FACULTY OF
BIOSCIENCE ENGINEERING

DESIGN OF AEROBIC GRANULAR SLUDGE REACTORS

BATCH VERSUS CONTINUOUS SYSTEMS

Margot Pennewaerde
Student number: 01505931

Promotor: Prof. dr. ir. Eveline Volcke
Tutors: ir. Laurence Strubbe & ir. Janis Baeten

Master's Dissertation submitted to Ghent University in partial fulfilment of the requirements for the degree of Master of Science in Bioscience Engineering: Chemistry and Bioprocess Technology

Academic year: 2019 - 2020

UNIVERSITEIT
GENT

Declaration of author rights

Ghent, June 2020

Author	Promotor
Margot Pennewaerde	prof. dr. ir. Eveline Volcke

Dankwoord

Met deze thesis komt een einde aan vijf mooie jaren studeren in Gent. Dit laatste jaar was intens, maar vooral heel erg interessant. Ik heb heel wat bijgeleerd en wil hiervoor enkele mensen in het bijzonder bedanken.

Eerst en vooral wil ik Laurence bedanken. Je stond altijd klaar om te luisteren naar nieuwe resultaten, om nieuwe inzichten te bespreken en goede raad te geven. Bedankt voor de vele interessante, aangename discussies! Verder wil ik ook Janis bedanken voor de kritische blik en leerrijke meetings die deze thesis zeker dat tikkeltje beter maakten. Ten slotte wil ik mijn promotor, professor Volcke, hartelijk bedanken voor de kans om mijn thesis in de BioCo groep te doen en me te verdiepen in dit interessante onderwerp. Ook bedankt voor de boeiende meetings en nieuwe standpunten die u aanbracht.

Ik wil ook graag mijn warme omgeving, mijn ouders, broer, vrienden en familie, bedanken voor de steun, goede raad en vooral het warme nest. Zonder jullie was dit allemaal veel moeilijker geweest.

Ik kijk uit en ben benieuwd naar wat nu komen zal.

Margot
Gent, juni 2020

Table of Contents

List of abbreviations

Abbreviation	Explanation
AOB	ammonium oxidizing bacteria
ASM2d	Activated Sludge Model No. 2d
A^2O	anaerobic-anoxic-aerobic wastewater treatment system
BOD	Biological oxygen demand
BSM1	Benchmark Simulation Model No. 1
BSM2	Benchmark Simulation Model No. 2
COD	chemical oxygen demand
DL	Diffusion limitation
DO	dissolved oxygen
DOHO	denitrifying ordinary heterotrophic organisms
DPAO	denitrifying phosphate accumulating organisms
EPS	extracellular polymeric substances
GAO	glycogen accumulating organisms
HRT	hydraulic retention time
NOB	nitrite oxidizing bacteria
OHO	ordinary heterotrophic organisms
PAO	phosphate accumulating organisms
P.E.	person equivalents
PHA	polyhydroxyalkanoates
PI	Proportional-Integral
PP	polyphosphate
rBCOD	readily biodegradable chemical oxygen demand
SBR	sequencing batch reactor
SRT	sludge retention time
SVI	sludge volume index
TSS	total suspended solids
VSS	Volatile suspended solids

List of symbols

Symbol	Explanation	Unit
English Alphabet		
AE	aeration energy	$kWh.d^{-1}$
A_{set}	Surface area of the settler	m^2
BOD_{crit}	BOD effluent criterion	$g\ BOD.m^{-3}$
BOD_{eff}	total BOD_5 concentration in effluent	$g\ BOD.m^{-3}$
C	total concentration N,P of COD in the continuous system	$g.m^{-3}$
COD_{crit}	COD effluent criterion	$g\ COD.m^{-3}$
COD_{eff}	total COD concentration in effluent	$g\ COD.m^{-3}$
D_{p1}	Denitrification potential	$g\ N.m^{-3}$
f_{cv}	COD/VSS ratio	$g\ COD.(g\ VSS)^{-1}$
$f_{N'ous}$	unbiodegradable soluble organic N fraction	-
f_{ns}	Non-settleable fraction	-
f_{x1}	anoxic volume fraction of bioreactor	-
f_{xt}	unaerated sludge mass fraction	-
h_{set}	Height of the settler	m
K_2	specific rate of denitrification in anoxic reactor at 15°C	$g\ N.(g\ VSS)^{-1}.d^{-1}$
KLa1-4	Oxygen transfer coefficient of reactors 1-4	d^{-1}
KLa5-6	Oxygen transfer coefficient of reactors 5-6	d^{-1}
$KLa6_{max}$	Maximal value for KLa6	d^{-1}
$KLa6_{min}$	Minimal value for KLa6	d^{-1}
KLa7	Oxygen transfer coefficient of reactor 7	d^{-1}
KLa_i	oxygen transfer coefficient of bioreactor *i*	d^{-1}
$K_{n,15}$	ammonium half saturation constant at 15°C	$g\ N.m^{-3}$
K_p	Proportional parameter of PI controller	depends on appl.
K_S	half-saturation coefficient	$g.m^{-3}$
$L_{TSS,eff}$	TSS load leaving the system with effluent	$kg\ TSS.m^{-3}$
$L_{TSS,in}$	TSS load coming into the system	$kg\ TSS.m^{-3}$
$L_{TSS,w}$	TSS load leaving the system with waste flow	$kg\ TSS.m^{-3}$
m	mass in the continuous wastewater system (COD, N or P)	g
ME	mixing energy	$kWh.d^{-1}$
N_c	nitrification capacity	$g\ N.m^{-3}$
N_{crit}	N effluent criterion	$g\ N.m^{-3}$
N_{eff}	total N concentration in effluent	$g\ N.m^{-3}$
N_s	concentration of influent N incorporated into the sludge	$g\ N.m^{-3}$
N_{ti}	Organic nitrogen in the influent	$g\ N.m^{-3}$
N_{te}	Organic nitrogen in the effluent	$g\ N.m^{-3}$
O_a	oxygen concentration in Q_{int}	$g\ O_2.m^{-3}$
O_s	oxygen concentration in Q_r	$g\ O_2.m^{-3}$
PE	pumping energy	$kWh.d^{-1}$
Q_i	effluent flow rate of bioreactor *i*	$m^3.d^{-1}$
$Q_{in,max}$	maximum influent flow rate based on BSM2 dynamic data	$m^3.d^{-1}$

Q_{in}	influent flow rate	$m^3.d^{-1}$
Q_{eff}	effluent flow rate	$m^3.d^{-1}$
Q_{int}	internal recycle flow rate	$m^3.d^{-1}$
Q_r	recycle flow rate	$m^3.d^{-1}$
Q_{set}	flow rate into settler	$m^3.d^{-1}$
Q_u	underflow rate	$m^3.d^{-1}$
Q_w	waste flow rate	$m^3.d^{-1}$
$Q_{w,max}$	Maximal value for Q_w	$m^3.d^{-1}$
$Q_{w,min}$	Minimal value for Q_w	$m^3.d^{-1}$
r_i	reaction rate of state variable	g *i*.m^{-3}.d^{1}
r_h	Hindered zone settling parameter	$m^3.(g\ TSS)^{-1}$
r_p	Flocculant zone settling parameter	$m^3.(g\ TSS)^{-1}$
r_{XOHO}	reaction rate of X_{OHO}	g COD.m^{-3}.d^{-1}
s	underflow sludge recycle ratio Q_r:Q_{in}	-
S	substrate concentration	g.m^{-3}
S_{Alk}	Alkalinity of the wastewater	(mole HCO_3^-).m^{-3}
S_F	Fermentable organic matter	g COD.m^{-3}
S_{N_2}	Dissolved nitrogen gas N_2	g N.m^{-3}
S_{NH_x}	Ammonium plus ammonia nitrogen: NH_4^+-N and NH_3-N	g N.m^{-3}
S_{No_x}	Nitrate plus nitrite nitrogen: NO_3^--N and NO_2^--N	g N.m^{-3}
S_{O_2}	Dissolved oxygen	g O_2.m^{-3}
$S^*_{O_2}$	oxygen saturation concentration in water	g O_2.d^{-1}
S_{PO_4}	Soluble inorganic phosphorus	g P.m^{-3}
S_U	Soluble undegradable organics	g COD.m^{-3}
S_{VFA}	Fermentation products (considered to be acetate)	g COD.m^{-3}
SRT_{min}	Minimal sludge retention time for nitrification	d
SRT_{reac}	sludge retention time in the biological reactor	d
SRT_{set}	sludge retention time in the settler	d
SRT_{tot}	total sludge retention time	d
T_i	Integral parameter of PI controller	depends on appl.
TSS_{crit}	TSS effluent criterion	g TSS.m^{-3}
TSS_{eff}	TSS concentration in the effllluent	g TSS.m^{-3}
v_0	maximum Vesilind settling velocity	$m.d^{-1}$
v_0'	Maximum settling velocity	$m.d^{-1}$
V_{1-2}	Volume of reactor 1 and 2	m^3
V_{3-4}	Volume of reactor 3 and 4	m^3
V_{5-7}	Volume of reactor 5,6 and 7	m^3
V_i	volume of bioreactor *i*	m^3
V_{layer}	Volume of one layer in settler	m^3
V_p	Volume of the biological reactor	m^3
$v_s(i)$	settling velocity in layer *i* of secondary settler	$m.d^{-1}$
V_{set}	Volume of the settler	m^3
X_{ANO}	Autotrophic nitrifying organisms	g COD.m^{-3}
X_{MeOH}	Metal-hydroxides	g $Fe(OH)_3$.m^{-3}

X_{MeP}	Metal-phosphates: $MePO_4$	g $FePO_4.m^{-3}$
X_{OHO}	Ordinary heterotrophic organisms	g $COD.m^{-3}$
$X_{OHO,i}$	X_{OHO} in bioreactor *i*	g $COD.m^{-3}.d^{-1}$
X_{PAO}	Phosphorus accumulating organisms	g $COD.m^{-3}$
$X_{PAO,PP}$	Stored polyphosphates in PAOs	g $P.m^{-3}$
$X_{PAO,Stor}$	Cell internal storage product of PAOs	g $COD.m^{-3}$
$X_{sc}(i)$	TSS concentration in layer *i* of secondary settler	g $TSS.m^{-3}$
V_{TOT}	total volume of the system	m^3
$X_{TSS,7}$	TSS concentration in bioreactor 7	g $TSS.m^{-3}$
$X_{TSS,7,sp}$	Set-point of TSS concentration in bioreactor 7	g $TSS.m^{-3}$
$X_{TSS,i}$	TSS concentration in bioreactor *i*	g $TSS.m^{-3}$
$X_{TSS, in}$	TSS concentration in influent of secondary settler	g $TSS.m^{-3}$
$X_{TSS, layer\ i}$	TSS concentration in layer *i* of settler	g $TSS.m^{-3}$
$X_{TSS,max}$	maximal TSS concentration in biological tank	g $TSS.m^{-3}$
$X_{TSS,reac}$	TSS concentration in biological reactor	g $TSS.m^{-3}$
$X_{TSS,w}$	TSS concentration in waste stream Q_w	g $TSS.m^{-3}$
XC_B	Slowly biodegradable substrates	g $COD.m^{-3}$
X_U	Particulate undegradable organics	g $COD.m^{-3}$
Greek Alphabet		
μ	specific process rate	d^{-1}
μ_{max}	Maximal specific process rate	d^{-1}
$\nu_{j,l}$	stoichiometric coefficient for component *i* in process *j*	g *i*.(g *j*)$^{-1}$
ρ_j	process rate of process *j*	g *j*.$m^{-3}.d^{-1}$
Stoichiometric parameters ASM2d		
$f_{S_U\_XC_B,hyd}$	Fraction of inert COD generated in hydrolysis	g $COD.(g\ COD)^{-1}$
Y_{OHO}	Yield for X_{OHO} growth	g $COD.(g\ COD)^{-1}$
Y_{PAO}	Yield for X_{PAO} growth per $X_{PAO,PHA}$	g $COD.(g\ COD)^{-1}$
$Y_{PP\_Stor,PAO}$	Yield for $X_{PAO,PP}$ requirement per $X_{PAO,Stor}$ stored	g $P.(g\ COD)^{-1}$
$Y_{Stor\_PP,PAO}$	Yield for $X_{PAO,PP}$ storage per $X_{PAO,Stor}$ utilized	g $COD.(g\ P)^{-1}$
Y_{ANO}	yield of autotrophic biomass per NO_3^- -N	g $COD.(g\ N)^{-1}$
$f_{X_U\_Bio,lys}$	Fraction of X_U generated in biomass decay	g $COD.(g\ COD)^{-1}$
$i_{N\_S_U}$	N content of S_U	g $N.(g\ COD)^{-1}$
$i_{N\_S_F}$	N content of S_F	g $N.(g\ COD)^{-1}$
$i_{N\_X_U}$	N content of X_U	g $N.(g\ COD)^{-1}$
$i_{N\_XC_B}$	N content of XC_B	g $N.(g\ COD)^{-1}$
$i_{N\_X_{Bio}}$	N content of biomass (X_{OHO}, X_{PAO}, X_{ANO})	g $N.(g\ COD)^{-1}$
$i_{P\_S_U}$	P content of S_U	g $P.(g\ COD)^{-1}$
$i_{P\_S_F}$	P content of S_F	g $P.(g\ COD)^{-1}$
$i_{P\_X_U}$	P content of X_U	g $P.(g\ COD)^{-1}$
$i_{P\_XC_B}$	P content of XC_B	g $P.(g\ COD)^{-1}$
$i_{P\_X_{Bio}}$	P content of biomass (X_{OHO}, X_{PAO}, X_{ANO})	g $P.(g\ COD)^{-1}$
$i_{TSS\_X_U}$	TSS to COD ratio for X_U	g $TSS.(g\ COD)^{-1}$
$i_{TSS\_XC_B}$	TSS to COD ratio for XC_B	g $TSS.(g\ COD)^{-1}$
$i_{TSS\_X_{Bio}}$	TSS to COD ratio for biomass (X_{OHO}, X_{PAO}, X_{ANO})	g $TSS.(g\ COD)^{-1}$

Kinetic parameters of ASM2d		
Hydrolysis of particulate substrate XC_B		
$q_{XC_B\_SB,hyd}$	Maximum specific hydrolysis rate	d^{-1}
$\eta_{qhyd,Ax}$	Correction factor for anoxic hydrolysis	-
$\eta_{qhyd,An}$	Correction factor for anaerobic hydrolysis	-
$K_{O_2,hyd}$	Half saturation/inhibition parameter for S_{O_2}	g $O_2.m^{-3}$
$K_{NO_x,hyd}$	Half saturation/inhibition parameter for S_{NO_x}	g $N.m^{-3}$
$K_{XC_B,hyd}$	Half saturation parameter for XC_B/X_{OHO}	g COD.(g COD)$^{-1}$
Heterotrophic organisms X_{OHO}		
$\mu_{OHO,Max}$	Maximum growth rate of X_{OHO}	d^{-1}
$q_{S_F\_VFA,Max}$	Rate constant for fermentation	g COD.(g COD)$^{-1}$.d^{-1}
$\eta_{\mu OHO,Ax}$	Reduction factor for anoxic growth of X_{OHO}	-
b_{OHO}	Decay rate for X_{OHO}	d^{-1}
$K_{O_2,OHO}$	Half saturation/inhibition parameter for S_{O_2}	g $O_2.m^{-3}$
$K_{S_F,OHO}$	Half saturation parameter for S_F	g COD.m^{-3}
$K_{S_F,fe}$	Half saturation parameter for fermentation of S_F	g COD.m^{-3}
$K_{S_{VFA},OHO}$	Half saturation parameter for S_{VFA}	g COD.m^{-3}
$K_{NO_x,OHO}$	Half saturation/inhibition parameter for S_{NO_x}	g $N.m^{-3}$
$K_{NH_x,OHO}$	Half saturation parameter for S_{NH_x}	g $N.m^{-3}$
$K_{PO_4,OHO}$	Half saturation parameter for S_{PO_4}	g $P.m^{-3}$
$K_{Alk,OHO}$	Half saturation parameter for S_{Alk}	(mole HCO_3^-).m^{-3}
Phosphorus accumulating organisms X_{PAO}		
q_{PAO,VFA_Stor}	Rate constant for S_{VFA} uptake rate ($X_{PAO,Stor}$ storage)	g COD.(g COD)$^{-1}$.d^{-1}
q_{PAO,PO_4_PP}	Rate constant for storage of $X_{PAO,PP}$	g P.(g COD)$^{-1}$.d^{-1}
$\mu_{PAO,Max}$	Maximum growth rate of X_{PAO}	d^{-1}
$\eta_{\mu\ PAO}$	Reduction factor for anoxic growth of X_{PAO}	-
b_{PAO}	Decay rate of X_{PAO}	d^{-1}
$b_{PP\_PO_4}$	Rate constant for lysis of $X_{PAO,PP}$	d^{-1}
b_{Stor_VFA}	Rate constant for respiration of $X_{PAO,Stor}$	d^{-1}
$K_{O_2,PAO}$	Half saturation/inhibition parameter for S_{O_2}	g $O_2.m^{-3}$
$K_{NO_x,PAO}$	Half saturation parameter for S_{NO_x}	g $N.m^{-3}$
$K_{S_{VFA},PAO}$	Half saturation parameter for S_{VFA}	g COD.m^{-3}
$K_{NH_x,PAO}$	Half saturation parameter for S_{NH_x}	g $N.m^{-3}$
$K_{PO_4,PAO,upt}$	Half saturation parameter for S_{PO_4} uptake ($X_{PAO,PP}$ storage)	g $P.m^{-3}$
$K_{PO_4,PAO,nut}$	Half saturation parameter for S_{PO_4} nutrient (X_{PAO} growth)	g $P.m^{-3}$
$K_{Alk,PAO}$	Half saturation parameter for S_{Alk}	(mole HCO_3^-).m^{-3}
K_{S,fPP_PAO}	Half saturation parameter for $X_{PAO,PP}/X_{PAO}$	g P.(g COD)$^{-1}$
$f_{PP\_PAO,Max}$	Maximum ratio of $X_{PAO,PP}/X_{PAO}$	g P.(g COD)$^{-1}$
K_{I,fPP_PAO}	Half inhibition parameter for $X_{PAO,PP}/X_{PAO}$	g P.(g COD)$^{-1}$
K_{fStor_PAO}	Saturation constant for $X_{PAO,Stor}/X_{PAO}$	g COD.(g COD)$^{-1}$
Autotrophic nitrifying organisms X_{ANO}		
$\mu_{ANO,Max}$	Maximum growth rate of X_{ANO}	d^{-1}

b_{ANO}	Decay rate of X_{ANO}	d^{-1}
$K_{O_2,ANO}$	Half saturation parameter for S_{O_2}	g O_2.m^{-3}
$K_{NH_x,ANO}$	Half saturation parameter for S_{NH_x}	g N.m^{-3}
$K_{Alk,ANO}$	Half saturation parameter for S_{Alk}	(mole HCO_3^-).m^{-3}
$K_{PO_4,ANO}$	Half saturation parameter for S_{PO_4}	g P.m^{-3}
Precipitation		
k_{PRE}	Rate constant for P precipitation	m^3.(g $Fe(OH)_3)^{-1}$.d^{-1}
k_{RED}	Rate constant for redissolution	d^{-1}
$K_{Alk,PRE}$	Saturation coefficient for alkalinity	(mole HCO_3^-).m^{-3}

Abstract

The starting point of this thesis is the demand to increase the treatment capacity of our existing continuous activated sludge plants for wastewater treatment in Flanders. This demand is driven by an increasingly high standard of living and an increasing amount of households connected to a sewage system (84% of the population in 2018 vs. 48% in 2000) (Vlaamse milieumaatschappij, 2019a). These wastewater treatment plants are usually continuous processes using activated sludge, where the bacteria that perform the conversions grow in flocs. However, this activated sludge has a the poor settling ability, which results in space consuming settlers and forms the bottleneck for scale-up of the conventional wastewater treatment plants. Opposite to the conventional activated sludge processes are wastewater treatment technologies based on aerobic granular sludge, i.e. bacteria grown in good settling granules. This promising aerobic granular sludge technology results in strong reduction of surface area, energy consumption and operational costs, which has led to over 70 full-scale applications worldwide (Royal HaskoningDHV, 2020a). Based on these advantages, it could be possible to increase the treatment capacity of the current continuous activated sludge plants by introducing aerobic granular sludge into the systems. The better settling ability of aerobic granular sludge leads to a higher biomass concentration for the same settler with a given surface area. However, it is important to realize that the proven applications of aerobic granular sludge are all batch configurations, contrary to the continuous design of the existing activated sludge plants. The replacement of activated sludge with aerobic granular sludge in continuous wastewater treatment is not straightforward and forms the topic of this thesis.

In this thesis it is questioned if refurbishment of the current continuous activated sludge plants into continuous aerobic granular sludge plants would be advantageous in terms of treatment capacity and energy consumption, in order to meet the effluent criteria. This was investigated by assuming that it is possible to cultivate aerobic granules with long-term stability into continuous systems. The latter research question is currently the focus of multiple international research groups, investigating this with experimental work. This thesis however focusses on the relation between the advantages of aerobic granular sludge and his process implementation. Based on a model simulation study in Matlab-Simulink, it was investigated whether the continuous system design and accompanied operating conditions could benefit from aerobic granular sludge compared to activated sludge. It was assumed that aerobic granular sludge differs from activated sludge based on two characteristics: better settleability and diffusion limitation. The latter occurs due to the compact structure of granules, which complicates the transport of substrates into the granule. This diffusion limitation effect is enhanced by the lower substrate concentration in a continuous reactor compared to a batch reactor, which was also taken into account. From the results, it was found that the better settling sludge increased the maximal treatment capacity of the continuous activated sludge system with about 40%. This positive effect was almost completely counteracted by diffusion limitation. In a strong diffusion limitation scenario, the maximal treatment capacity was approximately halved with aerobic granular sludge compared to activated sludge. In a moderate and probably more realistic diffusion limitation scenario, no significant difference was observed between the maximal treatment capacity of the continuous system with activated sludge and aerobic granular sludge. A disadvantage in case of aerobic granular sludge was the higher aeration energy needed. This research shows that diffusion limitation in continuous systems has a non-negligible negative effect that could possibly counteract the positive effect of better settling sludge compared to activated sludge.

Important to mention however is that no final judgement regarding the whether or not beneficial effect of replacing activated sludge with aerobic granular sludge in continuous systems can be made. The optimal operating conditions (anoxic reactors followed by aerobic ones) and the process control (e.g. oxygen control strategy in the reactors) were unchanged in this research. Further research is recommended regarding the optimization of the reactor design and operating conditions of the continuous system in order to fully benefit from the advantages of aerobic granular sludge.

Samenvatting

Dit werk vertrekt vanuit de vraag naar een toenemende behandelingscapaciteit van de waterzuiveringsinstallaties in Vlaanderen. Deze vraag wordt gedreven door een steeds hogere levensstandaard en het stijgende aantal huishoudens aangesloten op het rioleringssysteem (84% van de bevolking in 2018 vs. 48% in 2000) (Vlaamse milieumaatschappij, 2019a). Deze waterzuiveringsinstallaties zijn doorgaans continue processen die gebruik maken van actief slib, waarbij de bacteriën die de omzettingen bewerkstelligen in vlokken groeien. Dit actief slib is echter slecht bezinkbaar, wat resulteert in ruimteverslindende sedimentatietanks en een knelpunt vormt bij opschaling van conventionele waterzuiveringsinstallaties. Tegenover conventionele actiefslib-processen staan waterzuiveringstechnologieën gebaseerd op aeroob korrelslib, waarbij de bacteriën in zeer goed bezinkbare korrels groeien. De veelbelovende aeroob korrelslibtechniek resulteert in een sterke besparing van grondoppervlakte, energie en operationele kosten, wat sinds 2011 heeft geleid tot meer dan 70 nieuw gebouwde volle schaaltoepassingen wereldwijd (Royal HaskoningDHV, 2020a). Gezien de voordelen zou men er kunnen aan denken om de behandelingscapaciteit van de huidige actiefslibinstallaties te verhogen door het introduceren van korrelslib. De betere bezinkbaarheid van korrelslib leidt immers tot een hogere biomassaconcentratie voor eenzelfde sedimentatietank met gegeven oppervlakte. Het is echter belangrijk om zich te realiseren dat de bewezen toepassingen van korrelslib steeds batchreactoren betreffen, in tegenstelling tot de continu bedreven actiefslibinstallaties. Het vervangen van actief slib door korrelslib in continue waterzuiverings-installaties is niet rechtlijnig en vormt het onderwerp van deze masterproef.

Centraal staat de vraag of de omvorming van continue waterzuiveringsinstallaties werkend met actief slib tot aeroob korrelslibinstallaties voordelig zou zijn op het gebied van behandelingscapaciteit en energieverbruik, voor gelijkblijvende effluentnormen. Er werd hierbij van uitgegaan dat het cultiveren van aeroob korrelslib met langdurige stabiliteit in continue systemen op zich mogelijk is. Dit is immers een onderzoeksvraag waar zich momenteel reeds meerdere internationale onderzoeksgroepen op richten, via experimenteel werk. In dit masterproefwerk daarentegen ligt de focus op de relatie tussen de voordelen van korrelslib en zijn procesuitvoering. Op basis van een simulatiestudie in Matlab-Simulink werd onderzocht of men met een continu ontwerp en bijhorende procescondities, nog steeds voordeel zou kunnen halen uit aeroob korrelslib in vergelijking met actief slib. Er werd verondersteld dat aeroob korrelslib verschilt van actief slib op basis van twee kenmerken: een hogere bezinkingssnelheid en een sterkere diffusielimitatie. Diffusielimitatie is het resultaat van de compacte structuur van een korrel, wat het transport van substraten tot binnenin de korrel bemoeilijkt. Dit effect wordt nog versterkt door de lagere heersende substraatconcentratie in een continue reactor t.o.v. een batchreactor, die eveneens in rekening werd gebracht. Uit de resultaten bleek dat de betere bezinkbaarheid van aeroob korrelslib de maximale behandelingscapaciteit van het systeem deed stijgen met ongeveer 40%. Dit positieve effect werd echter nagenoeg volledig tenietgedaan door diffusielimitatie. In een scenario met sterke diffusielimitatie was de maximale behandelingscapaciteit van het continu systeem zelfs slechts half zo groot met korrelslib dan met actief slib. In een milder, wellicht realistischer scenario voor diffusielimitatie, was er geen significant verschil in maximale behandelingscapaciteit van het continu systeem met actief slib of korrelslib. Nadeel in geval van aeroob korrelslib was een hogere nodige beluchtingsenergie. Dit onderzoek toont aan dat diffusielimitatie in continue aeroob korrelslibsystemen niet verwaarloosbaar is en mogelijks het positieve effect van betere bezinkbaarheid van korrelslib t.o.v. actief slib teniet doet.

Het is echter belangrijk om op te merken dat op basis van deze resultaten nog geen finale uitspraak kan worden gedaan omtrent het al dan niet gunstig effect van het vervangen van actief slib door korrelslib in continue installaties. De procesconfiguratie (anoxische tanks gevolgd door aerobe) en procesregeling (bv. zuurstofcontrole strategie in de reactoren) werd immers ongewijzigd gelaten. Verder onderzoek is aangewezen naar optimalisatie van het reactorontwerp en -bedrijf om zo de voordelen van aeroob korrelslib ten volle te benutten.

1. Introduction

Since several years, conventional wastewater treatment has been dealing with low volumetric loading rates and a high energy consumption (Van Haandel & Van der Lubbe, 2007; Pronk *et al.*, 2017). Especially with the increasing standard of living and an increasing amount of households connected to a sewage system constant improvements are needed (Vlaamse milieumaatschappij, 2019a). The question arises how these challenges can be met in an efficient way. Over the past 20 years, aerobic granular sludge is presented as a promising technology to meet these challenges. Conventional activated sludge flocs, i.e. suspended microorganisms forming bulky aggregates, are converted into compact aerobic granules. This results in 25-75% less land area, 20-50% less energy and up to 7-17% less costs compared to conventional activated sludge plants (Pronk *et al*, 2017). The conventional use of aerobic granular sludge is in batch systems, but continuous systems are under research as well (Jahn *et al.*, 2019).

The aim of this thesis is to gain further insight in continuous processes with aerobic granular sludge. Given that the current continuous systems are not depreciated, yet cannot meet the demand for higher treatment capacity, continuous aerobic granular sludge systems seem promising. Better settleability of granules could lead to higher biomass concentrations in the existing continuous systems, possibly resulting in a higher treatment capacity. Before researching how to get stable granules in a continuous flow reactor, it is needed to investigate the overall effect of granules on the performance of continuous reactors. In this thesis it is questioned if refurbishment of the current continuous activated sludge plants into continuous aerobic granular sludge plants would be advantageous in terms of treatment capacity and energy consumption, in order to meet the effluent criteria. This was investigated by developing the comparison between continuous systems with activated sludge and with aerobic granular sludge.

The comparative study is obtained in different steps. In the literature review, a state-of-the-art on current wastewater treatment with activated sludge and aerobic granular sludge is given. Both the typical aerobic granular sludge implementation in batch systems and perspectives on aerobic granular sludge in continuous systems are discussed and compared based on literature findings.
The chapter 'Materials and methods' describes the mathematical model based on the Benchmark Simulations Model No. 1 (BSM1) in Matlab-Simulink. A continuous activated sludge system serves as the reference model. Furthermore, this model is adapted to make it representable as a continuous design with aerobic granular sludge based on two characteristics: better settleability and diffusion limitation.
In the chapter 'Results and discussion', the differences between both continuous systems are elucidated to answer the research question. Both the maximal treatment capacity and energy consumption in order to meet the effluent criteria were calculated and compared for both systems.
Conclusions are summarized in the chapter 'General conclusions' and 'Recommendations for further research' are given.

2. Literature review

In this chapter, literature findings on the design of aerobic granular sludge systems are gathered. In the first section, the importance of wastewater treatment is explained. Subsequently, the biological removal processes performed in both activated sludge and aerobic granular sludge wastewater treatment plants are explained in section 2.2. In section 2.3, the differences between the conventional activated sludge and aerobic granular sludge are stated. Furthermore, two design possibilities for wastewater treatment with activated sludge, namely continuous and batch systems are explained in section 2.4. Following this, conventional aerobic granular sludge technology in batch systems is stated in section 2.5. The potential of aerobic granular sludge in continuous systems on the other hand, is explained in section 2.6. Lastly, the conclusions and research objectives for the continuation of this thesis are given in section 2.7.

2.1 Importance of wastewater treatment

Wastewater is produced by the water consumption of domestic residences, industry and agriculture. These sectors are polluting the groundwater with various contaminants (European Commission, 2019). These contaminants are mostly organic compounds, e.g. proteins, fats and carbohydrates, and nutrients, i.e. nitrogen and phosphorus. The production of wastewater leads to two types of risks. Firstly, pathogens present in the wastewater have an important effect on human health (Shannon *et al.*, 2007). Secondly, wastewater directly affects aquatic and terrestrial ecosystems (European Commission, 2019). Eutrophication occurs, which means that due to the availability of nutrients derived from wastewater in the receiving water, excessive growth of algae occurs (Van Haandel & Van der Lubbe, 2007). Due to oxygen usage of bacteria for decay of these algae, the water can become poor in oxygen, which can lead to the death of aquatic organisms.

Biological wastewater treatment has a tremendous impact on the world by protecting human health and the environment. During this process, the removal of organic matter (COD), nitrogen (N) and phosphorus (P) from the wastewater occurs. Pathogen concentrations decrease by at least a 10-fold after wastewater treatment. This is realized by the embedding of pathogens in the waste sludge and by the lethal effect of aeration on pathogens (Shannon *et al.*, 2007; Wery *et al.*, 2008). Eutrophication on the other hand, is tackled by achieving removal rates of more than 90% for nitrogen and more than 60% for phosphorus depending on the strength of the wastewater (Metcalf & Eddy, 2004; European Commission, 2016). Removal rates of more than 90% for organic matter prevent oxygen depletion in the receiving water (European Commission, 2016).

Wastewater treatment regarding COD, N and P are controlled by legislation like the Urban Waste Water treatment Directive and the European Water Framework Directive. This results in effluent criteria, depending on the receiving water, e.g. a COD concentration of 125 g $COD.m^{-3}$, total suspended solids concentration of 35 g $TSS.m^{-3}$ and a total nitrogen and phosphorus concentration of respectively 10 g $N.m^{-3}$ and 2 g $P.m^{-3}$ (Council of European Communities, 1991). A good performance of the wastewater treatment has to be guaranteed, since these standards will only become stricter in the future (Jeppsson *et al.*, 2002). The European Water Framework Directive has postulated that by 2027, all water in brooks and rivers have to meet the previously mentioned criteria. In 2018, the average degree of purification in Flanders, which is defined as the amount of people whose wastewater is connected to a sewage system to the total amount of people, was 84%, evolving from 26% in 1991

(Vlaamse milieumaatschappij, 2019a,b). Another method that is more and more implemented is the separation of non-polluted water like rainwater from wastewater, which is not easy and has high costs. This separated sewer system results in a better efficiency since it helps to prevent unnecessary dilution and thus optimizes the performance of the wastewater treatment plant (e.g. energy for transport of wastewater to plant) (Tobey & Smets, 1996; Wavin, 2017). It also leads to less fluctuating influent flow rates into the wastewater treatment plant.

2.2 Biological removal of organic matter, nitrogen and phosphorus

Conventional wastewater treatment performing the purification of wastewater to meet the effluent criteria consists of physical, chemical and biological processes. In the biological processes, microorganisms - suspended in aerated water - are responsible for the removal of organic matter, nitrogen and phosphorus, which takes place under different conditions. Table 2.1 summarizes which microbial groups occur under each of these operating conditions. In addition, for each microbial group, their function and respective reaction are given.

Table 2.1: Summary of the different microbial groups active under different conditions in a conventional wastewater treatment process. For each group, their function and respective reaction is given (based on Yuan *et al.*, 2012; Bengtsson *et al.*, 2018; Rollemberg *et al.*, 2018). Abbreviations: (D)PAO: (denitrifying) phosphate accumulating organisms, (D)OHO: (denitrifying) ordinary heterotrophic organisms, (D)GAO: (denitrifying) glycogen accumulating organisms, AOB: ammonium oxidizing bacteria, NOB: nitrite oxidizing bacteria, VFA: volatile fatty acids, PHA: polyhydroxyalkanoates, PP: polyphosphate.

Condition	Microbial group	Function	Reaction
anaerobic	PAO/GAO	COD removal	VFA → PHA
anoxic	DOHO/DPAO/DGAO	denitrification	NO_3^- → N_2
	DOHO	COD removal	org C + NO_3^- → CO_2 + N_2 + H_2O
	DPAO	P removal	PO_4^{3-} → PP + biomass
	DPAO/DGAO	glycogen production	PHA → glycogen + biomass
aerobic	OHO	COD removal	org C + O_2 → CO_2 + H_2O
	AOB,NOB	nitrification	NH_4^+ + $2O_2$ → NO_3^- + H_2O + $2H^+$
	PAO	P removal	PO_4^{3-} → PP + biomass
	PAO/GAO	glycogen production	PHA → glycogen + biomass

Nitrogen is removed from the wastewater by a combination of nitrification and denitrification, which take place under aerobic and anoxic conditions, respectively. Nitrification is carried out by autotrophic bacteria and consists of two steps. Ammonium NH_4^+ is first converted to nitrite NO_2^- by ammonium oxidizing bacteria (AOB), followed by oxidation of NO_2^- to nitrate NO_3^- by nitrite oxidizing bacteria (NOB) (Focht & Chang, 1975; Wagner et al., 2002). During denitrification, NO_3^- is converted to the harmless N_2, which leaves the water into the atmosphere.

Phosphorus removal takes place under alternating anaerobic and aerobic or anoxic conditions. Under anaerobic conditions, phosphate accumulating organisms (PAO) take up volatile fatty acids, and store them in the form of polyhydroxyalkanoates (PHA) (Comeau *et al.*, 1986; Yuan *et al.*, 2012). Energy to do this is obtained by glycolysis and by hydrolysing internal stored polyphosphate, resulting in the release of phosphate PO_4^{3-} to the water (Yuan *et al.*, 2012). Under subsequent aerobic or anoxic conditions, PAO use the power from reduction of oxygen or nitrate to oxidize the anaerobically stored PHA. The oxidation of PHA produces energy for cell growth, glycogen synthesis and phosphate uptake, which is internally stored as polyphosphate (PP) (Comeau *et al.*, 1986; Oehmen *et al.*, 2007). In the

aerobic or anoxic phase, about 18% more P is stored than there was released during the last anaerobic phase (Clayton *et al.*, 1991). This net P removal is obtained due to a higher biomass concentration performing the phosphate uptake then there was during the previous anaerobic phosphate release. In case of the denitrifying PAO (DPAO) under anoxic conditions, simultaneous denitrification and P removal occurs. This results in lower aeration costs, cell yields and carbon requirements (Lu *et al.*, 2016). Glycogen accumulating organisms (GAO) are also active under alternating anaerobic and aerobic conditions. However, these organisms do not perform P removal, but only function on glycolysis and glycogen synthesis (Table 2.1). Possible competition between PAO and GAO for organic carbon can be imposed in favour of PAO by applying high P:COD ratios, low COD:N ratios and high dissolved oxygen (DO) concentrations (Yuan *et al.*, 2012; Rollemberg *et al.*, 2018; Carrera *et al.*, 2019).

Organic matter (COD) is removed under aerobic, anoxic, as well as anaerobic conditions. Ordinary heterotrophic bacteria consume organic matter with oxygen (O_2) as electron acceptor. The organic carbon is converted to CO_2 and leaving the water (Clayton *et al.*, 1991). Secondly, the denitrification under anoxic conditions also requires organic carbon. Lastly, under anaerobic conditions, PAO/GAO store volatile fatty acids, which is rBCOD (readily biodegradable COD) (Yuan *et al.*, 2012).

2.3 Activated sludge versus aerobic granular sludge

Both activated sludge and aerobic granular sludge can be used to remove organic matter, nitrogen and phosphorus from wastewater, like explained in section 2.2. However, there are some differences in structure and characteristics of both options.

Activated sludge are suspended microorganisms that form bulky aggregates called flocs. They are the most commonly applied sludge structures for purifying both municipal and industrial wastewater. Advantages of activated sludge processes are good effluent quality at reasonable cost, high process stability and relative ease of operation (Van Haandel & Van der Lubbe, 2007).

Aerobic granules are developed and maintained under aerobic conditions and are defined as ‘aggregates of microbial origin, which do not coagulate under reduced hydrodynamic shear, and which settle significantly faster than activated sludge flocs’ (Bathe *et al.*, 2005). This definition consists of three parts. Firstly, these aggregates of microbial origin are self-immobilized biofilms without the need of carrier material (Bathe *et al.*, 2005; McSwain *et al.*, 2005). A spherical shape is the optimal configuration for biofilms, since this results in the maximal surface to volume ratio, leading to good mass transfer at the surface of the granules (de Kreuk & van Loosdrecht, 2004). Secondly, in contrast to flocs, granules do not coagulate but settle as individual units (de Kreuk *et al.*, 2007). Lastly, due to their fast settling velocity, they are able to operate at short hydraulic retention times (HRT) (Van Haandel & Van der Lubbe, 2007). Later on, some additions to this definition were made. The minimum diameter of an aerobic granule to make sure that all these criteria are being met, is defined by 0.2 mm (de Kreuk *et al.*, 2007). Furthermore, granules must have a certain physical strength, resulting in toleration for high shear forces (Gao *et al.*, 2011). Granular sludge can treat both municipal and industrial wastewater (Liu *et al.*, 2017).

Aerobic granules show some advantages compared to activated sludge. In Table 2.2, a comparison of the main differences in characteristics of activated sludge and aerobic granules is given. The most important difference - in fact the main driver of the emergence of aerobic granules - is their better settling velocity (Schwarzenbeck & Wilderer, 2005; Anuar *et al.*; 2007; Caluwé, 2018). This ensures that higher biomass concentration in the system can be obtained, because the separation of sludge from the clean effluent in enhanced. Hence, for the same treatment volume, less reactor volume is needed, leading to a reduction in the required surface area and lower investment costs (Bathe *et al.*, 2005). Secondly, aerobic granules are able to withstand shock-loading rates up to 15 kg $COD.m^{-3}.d^{-1}$ (Li *et al.*, 2005; Gao *et al.*, 2011). Another advantage of aerobic granules is the fact that they are better at treating wastewater containing less degradable substrates, such as phenol (Tay *et al.*, 2005; Kent *et al.*, 2018). Aerobic granules are less susceptible to the toxicity of phenol since a large part of the biomass is not exposed to this high phenol concentration (Liu & Tay, 2004). The latter is due to the diffusion limitation in granules, which is also a possible disadvantage of aerobic granules. Due to this limited diffusion of oxygen and substrates into the core of granules, the metabolic activity of the granule could be decreased (Wang *et al.*, 2004; Li & Liu, 2005). Another possible disadvantage is the start-up of the system, because the formation of granules takes some time (Bathe *et al.*, 2005). This problem could be solved by using an inoculum of granules from another installation. In this way, further granulation (i.e. the formation of granules) is fastened significantly (Gao *et al.,* 2011). On top of that, achieving long-term stability of these granules is also a key factor for stable operation, which is not evident and requires extra attention (Bathe *et al.*, 2005; Van Haandel & Van der Lubbe, 2007; Franca *et al.*, 2018).

Table 2.2: Comparison of characteristics of activated sludge and aerobic granules (SVI30 = sludge volume index, volume occupied by the sludge after 30 minutes of settling) (Hu *et al.*, 2005; Li *et al.*, 2007; Kent *et al., 2018;* Rollemberg *et al.*, 2018; Van Haandel & Van der Lubbe, 2007).

Characteristic	Activated sludge	Aerobic granules
Settling velocity [$m.h^{-1}$]	2-10	10-90
Size [mm]	<0.2	0.2-5
SVI30 [$mL.g^{-1}$]	100-120	20-50
Biomass concentration [kg $TSS.m^{-3}$]	3-5	10-15

2.4 Continuous versus batch systems with activated sludge

A distinction is made between two different design configurations to execute biological wastewater treatment, i.e. a continuous or a batch design. A combination of anaerobic, anoxic and aerobic phases are needed to perform removal of organic matter, nitrogen and phosphorus (Table 2.1). Hence, these conditions have to be incorporated in the design and operation of both continuous (section 2.4.1) and batch (section 2.4.2) systems. Lastly, the implementation of both systems, together with their differences and challenges is given in section 2.4.3.

2.4.1 Continuous systems

The conventional design for wastewater treatment is a continuous flow reactor (Figure 2.1). In a continuous system, the various biological conversions are carried out in separate tanks. The system is thus called space-oriented. The water flows from one tank to the other and the volume of each tank is constant (Irvine *et al.*, 1989).

The general set-up constitutes of multiple reactors mostly in a sequence anaerobic-anoxic-aerobic (A^2O) where the bioconversion reactions as given in Table 2.1 occur (Zeng *et al.*, 2010). The biological tanks are followed by a settler in which the sludge is separated from the purified water (Pitman, 1991; Van Haandel & Van der Lubbe, 2007). The settled sludge is partially recycled and partially wasted. The recycle ratio Q_r:Q_{in} mostly has a value between 0.5 and 1.5, with Q_{in} [$m^3.d^{-1}$] the influent flow rate and Q_r [$m^3.d^{-1}$] the recycled sludge flow rate back to the anaerobic tank (Figure 2.1) (Pitman, 1991). Alternating phases of anaerobic and aerobic/anoxic conditions are needed for the growth of PAO and consequently for the removal of phosphorus. The C-requirement for both the anaerobic storage of PHA and the denitrification explains why the anaerobic and anoxic tanks are placed before the aerobic ones (He *et al.*, 2016). If the aerobic tank would be placed first, all COD would be aerobically converted before N and P removal could take place. With this in mind, sufficient COD has to be present in the wastewater to obtain good N and P removal (COD:N ratio of 5-10 g COD.(g N)$^{-1}$) (Isaacs & Henze, 1995). Since most of the nitrogen in the influent stream is present in the form of ammonium, also an internal recycle stream from the aerobic to the anoxic tank is needed to denitrify the just formed NO_3^-, thus optimizing N removal (Figure 2.1).

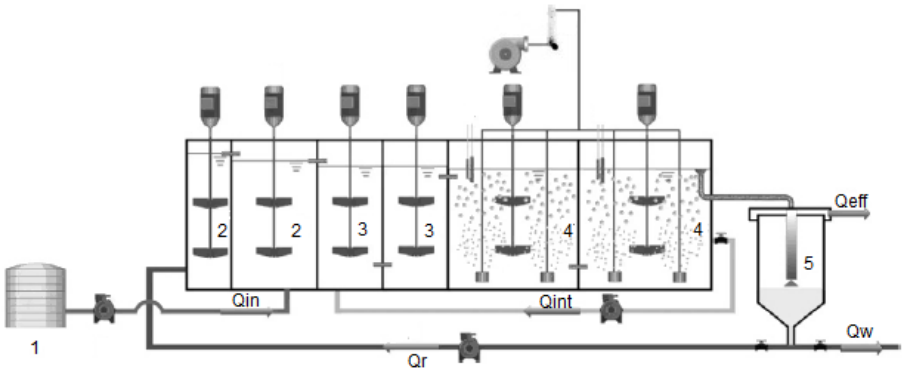

Figure 2.1: General set-up of a continuous waste water treatment plant (A^2O) (1: influent tank, 2: anaerobic tanks, 3: anoxic tanks, 4: aerobic tanks, 5: settler, Q_{in}: influent flow rate [$m^3.d^{-1}$], Q_w: waste sludge flow rate [$m^3.d^{-1}$], Q_r: recycled sludge flow rate [$m^3.d^{-1}$], Q_{eff}: effluent flow rate [$m^3.d^{-1}$], Q_{int}: internal recycle flow rate [$m^3.d^{-1}$]). The first out of two anaerobic tanks can also be named the pre-anoxic zone, since there can be NO_3^- embedded in the recycled sludge (based on Zeng *et al.*, 2010).

2.4.2 Batch systems

Batch systems are time-oriented, i.e. the different conditions occur in the same tank at different points in time. Flow rate, energy use and tank volume vary according to a pre-determined, periodic operating strategy (Irvine *et al.*, 1989; Mahvi, 2008).

The conventional batch system is a sequencing batch reactor (SBR), running through cycles consisting of five phases (Figure 2.2). These five phases are the fill, react, settle, draw and idle phase (Mahvi, 2008; Shaw *et al.*, 2009). The fill and react phases allow that alternating anaerobic, anoxic and aerobic phases can occur through interrupted aeration if this is needed for the particular purification strategy. As a result, a sequence similar to the one imposed to a continuous system can be used and removal of COD, N and P can be obtained. In the draw phase, the purified water is partially removed and the idle phase allows removal of waste sludge (Irvine *et al.*, 1989; Shaw *et al.,* 2009). The volume exchange ratio quantifies which fraction of the reactor volume is discharged during the draw phase (Kent *et al.*,2018). To allow the treatment of a continuous influent stream, a set of at least two SBR tanks

operating parallel, combined with an optional buffer tank can be used (Irvine *et al.*, 1989; Mahvi *et al.*, 2004; Simon *et al.*, 2006).

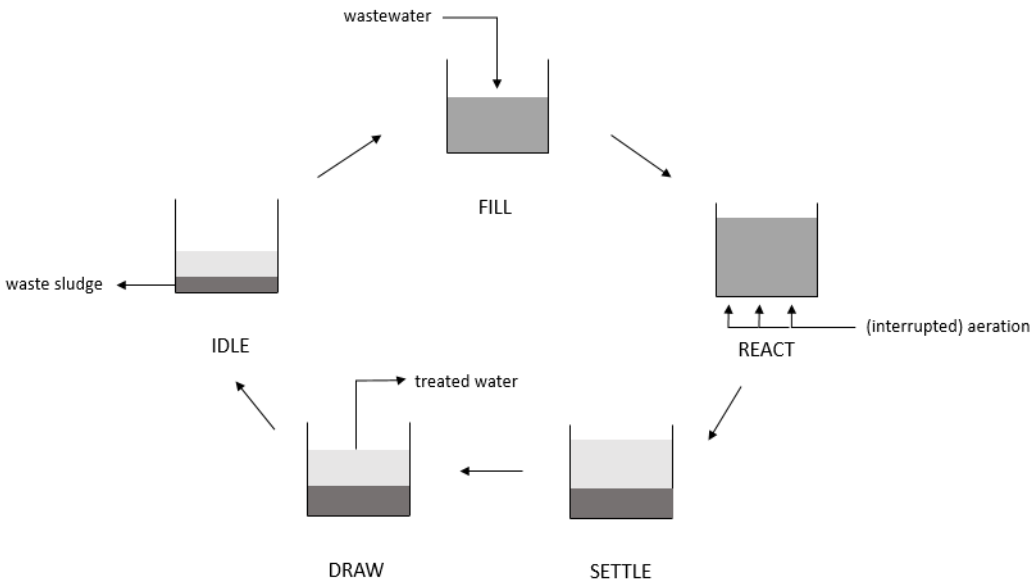

Figure 2.2: General cycle of a sequencing batch reactor (based on Mahvi, 2008).

2.4.3 Comparison continuous versus batch: implementation, differences and challenges

Both continuous and batch processes can be used in combination with activated sludge. In Flanders, a continuous wastewater treatment plant with activated sludge is the conventional procedure. In most of these plants - 95% of the plants bigger than 1000 P.E. (person equivalents) - the oxidation is done in an oxidation ditch. This is a carrousel type of reactor where the water flows in a cyclic pattern. On the contrary, batch systems are not used for the treatment of municipal wastewater in Flanders. Two reasons for this trend are given by Aquafin, the company responsible for management of the infrastructure for wastewater treatment in Flanders. The varying influent flow rate due to a combined sewer system (wastewater + rainwater) and the entire automation of the batch process. Batch systems cannot handle the varying influent flow rate due to fluctuating weather conditions very well, since it is hard to plan this into the cycles. Furthermore, a batch process requires more sophisticated control, called batch scheduling, which is not interesting in plants where not always an operator is present. Hence, the risk of failure in the automatically regulated cycle is too high (Boonen, I., Aquafin, personal communication, December 9, 2019). Nowadays however, interest is regained in SBR systems for activated sludge because of their compactness and better process control (Van Haandel & Van der Lubbe, 2007).

Advantages of continuous systems are the low maintenance and sophistication and the low installed aeration capacity compared to batch systems (EPA, 1999; Van Haandel & Van der Lubbe, 2007; Mahvi, 2008). Batch reactors on the other hand have a single tank configuration, small foot print, flexibility in designing the cycles and low capital cost (Irvine *et al.*, 1989; EPA, 1999; Mahvi, 2008). It can be pointed out that process control is pushed forward as an advantage in both continuous and batch systems. It seems that in continuous systems, the control aspect means that the system works quite well on his own and requires less work of the operator, while in batch systems, the system can be designed very

case-specific based on the composition of the wastewater, but requires more insight of the operator to design and run the perfect cycle.

Although these activated sludge processes work well, some challenges can be identified. Due to a growing world population and a higher standard of living, the amount of wastewater keeps increasing and less space is available. Hence, a higher treatment capacity is needed in the current wastewater treatment plants. In the conventional continuous activated sludge systems, this would mean that higher biomass concentrations are desired. However, the settler - which is the limiting factor of the process - does not make this possible (Pitman, 1991; Genesis water tech, 2019). Activated sludge has a relatively poor settling characteristics. Hence, the required area for the settler in order to prevent sludge blanket overflow can become quite large (Anuar *et al.*, 2007). The resulting low biomass concentration (3-5 kg TSS.m^{-3}) in activated sludge systems leads to large treatment volumes per reactor and high energy requirements for pumping (Van Haandel & Van der Lubbe, 2007; Pronk *et al.*, 2017). Hence, the relatively low treatment capacity of the activated sludge system is an important drawback to keep in mind for new wastewater treatment technologies.

2.5 Aerobic granular sludge in batch systems

2.5.1 Introduction

The bottlenecks of the activated sludge process can partly be handled by aerobic granular sludge. Aerobic granular sludge in SBR is a relative new biotechnological process. Formation and application of aerobic granular sludge has only been reported since the late 1990s (Morgenroth et al., 1997; Beun et al., 1999; Adav et al., 2008). From then on, the aerobic granular sludge technology has experienced a big growth in the wastewater treatment field. Most of this research, and almost all implementations were done in batch reactors (Gao et al., 2011; Bengtsson et al., 2018).

In this section, the knowledge on aerobic granular sludge technology obtained in these batch systems is discussed. Firstly, establishing stable granulation in a batch reactor is explained (section 2.5.2). Subsequently, the practical implementation (section 2.5.3) and the comparison with conventional activated sludge systems (section 2.5.4) are given.

2.5.2 Stable granulation in batch systems

The formation of granules happens through cell-to-cell aggregation of microorganisms (Ivanov *et al.,* 2005; Liu *et al.*, 2005a). Generally, it occurs in four steps. First, there is random movement and collision of cells, which subsequently leads to reversible cohesion through cell surface hydrophobicity increase. Thirdly, further irreversible aggregation and growth occur and a network of connection through EPS (extracellular polymeric substances) is formed. These EPS can be proteins or polysaccharides that are formed by the microorganisms. Due to the excretion of these substances, the cell surface hydrophobicity increases. Finally, the granules are shaped into the right form by an imposed shear force (Gao *et al.*, 2011; Kent *et al.*, 2018).

The formation of granules in SBR does not happen spontaneously. The sludge in the SBR is subject to different phases in a batch system, leading to so-called feast-famine conditions (Table 2.3). During the fill phase and the first part of the react phase (degradation phase), the readily biodegradable matter (rBCOD) present in the wastewater is used. This usage of rBCOD is done by (D)PAO/(D)GAO under

anaerobic conditions during the fill phase and by OHO and PAO/GAO under aerobic conditions in the react phase. Mostly, the aerobic degradation phase is fairly short, because all of the organic matter is already taken up by PAO/GAO during the anaerobic phase. Hence, the presence of rBCOD indicates the feast period. When there is no external rBCOD left anymore, the famine period begins. During this starvation period, the PAO/GAO grow on the previously stored material. It is important to realize that although there is no rBCOD left in the wastewater, growth of the biomass could still occur during the famine period (de Kreuk & van Loosdrecht, 2004; Bathe *et al.*, 2005; Liu *et al.*, 2005a; Lübken *et al.*, 2005; Van Haandel & Van der Lubbe, 2007; Bengtsson *et al.*, 2018). The bacteria that are able to survive this famine period - and thus are able to store rBCOD as PHA - will be favorised in the reactor (Caluwé, 2018). The longer the famine period, the better the selection for PAO/GAO and the bigger the size of the granules (Gao *et al.*, 2011; Devlin & Oleszkiewicz, 2018).

Table 2.3: Schematic representation of the degradation of organic matter during the fill and react phases in a typical sequencing batch reactor (SBR) cycle. Abbreviations: rBCOD: readily biodegradable chemical oxygen demand, PHA: polyhydroxyalkanoates, (D)PAO: (denitrifying) phosphate accumulating organisms, (D)GAO: (denitrifying) glycogen accumulating organisms, OHO: ordinary heterotrophic organisms.

fill	anaerobic	storage of rBCOD as PHA by (D)PAO/(D)GAO	FEAST
react	aerobic	DEGRADATION rBCOD degraded by OHO usage PHA by PAO/GAO	
	aerobic	STARVATION usage PHA by PAO/GAO	FAMINE

The general distribution of the microorganisms in the granule depends on both these feast-famine conditions and the oxygen gradient due to diffusion limitation. Firstly, the organisms that are selected under these feast-famine conditions are slow-growing bacteria, in particular (D)PAO/(D)GAO (de Kreuk & van Loosdrecht, 2004; de Kreuk *et al.*, 2005b; McSwain *et al.*, 2005). Slow-growing organisms make sure that a stable, compact and dense granule is formed (Gao *et al.*, 2011; Bengtsson *et al.*, 2018). Due to the slow growth, the organisms can approach each other more closely. This type of growth resembles the formation of crystals (de Kreuk *et al.*, 2005b). Faster growing organisms do not have enough time to approach and thus form more floc-like structures. Hence, the resulting granule has the slowest growing organisms in the core, and the fastest growing organisms towards the surface. A second important aspect in the distribution of microorganisms in an aerobic granule is the oxygen gradient. The granules are grown aerobically, which results in a redox profile along the radius of the granule (van Loosdrecht *et al.,* 2005; Van Haandel & Van der Lubbe, 2007). This means that the granule is partially aerobic and partially non-aerobic, determining which organisms can grow in each zone of the granule (Bengtsson *et al.*, 2018). As an illustration, anaerobic organisms grow in the anaerobic core of the granule, although their actual growth rate could possibly be higher than e.g. nitrifying organisms that are more on the outside of the granule because they need oxygen (Mosquera-Corral *et al.*, 2005; van Loosdrecht *et al.*, 2005). Hence, the resulting granule has microorganisms distributed from the

outside to the inside of the granule as follows: obligated aerobic, facultative aerobic and obligated anaerobic organisms (Ivanov *et al.*, 2005).

The resulting general structure of an aerobic granule is pictured in Figure 2.3. In the aerobic zone, the aerobic heterotrophic organisms (OHO, PAO, GAO) and the autotrophic nitrifying bacteria (AOB,NOB) are present. In the anaerobic/anoxic zone - depending on the presence of NO_3^- - the denitrifying organisms (DOHO, DPAO) occur (Bengtsson *et al.*, 2018; Rollemberg *et al.*, 2018). Generally, the size of the anaerobic zone is kept sufficiently small, because anaerobic bacteria can produce acids and gasses via fermentation and thus cause floating of the granules. Since this would lead to inadequate settling, a too large anaerobic zone should be avoided (Kent *et al.*, 2018).

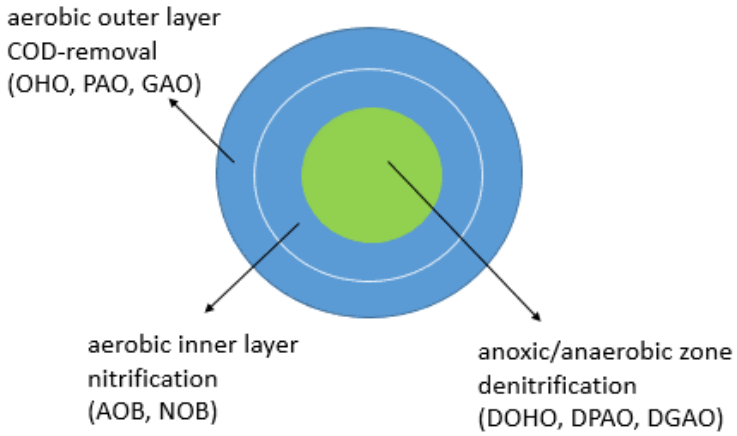

Figure 2.3: Distribution of microorganisms in an aerobic granule. Different zones are indicated, each with the corresponding main reactions occurring (Table 2.1) and the microbial groups active. Abbreviations: COD: chemical oxygen demand, (D)OHO: (denitrifying) ordinary heterotrophic organisms, (D)PAO: (denitrifying) phosphate accumulating organisms, (D)GAO: (denitrifying) glycogen accumulating organisms, AOB: ammonium oxidizing bacteria, NOB: nitrite oxidizing bacteria (based on Bengtsson *et al.*, 2018).

In the aerobic, anoxic and anaerobic zone of the granule, the different reactions described in Table 2.1 occur (Bengtsson *et al.*, 2018). This differs with activated sludge, where these reactions occurred in different tanks in continuous systems or at different points in time in SBR (Irvine *et al.*, 1989). In the aerobic outer layer, PAO/GAO grow on internal stored material, OHO aerobically degrade COD and autotrophic bacteria perform nitrification. In the anoxic inner layer, denitrification by DOHO or DPAO/DGAO occurs, whereby simultaneous nitrification and denitrification within the aerobic tank is possible. This means that the just nitrified NO_3^- diffuses to the core of the granule and is denitrified to N_2 (Li *et al.*, 2005; Gao et al., 2011).

Applying feast-famine is mostly not enough to ensure that granules are formed and long-term stabilization is achieved (Liu *et al.*, 2005a; Kent *et al.,* 2018). Extra selection pressures have to be imposed to the system because of instability due to fast growers like OHO or exposure to varying conditions (Bathe *et al.*, 2005; de Kreuk *et al.*, 2005a). The most used selection pressure is based on the settling velocity. Short settling times are imposed and under those circumstances, the particles with the highest settling velocity - i.e. the granules - are selected. In other words, the wash-out of less dense flocs and suspended solids is forced (de Kreuk *et al.*, 2005a; McSwain *et al.*, 2005; Van Haandel & Van der Lubbe, 2007). Instead of selecting on the settling time, the settling velocity can also be controlled through control of the volume exchange ratio of the SBR cycle at a fixed, relative short settling time. High ratios of 60-80% are needed for successful granulation. By imposing that a high fraction of the wastewater is discharged after each cycle, the less dense particles will be discharged

and only the best settling particles will stay in the reactor (Liu *et al.*, 2005a). As a side note can be noticed that the HRT can get low in this case. Hence, care has to be taken to ensure the effluent criteria are met. The settling velocity selection pressure is a key aspect, because when this is not controlled, aerobic granulation could fail (Liu *et al.*, 2005a).

Another option to facilitate the granulation is the shear rate selection pressure, i.e. imposing high shear rates to let the granulation occur more smoothly (de Kreuk *et al.,* 2005a*;* Van Haandel & Van der Lubbe, 2007). Shear is not a primary inducer of granulation, but can be important when also fast growing organisms (e.g. OHO) are desired in the granule. The faster organisms grow, the more shear they need to approach close enough to form a compact granule (Bathe *et al.*, 2005; Liu *et al.*, 2005a; Van Loosdrecht *et al.*, 2005; Bengtsson *et al.*, 2018). No effect of DO, substrate loading rate or substrate composition is noticed on the granulation process (Liu *et al*., 2005a; Kent *et al.*, 2018). Possible selection pressures and the optimization of these techniques still is an important research topic, especially for scale-up (Gao *et al.,* 2011).

2.5.3 Practical implementation of aerobic granular sludge in batch systems

Batch-wise operated aerobic granular sludge systems are mostly implemented in a bubble column SBR configuration (Figure 2.4(a)). The anaerobic feeding is not mixed and feeding takes place from the bottom of the tank, which means that the influent water flows through the settled bed of granules in a plug flow-like pattern (de Kreuk & van Loosdrecht, 2004; Liu *et al.,* 2005a; Pronk *et al.*, 2015). This technique enhances the feast effect as a substrate gradient develops along the height of the sludge bed, leading to better diffusion into the granules (Kent *et al.,* 2018). This better diffusion is due to the high local substrate concentrations that can occur due to plug flow in contrast to the relatively low concentration in a completely mixed reactor.

An alternate option is an airlift SBR (Figure 2.4(b)), which consists of a central column along which the water is brought up, after which it flows back down through the outer column. Influent can enter from the top and leave at the bottom of the reactor or vice versa (Liu *et al.*, 2005a; Espinosa-Ortiz *et al.,* 2016). An airlift reactor can apply higher local shear rates due to the circular flow pattern, which results in higher stability, particularly interesting in case of presence of fast growing organisms (Zhou *et al.*, 2013b). The liquid recirculation in the airlift SBR also results in better mass and heat transfer and better mixing (Onken & Weiland, 1983; Kawase & Moo-Young, 1990). A disadvantage of airlift SBRs is the more expensive design (de Kreuk & van Loosdrecht, 2004). Aeration occurs in both cases at the bottom of the reactor.

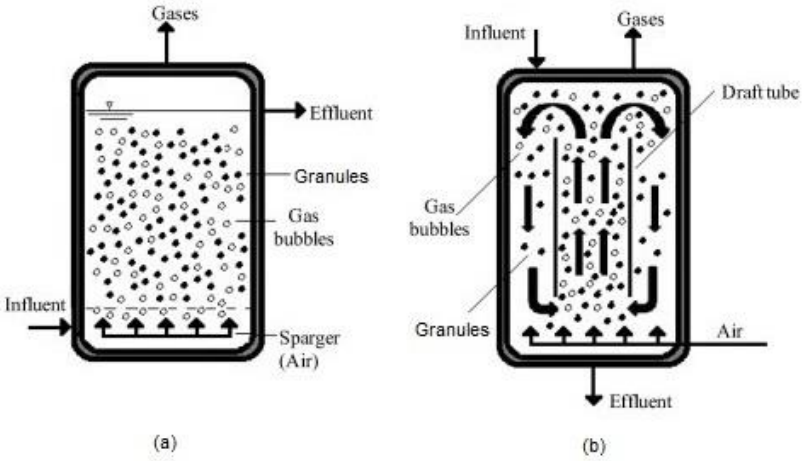

Figure 2.4: Types of sequencing batch reactor (SBR) used in combination with aerobic granular sludge to treat wastewater: (a): bubble column SBR, (b): airlift SBR (Espinosa-Ortiz *et al.,* 2016).

Most applications in practice appear under the commercial name Nereda (Royal HaskoningDHV, 2020b). This configuration uses simultaneous feeding and decanting in a configuration similar to a bubble column SBR (Figure 2.4(a)) (Pronk *et al.*, 2017). The first full scale reference of a Nereda plant in operation was in 2011 in a municipal wastewater treatment plant in Epe, The Netherlands (Van der Roest *et al.*, 2011; Royal HaskoningDHV, 2020c). Today, more than 70 plants worldwide are under construction or in operation (Royal HaskoningDHV, 2020a). In Belgium, one Nereda plant is in operation, namely in Sappi Lanaken Press Paper N.V., since 2018. The highly polluted industrial wastewater from paper pulp production is treated through consecutively pre-treatment, anaerobic treatment and a Nereda system to achieve sufficient purification (Cobelpa, n.d.; Royal HaskoningDHV, 2020b). The system can handle a peak flow of 600 $m^3.h^{-1}$ (Royal HaskoningDHV, 2020b). Nereda treatment plants have been shown to achieve similar or improved enhanced biological nutrient removal when compared to similarly loaded activated sludge systems (Pronk *et al.*, 2017).

2.5.4 Comparison with conventional activated sludge systems

Aerobic granular sludge in SBR indicates some advantages compared to the conventional continuous activated sludge process, including 25-75% less surface area needed, reduction of 20-50% energy consumption and significant lower investment (15-30% on average) and operational costs (total annual cost reduction of 7-17%) (de Bruin *et al.*, 2004; Pronk *et al*, 2017). Reasons for the reduction in treatment system footprint are the higher biomass concentrations that can be imposed and the non-use of secondary settling tanks in case of the SBR design. Additionally, 20-25% energy consumption reduction is obtained because no mixing devices are needed in separate anaerobic and anoxic tanks, neither is pumping energy for transport from and to the settler needed (Bathe *et al.*, 2005; Pronk *et al.*, 2017; Caluwé, 2018). These reductions in surface area and energy consumption result in a reduction of both the investment and operational costs. On top of that, aerobic granular sludge in a SBR configuration is a compact system that handles better complex loads (Bathe *et al.*, 2005). The latter can be explained by diffusion limitation. Furthermore, SBR with his feast-famine conditions leads to an accelerated treatment of the water. The bacteria are starved during famine periods, which means that during feast phases, they take up the organic matter and nutrients much faster. In contrast, under continuously fed conditions, there is no such pressure since the food is constantly present (Emis, 2015; Caluwé, 2018; Caluwé *et al.*, 2018).

There are however some disadvantages of aerobic granular sludge in SBR compared with the conventional activated sludge system. Batch systems require a complex planning due to the discontinuous nature of the process. Furthermore, the robustness and stability of granules is - even under the described selection pressures - uncertain. Lastly, bigger aeration equipment is needed due to the fact that the aeration per COD load is more or less the same as for activated sludge, but the biomass concentration is higher (Mahvi *et al.*, 2004; Bathe *et al.*, 2005).

Based on these observations, it can be concluded that aerobic granular sludge in SBR is a promising technology. However, the current infrastructure in Flanders consists for the biggest part of continuous plants. The question arises whether it would not be more efficient to combine the advantages of aerobic granular sludge with the existing continuous systems.

2.6 Potential of continuous aerobic granular sludge systems

Aerobic granular sludge could potentially be used in continuous systems. The reason why this might be an interesting option is explained in the first section 2.6.1. Subsequently, the challenges for stable granulation are discussed in section 2.6.2. In section 2.6.3, the current implementation status of aerobic granular sludge in continuous systems is given, followed by the comparison with aerobic granular sludge in batch systems in section 2.6.4.

2.6.1 Rationale for implementing aerobic granular sludge in continuous systems

Aerobic granular sludge in continuous systems indicates some opportunities in the wastewater treatment field. Firstly, retrofitting the existing plants with aerobic granular sludge could possibly lead to an increased hydraulic treatment capacity (Zheng *et al.*, 2006; Van Haandel & Van der Lubbe, 2007; Manea & Bumbac, 2019). The reason for this would be the higher biomass possible in the biological tank because of better settling sludge. On the other hand, aerobic granules could allow constructing more compact continuous wastewater treatment plants with smaller settlers (or other separation units), which would result in a lower cost (Jahn *et al.*, 2019). Secondly, if a new design should be chosen, continuous systems with aerobic granular sludge show advantages compared to SBRs with aerobic granular sludge. Continuous systems are easier to operate and control, have high equipment utilization rate and lower installation costs (Juang *et al.*, 2010; Zou *et al.*, 2018).

Introducing aerobic granules in continuous systems is a new endeavor in the wastewater treatment research area (Kent *et al.*, 2018). Its potential is confirmed by experimental data in the last couple of years and worldwide research on aerobic granules in continuous systems is ongoing (Juang *et al.*, 2010; Corsino *et al.*, 2016; Manea & Bumbac, 2019). Hence, it is important to realize that aerobic granular sludge in practical applications is until now only used in SBR and all of the undermentioned information is obtained with lab-scale research (Jahn *et al.*, 2019). The emphasis of most of this research concerns the formation and stabilization of granules in continuous systems. Nonetheless this is important for realization of this technology in full-scale, the actual better performance of continuous systems with aerobic granular sludge compared to conventional continuous systems with activated sludge is yet to be proven.

2.6.2 Establishing stable granulation in continuous systems

Establishing stable granulation in continuous systems is not self-evident. There are two important points of difference for granulation between continuous and batch systems, explained in the first section. Keeping these points of difference in mind, three crucial parameters for stable granulation have to be taken into account. These parameters are discussed in the second section. At present, it is still difficult to cultivate aerobic granules directly and maintain long-term stability in a conventional continuous flow reactor. Possible actions to improve this granulation are discussed in the last section.

2.6.2.1 Points of attention

A first important point of attention for granule formation and stabilization is the difference in reactor geometry between continuous flow and batch reactors (Morales *et al.*, 2012). Ideally, the existing continuous wastewater treatments plants could introduce aerobic granular sludge into their system and thus take advantage of their better settling characteristics. However, lab-scale attempts for aerobic granular sludge in continuous systems are not yet conform with the existing activated sludge continuous plants. Many different designs are being investigated, with the biggest differences on the level of the solid-liquid separation (Kent *et al*, 2018). This separation can either be done internal or external. Internal separation results in configurations that have many similarities with the SBR configuration. Continuous feeding occurs at the bottom of the reactor, together with continuous withdrawal at the top of the reactor. External separation includes continuous water influent from the biological tank, combined with continuous effluent and waste sludge, for example with a conventional settler. The geometry of continuous systems compared to SBR is particularly different in case of external separation (Kent *et al.*, 2018).

Another point of attention is the difference in operating conditions between batch and continuous systems (Morales *et al.*, 2012). Due to the completely mixed operation conditions in most continuous configurations, the substrate concentration in the reactor is everywhere and always as low as in the effluent. The lower substrate concentrations result in lower substrate gradients in the granules and thus poor diffusion (Corsino *et al.,* 2016). This is completely different from the steep substrate gradient from beginning to the end in a typical SBR cycle, together with the plug flow feeding conditions (Bengtsson *et al.*, 2018). The lower substrate diffusion in continuous systems leads to different substrate degradations kinetics, microbial activity and physical characteristics of the sludge (Liu *et al.*, 2015). These differences in geometry and operating conditions are important to keep in mind for the development of aerobic granular sludge in continuous systems (Xin *et al.*, 2017; Kent *et al.*, 2018; Zou *et al.*, 2018).

2.6.2.2 Three important parameters for stable granulation

The specific necessary conditions to ensure granule formation and long-term stabilization are well-known, namely feast/famine conditions, an additional selection pressure to ensure wash-out of flocs (e.g. settling velocity-based) and high shear rates (Morales *et al.*, 2012; Corsino *et al.*, 2016; Zou *et al.*, 2018). Specific care has to be taken - especially for the first two parameters - when designing the continuous process, because failure of these parameters can result in formation of flocs.

The first important aspect for granulation and stabilization is feast-famine conditions combined with alternating anaerobic/aerobic phases to select slow-growing biomass (Van Loosdrecht *et al.*, 2005). If no feast-famine occurs, decreasing granulation rates and poor diffusion into the granules are observed (Jahn *et al.*, 2019). There are many options to induce substrate gradients along the continuous reactor. Two aerobic reactors in series are a possible configuration: a first small reactor under feast conditions (high rBCOD concentration), followed by a large famine tank (low rBCOD concentration) (Figure 2.5(a)) (Devlin & Oleszkiewicz, 2018). The first aerobic tank is called the selector zone because it selects the mircoorganisms that are able to store organic matter (Kent *et al.*, 2018). Furthermore, it is also possible to use multiple baffled reaction chambers in series (Figure 2.5(b)). Substrate-rich influent comes in and the substrate concentrations are lower more towards the end of the reactor (Li *et al.*, 2015; Corsino *et al.*, 2016). A variation to this is a multi-pass system with step feeding, which means that influent is fed to every other pass (Kent *et al.*, 2018). A last possibility is to cycle through forward and reverse flow in a reactor and thus introduce alternating feast-famine conditions in each zone of the reactor (Figure 2.5(c)) (Li *et al.*, 2015). The feast-famine conditions have to be combined with alternating aerobic and anaerobic phases. A separate anaerobic tank like in the conventional system (Figure 2.5(a)) or alternating aerobic and anaerobic zones (Figure 2.5(b,c)) can be used (Corsino *et al.*, 2016).

Whether feast-famine conditions are really necessary for formation and stabilization of granules - especially on lab-scale - is not clear and varying opinions are mentioned in literature (Van Loosdrecht *et al.*, 2005; Rocktaschel *et al*., 2013; Kent *et al.*, 2018). It also has to be noted that it is not very clear when a configuration is defined as plug flow. After all, most continuous flow reactors have a plug flow-like pattern in practice (Kent *et al.*, 2018). The question is whether this is enough for selection of the slow growers or not. At low substrate concentrations (like in the conventional continuous systems), diffusion limitation could become important for the performance of the continuous system with aerobic granular sludge. More insight in the deterioration of the performance of this system due to low substrate concentrations is needed, because this will tell how important these feast-famine conditions really are.

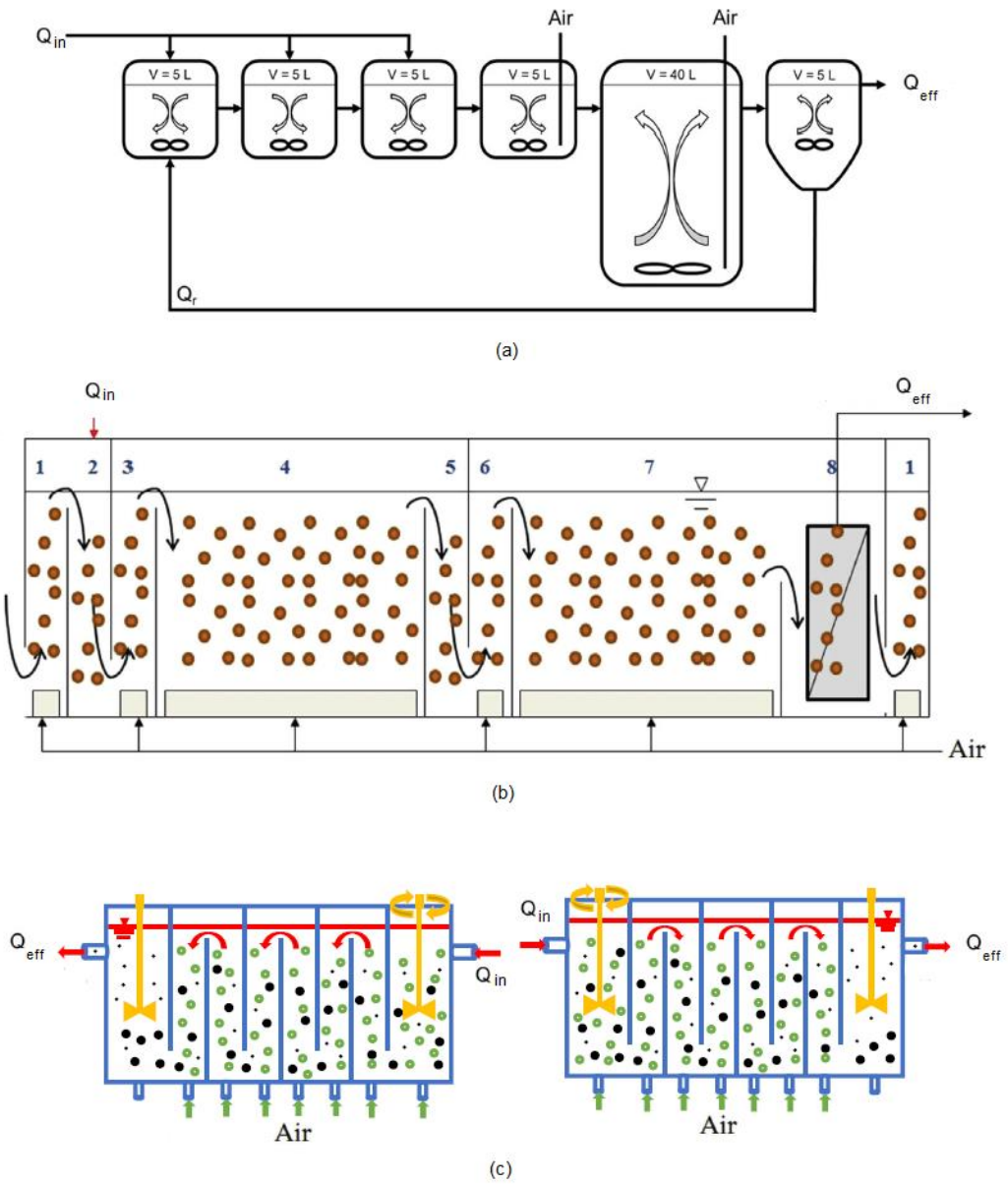

Figure 2.5: Implementing feast-famine combined with anaerobic/aerobic phases into continuous flow systems. (a): continuous flow reactor configuration with first 3 non-aerated tanks, each receiving one third of the incoming flow, followed by 2 aeration tanks: one small feast (selector) tank and one larger famine tank, with at the end a mixed clarifier (Devlin & Oleszkiewicz, 2018), (b): a multi-baffled membrane bioreactor with alternating aerobic and anaerobic zones. Important to notice is that the separation based on membranes is ideal. This means that all biomass is retained, i.e. both the granules and the flocs. No extra selection pressure is imposed in this case because a random part of retained biomass is wasted (Corsino *et al.*, 2016), (c): a multi-baffled continuous flow reactor in forward- and reverse mode, inducing alternating feast-famine conditions in each zone in the reactor. A rather strange method for aeration is used because all the zones are aerated, except the last settling zone (Kent *et al.*, 2018, based on Li *et al.*, 2015) (Q_{in}: influent flow rate [$m^3.d^{-1}$], Q_r: recycle flow rate [$m^3.d^{-1}$], Q_{eff}: effluent flow rate [$m^3.d^{-1}$]).

The second crucial parameter for formation and stabilization of aerobic granules is an appropriate extra selection pressure to ensure flocculent sludge wash-out. Two possible selection pressures can be used, namely the settling velocity selection pressure and the particle size selection pressure.

The first option - which was also the conventional method in SBR - is the settling velocity-based selection pressure. In contrast to batch systems, in continuous systems the settler is continuously fed and effluent continuously leaves (Liu *et al.*, 2014; Li *et al.*, 2016). Full-scale secondary clarifiers are typically designed with significantly long settling times to deal with these disturbances (Kent *et al.*, 2018). This aspect makes it difficult to impose short settling times according to the classical settling velocity-based selection pressure (Liu *et al.*, 2014). Hence, there is a need for a continuous system equipped with an effective mechanism for continuously separating faster settling solids from the treated water and retaining them within the system. In case of internal solid-liquid separation, the HRT is controlled (Kent *et al.*, 2018). This means that the treatment rate is controlled which can be realized in an airlift reactor (Figure 2.6(a)) (Qian *et al.*, 2017). The lower the HRT, the higher the treatment rate and the higher the selection for the heaviest particles (granules) (Kent *et al.*, 2018). The effluent quality of course still has to be ensured, so the treatment rate cannot become too high. Another technique is a three-phase separator, where baffles within the reactor are used to select the fastest settling particles (Figure 2.6(b)) (Ramos *et al.*, 2016). In systems with external separation a baffled settling tank can be used to ensure the selection pressure. An example is a two-zone settler (Figure 2.6(c)) (Zou *et al.*, 2018; Manea & Bumbac, 2019). A movable baffle can adjust the height of baffle to liquid level, thereby creating different selection pressures (Zou *et al.*, 2018). Another possibility is a mixed clarifier (Figure 2.5(a)). Mixing results in more turbulence during settling and therefore higher selective pressures for rapidly settling particles (Devlin & Oleszkiewicz, 2018). Furthermore are also inclined plate and tube settlers an option (Figure 2.6(d)). These are tilted configurations with increased surface area over which the solids may settle (Tarpagkou & Pantokratoras, 2014). These inclined settlers are compact and already being used in drinking water treatment, so they should be easy to adapt in full-scale (Kent *et al.*, 2018). Nevertheless that all these methods seem very interesting, it is important to point out that the original advantage of using the current infrastructure (i.e. conventional continuous flow systems) would be nullified if one of the abovementioned configurations is used.

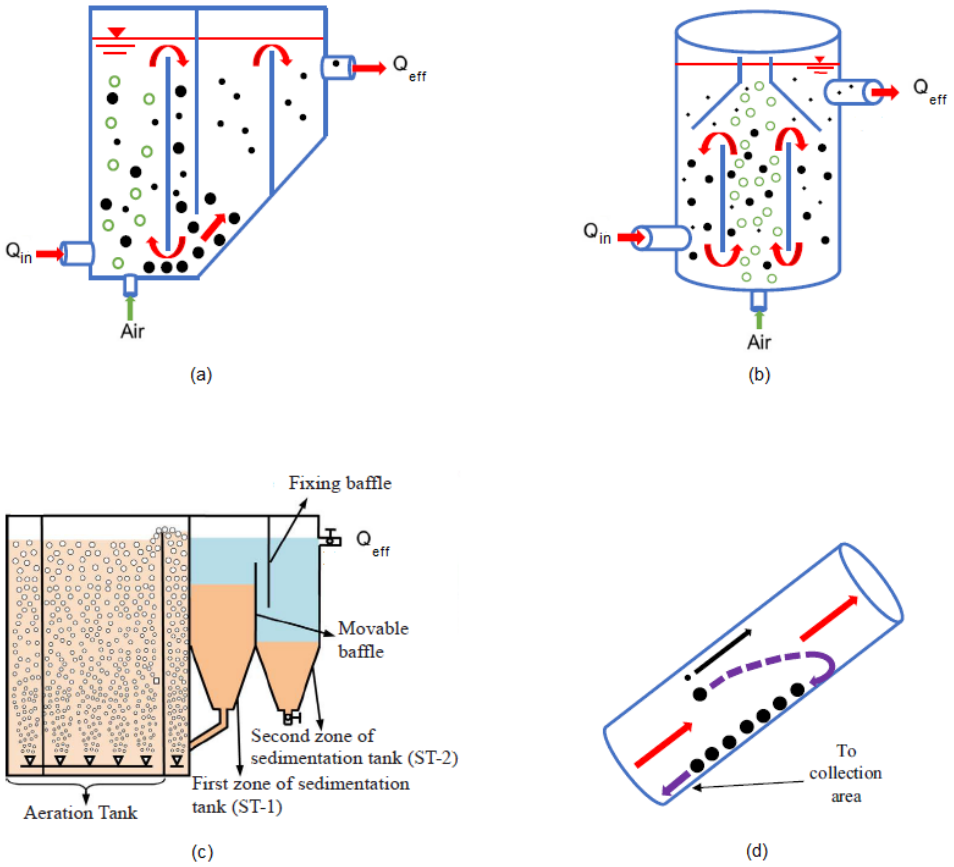

Figure 2.6: Implementing settling velocity-based selection pressure in continuous systems. (a): an airlift reactor with internal baffled settling zone (Kent *et al.*, 2018, based on Qian *et al.*, 2017), (b): an airlift reactor with an internal three-phase separator on top (Three-phase separator: the liquid flows up through the middle of the device, where liquid-gas separation occurs. The remaining liquid-solid slurry is directed towards the sides, where the solids settle out of the liquid) (Kent *et al.*, 2018, based on Ramos *et al.*, 2016), (c): airlift reactor with external two-zone settler. By decreasing the height of the movable baffle, the associated selected settling time is decreased (Zou *et al.*, 2018), (d): external inclined plate settler to be used in combination with a biological tank (Kent *et al.*, 2018) (Q_{in}: influent flow rate, Q_{eff}: effluent flow rate).

A second option that is being investigated as extra selection pressure is the particle-size selection pressure, which is based on the difference in particle size between flocs and granules (Liu *et al.*, 2014). This can be realized using a sludge selective tank, i.e. a sieve that retains particles of a selected size (Liu *et al.*, 2012). Both internal and external sieves are possible and aerators can be installed under the sieve to avoid clogging, which of course than results in higher aeration energy. The retained large granules are send back to the reactor (in case of external separation) and the small flocs pass through the sieve with the effluent (Kent *et al.*, 2018). The granulation rate can be controlled by adjusting the sieve aperture (per example range of 0.1-1.0 mm) (Liu *et al.*, 2014). The aerobic granules cultivated by particle-size selection pressure have a larger diameter, lower settling velocity and a higher specific rate of nitrification, denitrification and phosphorus removal compared to the ones obtained with settling velocity-based selection pressure (Liu *et al.*, 2014). Advantages of particle-size selection pressure are the fact that these reactors are easy to operate, convenient for large-scale application and better COD removal. The latter is due to better removal of dead or collapsed granules that settle well and thus would be maintained with the settling velocity-based selection pressure. A disadvantage is the fact

that poor-settling, large biomass (not granule-like) remains in the reactor, which can result in higher SVI (Liu *et al.*, 2014). Working with sieves could also cause drawbacks including clogging and thus high maintenance. A last option that combines the settling and particle size selection pressure is a hydrocyclone (Ford *et al.*, 2016). Vortexing is used to separate the biomass based on both the density and the size of the particles. This also decreases the required size for the clarifiers (Kent *et al.*, 2018).

The last parameter influencing granulation and stabilization of granules in continuous systems is high shear rate. High shear rates are especially important if fast-growing organisms are present in the system (Van Loosdrecht *et al.*, 2005). Shear depends on the flow patterns in a reactor. High shear rates in an internal separation system are provided with an airlift reactor (Figure 2.6(a,b)) due to the cyclic movement (Zhou *et al.*, 2013b). This is also the most interesting way to inhibit damage to the sludge, since no return sludge equipment is needed. In the case of the conventional external separation system, the shear is provided in the biological reactor by the mixing devices in the anaerobic and anoxic tanks (Xin *et al.*, 2017). To avoid damage to the granules, the best option for the return sludge equipment are peristaltic pumps (Kent *et al.*, 2018).

2.6.2.3 Additional actions to speed up granulation in continuous systems

Since granular sludge in continuous systems usually has poor stability or high probability of sludge bulking, some additional measures can be taken (Xin *et al.*, 2017). Stimulating granule formation can be done in various ways. This is especially important in case of continuous systems because of the higher competition between flocs and granules. Flocs can handle better the low substrate concentrations since they have a higher specific surface area and thus a higher specific substrate utilization rate (Liu *et al.*, 2015; Kent *et al.*, 2018). First of all, the addition of pre-grown microbial cultures is used in practice to speed up aerobic granule formation or improving its stability (Kent *et al.*, 2018). Secondly, pre-grown granules cultivated in SBR can be inoculated into the continuous system (Devlin & Oleszkiewicz, 2018; Manea & Bumbac, 2019). This is a widely used and efficient method. Chen *et al.* (2016) has concluded that better stability can be obtained by growing the granules in SBR under similar conditions as the continuous conditions that it will be inoculated in. It has to be pointed out that even if stable granules are inoculated into a continuous system, the stability of the granules still has to be maintained (Corsino *et al.*, 2016; Zou *et al.*, 2018). A third possible strategy is adding micropowder made of excess sludge to the system. The micropowder acts as a nucleus upon which bacterial attachment is possible (Zou *et al.*, 2018). Finally, in a similar manner Ca^{2+} ions can be added to the system. The Ca^{2+} ions help in the fast formation of granules by adsorbing onto the negatively charged surface of bacteria. By doing this, the electrostatic repulsion when sludge approaches is reduced and better and faster aggregation occurs (Zhou *et al.*, 2013a; Xin *et al.*, 2017). Not only does this improve the granulation, but also the long-term stability because a more compact granule with high physical stability, increased density and higher settling ability is formed (lower SVI) (Liu *et al.*, 2015; Xin *et al.*, 2017). However, excessive metal precipitation is harmful in terms of microbial activity and substrate degradation. The metals in the granule would inhibit the diffusion of substrates into the granule even more (Liu *et al.*, 2015).

2.6.3 Implementation status of continuous aerobic granular sludge systems

Currently, researches are primary investigating continuous systems on lab-scale, but already some small steps are being made to practical application possibilities. Many different design possibilities have already been tried in the lab, most of them being sufficiently complicated (like a three phase separator, internal sieves, etc). These designs are too complex to be implemented in practice in full-scale operation (Liu *et al.*, 2015). It also has to be taken into account that the time required for granulation - even after inoculation - will be longer in full-scale plants than observed in a laboratory setting (Kent *et al.*, 2018). EssDe, a Swiss company, has developed a process called S::Select, where a mixture of flocs and granules is used for continuous wastewater treatment. This technique appears to be already implemented in the wastewater treatment plant in Glarnerland, where significant higher loads (doubled or tripled) can be treated without deterioration of the effluent quality (EssDe, n.d. a). In order to prevent the overgrow of fast-growing heterotrophic bacteria compared to the slower growing organisms, the granules are regularly being shaved in a specially designed hydrocyclone (EssDe, n.d. b).

Regardless of the fact that continuous aerobic granular sludge technology is promising , it still needs further research before it can be put into practice. Feast-famine conditions, extent of granulation and selection pressure mechanisms are some of the hot topics in research right now (Corsino *et al.*, 2016; Kent *et al.*, 2018). On top of that, it is not sure that some methods regardless of the fact that they work on lab-scale, also will work in full-scale. Only hydrocyclones have already been researched in full-scale, and optimization is also still needed (Kent *et al.*, 2018). More insight in the needed conditions to ensure a good working system with a high treatment capacity, good effluent quality and acceptable energy consumption should be obtained. More knowledge will also help in further verifying long-term stability. Up until now, the reported stability varies greatly. The longest projects so far were in operation for around one year. However, the biggest lack in information on aerobic granular sludge in continuous systems concerns the performance of this system. Would introducing aerobic granular sludge in continuous systems actually benefit the process compared to activated sludge? If so, is it possible to quantify these improvements? Getting to know the answers to these questions first and foremost seems the smartest technique, because in case of bad performance, all of the other efforts would not be necessary.

2.6.4 Comparison with aerobic granular sludge in batch systems

Although the properties of granules developed and maintained under continuous conditions are similar to the ones in SBR, an important difference can be noticed (Kent *et al.*, 2018). Granules in continuous systems have a smaller diameter as a result of the lower substrate concentration in the reactors (Jahn *et al.*, 2019). Another possible reason for this smaller granules is the higher shear in continuous systems because of stirring in the anaerobic and anoxic tanks. Granule sizes in continuous systems are around 0.2 mm (Jahn *et al*, 2019). Based on the previously mentioned definition of aerobic granules, this diameter just fits within the determined range (0.2-5 mm) (de Kreuk *et al.*, 2007; Rollemberg *et al.*, 2018). The smaller diameter prevents the formation of a sufficiently large anoxic core in which denitrifiers can occur (Liu *et al.*, 2012; Corsino *et al.*, 2016). It should be noted that an extra anoxic zone is needed in continuous systems to efficiently remove nitrogen.

In Table 2.4, an evaluation of aerobic granular sludge technology of both batch and continuous systems is made. The advantages of aerobic granules make this technique a very promising technology in wastewater treatment. Whether this technology should be implemented in batch or continuous systems is a more difficult question. Batch systems are up until now most investigated and thus better described. They currently have a higher possibility of a good working process with stable granules (Morales *et al.*, 2012; Zou *et al.*, 2018; Manea & Bumbac, 2019). However, the advantages and opportunities that continuous processes can deliver should not be neglected. Further research will clarify whether continuous operating conditions can ensure stable granules that treat the wastewater at high treatment capacity.

Table 2.4: Evaluation of aerobic granular sludge technology and comparison between batch and continuous configurations (Irvine *et al.*, 1989; Schwarzenbeck & Wilderer, 2005; Tay *et al.*, 2005; Mahvi, 2008; Pronk *et al.*, 2017; Caluwé, 2018; Kent *et al.*, 2018; Zou *et al.*, 2018)

	Aerobic granules	
advantages	high settling velocity → higher biomass concentration surface area reduction or higher volumetric loading rate ability to withstand higher concentrations of toxic compounds	
disadvantages	diffusion limitation uncertain long-term stability of granules	
configuration	**Batch**	**Continuous**
differences	time-oriented 1 tank with planned cycle variable volume	space-oriented flow between different tanks constant volume
advantages	small footprint flexibility well described process	majority of current infrastructure low maintenance and sophistication
disadvantages	complex planning	further research needed

2.7 Conclusions and research objectives

The conventional wastewater treatment with activated sludge is a well working process, but has a high footprint and consumes a lot of energy (Van Haandel & Van der Lubbe, 2007; Pronk *et al.*, 2017). Due an increasingly high standard of living and an increasing amount of households connected to a sewage system (84% of the population in 2018 vs. 48% in 2000) (Vlaamse milieumaatschappij, 2019a), a higher treatment capacity is needed in Flanders. However, because of the poor settling ability of the activated sludge flocs, space consuming settlers would be required forming the bottleneck for scale-up of the conventional wastewater treatment plants. Given the limited space in Flanders and the high cost of these installations, other options should be investigated.

Last couple of years, a new process is available where bacteria, purifying the water, are grown in good settling aerobic granules. This aerobic granular sludge is primary used in batch reactors, resulting in strong reduction of surface area, energy consumption and operational costs which had led to worldwide already more than 70 full-scale batch plants in operation (Royal HaskoningDHV, 2020a).

The current shortcomings in continuous activated sludge plants and the advantages of aerobic granular sludge could be combined to an interesting opportunity. Refurbishment of the current continuous activated sludge plants into continuous aerobic granular sludge plants could presumably increase the treatment capacity because of the better settling velocity of granules and thus the higher biomass concentration in the biological reactor. However, since the proven applications of aerobic granular sludge are all batch configurations, it should first be investigated whether the operating conditions of the existing continuous activated sludge system, i.e. the conventional continuous design with low substrate concentrations and associated control strategies (e.g. oxygen control), could be combined with aerobic granular sludge into a good performing system. The replacement of activated sludge with aerobic granular sludge in continuous wastewater treatment is not straightforward and forms the topic of this thesis.

There will obviously be some challenges to ensure formation and stabilization of granules into continuous systems. Since these challenges seem to be the only topic of research on aerobic granular sludge in continuous systems, this is not the focus of this thesis. Assuming that it would be possible to cultivate stable granules in continuous systems and that long-term stability of the granules is achieved, the following research question was answered:

"Would continuous aerobic granular sludge plants have a higher treatment capacity and/or lower energy consumption compared to the conventional activated sludge plants with the same design and effluent criteria?".

3. Materials and methods

This chapter describes the mathematical model that was used to compare activated sludge with aerobic granular sludge in a continuous flow reactor. The goal was to investigate the differences between both cases in maximal treatment capacity and energy consumption in order to reach the effluent criteria. The mathematical model was implemented in Matlab-Simulink as described by Flores-Alsina *et al.* (2015). The reference model describing a continuous system with a secondary settler is presented in the first section 3.1. Subsequently, the optimization of the reference model to the actual activated sludge model is given in section 3.2. Then, this activated sludge model was modified to a continuous aerobic granular sludge model, which is described in section 3.3. Lastly, a description of the simulation procedure is given in section 3.4.

3.1 Reference model

3.1.1 Reactor design and operating conditions

A continuous activated sludge wastewater treatment plant was modelled in Matlab-Simulink as described by Flores-Alsina *et al.* (2015), but without the primary clarifier and sludge processing units (Figure 3.1). This model was based on the Benchmark Simulations Model No. 1 (BSM1) as presented by Alex *et al.* (2008b) and Gernaey *et al.* (2014). Design parameters and sludge characteristics were identical to Solon *et al.* (2017) (Table 3.1).

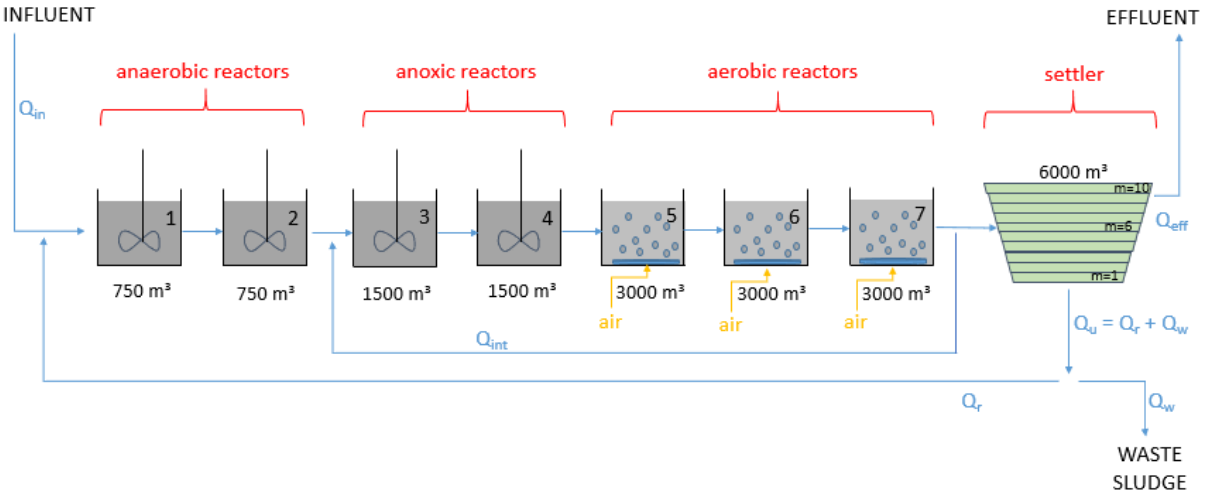

Figure 3.1: Reference design of the modelled continuous wastewater treatment system implemented in Matlab-Simulink: two anaerobic bioreactors (1 and 2), two anoxic bioreactors (3 and 4) and three aerobic bioreactors (5, 6 and 7), followed by a 10-layered settler (different layers indicated as 'm'). The blue arrows represent the mixed liquor flows. The settler separates the wastewater in the effluent and the underflow. Part of this underflow is wasted as waste sludge. The influent composition is constant (BSM2 influent data; Table A.1). Q_{in}: influent flow rate [$m^3.d^{-1}$], Q_{eff}: effluent flow rate [$m^3.d^{-1}$], Q_u: underflow rate [$m^3.d^{-1}$], Q_r: recycle sludge flow rate [$m^3.d^{-1}$], Q_w: waste sludge flow rate [$m^3.d^{-1}$], Q_{int}: internal recycle flow rate [$m^3.d^{-1}$].

Table 3.1: Reference design parameters and sludge characteristics of the BSM1 and/or BSM2 model used to describe a continuous activated sludge system. The BSM1 data is given by Alex *et al.*(2008a) and the BSM2 data by Alex *et al.* (2008b). The combination of data is as described by Solon *et al.* (2017).

Symbol	Definition	Value	Unit	Based on
Q_w	Waste sludge flow rate	300	$m^3.d^{-1}$	BSM2
Q_r	Recycle sludge flow rate	18 446	$m^3.d^{-1}$	BSM1
Q_{int}	Internal recycle flow rate	55 338	$m^3.d^{-1}$	BSM1
V_{1-2}	Volume of bioreactor 1 and 2	750	m^3	BSM2
V_{3-4}	Volume of bioreactor 3 and 4	1500	m^3	BSM2
V_{5-7}	Volume of bioreactor 5,6 and 7	3000	m^3	BSM2
V_{set}	Volume of the settler	6000	m^3	BSM1/2
A_{set}	Surface area of the settler	1500	m^2	BSM1/2
h_{set}	Height of the settler	4	m	BSM1/2
$K_La1\text{-}4$	Oxygen transfer coefficient of bioreactors 1-4	0	d^{-1}	BSM2
$K_La5\text{-}6$	Oxygen transfer coefficient of bioreactors 5-6	120	d^{-1}	BSM2
K_La7	Oxygen transfer coefficient of bioreactor 7	60	d^{-1}	BSM2
v_0'	Maximum settling velocity	250	$m.d^{-1}$	BSM1/2
v_0	Maximum Vesilind settling velocity	474	$m.d^{-1}$	BSM1/2
r_h	Hindered zone settling parameter	0.000576	$m^3.(g\ TSS)^{-1}$	BSM1/2
r_p	Flocculant zone settling parameter	0.00286	$m^3.(g\ TSS)^{-1}$	BSM1/2
f_{ns}	Non-settleable fraction	0.00228	-	BSM1/2

The composition of the mixed liquor flows (indicated by the blue arrows in Figure 3.1) flowing through the system was simulated over time. The mixed liquor entered the plant with the influent, which had a constant composition (constant BSM2 influent data from Alex *et al.* (2008b); Table A.1). The water then flowed through seven perfectly mixed bioreactors (i.e. the concentration was the same in the bioreactor and their respective effluent), followed by a settler. An internal recycle flow rate Q_{int} [$m^3.d^{-1}$] and underflow recycle flow rate Q_r [$m^3.d^{-1}$] were present. Clean effluent leaved the system with Q_{eff} [$m^3.d^{-1}$] and waste sludge with Q_w [$m^3.d^{-1}$]. The temperature was kept constant throughout the whole system at 14.86 °C (BSM2 constant influent data).

3.1.2 Settler: 10-layered tank

The secondary settler was modelled as a 10-layered tank based on Takacs *et al.* (1991) (Figure 3.1). No biological reactions occurred in this settler. The distribution of sludge in the settler was modelled, i.e. higher sludge concentrations occurred more towards the bottom of the settler. The settling velocity v_s [$m.d^{-1}$] of the particles in each layer *i* was calculated by Eq. 3.1 using the settling parameters as given in Table 3.1 (Takacs *et al.*, 1991; Alex *et al.*, 2008b). The minimum of the maximum settling velocity v_0' [$m.d^{-1}$] and the expression based on the maximum Vesilind settling velocity v_0 [$m.d^{-1}$] was taken (Eq. 3.1).

$$v_s(i) = \min\left(v_0', v_0\left(e^{-r_h(X_{sc}(i)-f_{ns}X_{TSS,in})} - e^{-r_p(X_{sc}(i)-f_{ns}X_{TSS,in})}\right)\right)\ (v_s > 0)\ [m.d^{-1}] \qquad \textbf{Eq. 3.1}$$

with $X_{sc}(i)$ = TSS concentration in layer *i* [$g\ TSS.m^{-3}$]

$X_{TSS,in}$ = TSS concentration in influent of settler [$g\ TSS.m^{-3}$]

other parameters: see Table 3.1

3.1.3 Biological conversions: ASM2d

The Activated Sludge Model No. 2d (ASM2d) developed by Henze *et al.* (2000), including some corrections by Hauduc *et al.* (2010) was used to simulate the biological removal of organic matter, nitrogen and phosphorus (more details in Appendix A.2 to A.6). Table 3.2 lists the model state variables. These variables were used to describe the biological reactions occurring in the system performed by the ordinary heterotrophic organisms X_{OHO} [g COD.m^{-3}], the phosphorus accumulating bacteria X_{PAO} [g COD.m^{-3}] and the autotrophic nitrifying organisms X_{ANO} [g COD.m^{-3}]. X_{OHO} and X_{PAO} perform COD removal and denitrification, while X_{ANO} carry out nitrification and X_{PAO} additionally perform P removal. The stoichiometric and kinetic parameters at 14.86 °C (Tables A.2 and A.3), the process rates (Table A.4), the complete stoichiometric ASM2d matrix (Table A.5) and a short explanation on the simulation of the state variables (Appendix A.6) is added in the Appendix.

Table 3.2: State variables of the model, their respective definition and unit (Henze *et al.*, 2000). 'S' stands for soluble variables, while 'X' represents particulates. The notation is based on Corominas *et al.* (2010).

State variable	Definition	Unit
S_{O_2}	Dissolved oxygen	g O_2.m^{-3}
S_F	Fermentable organic matter	g COD.m^{-3}
S_{VFA}	Fermentation products (considered to be acetate)	g COD.m^{-3}
S_U	Soluble undegradable organics	g COD.m^{-3}
S_{NH_x}	Ammonium plus ammonia nitrogen: NH_4^+-N and NH_3-N	g N.m^{-3}
S_{N_2}	Dissolved nitrogen gas N_2	g N.m^{-3}
S_{No_x}	Nitrate plus nitrite nitrogen: NO_3^--N and NO_2^--N	g N.m^{-3}
S_{PO_4}	Soluble inorganic phosphorus	g P.m^{-3}
S_{Alk}	Alkalinity of the wastewater	(mole HCO_3^-).m^{-3}
X_U	Particulate undegradable organics	g COD.m^{-3}
XC_B	Slowly biodegradable substrates	g COD.m^{-3}
X_{OHO}	Ordinary heterotrophic organisms	g COD.m^{-3}
X_{PAO}	Phosphorus accumulating organisms	g COD.m^{-3}
$X_{PAO,PP}$	Stored polyphosphates in PAOs	g P.m^{-3}
$X_{PAO,Stor}$	Cell internal storage product of PAOs	g COD.m^{-3}
X_{ANO}	Autotrophic nitrifying organisms	g COD.m^{-3}
X_{TSS}	Total suspended solids	g TSS.m^{-3}
X_{MeOH}	Metal-hydroxides	g $Fe(OH)_3$.m^{-3}
X_{MeP}	Metal-phosphates: $MePO_4$	g $FePO_4$.m^{-3}

3.1.4 Optimal recycle ratios

To make a fair comparison between simulations with different influent flow rates Q_{in}, the recycle flows, i.e. the underflow recycle flow rate Q_r and the internal recycle flow rate Q_{int} were adapted to the imposed influent flow rate. A fixed underflow ratio of Q_r:Q_{in} = 1.5 was chosen, as often applied in practice to prevent denitrification in the settler (Vrecko *et al.*, 2006; Henze *et al.*, 2008). The internal recycle ratio Q_{int}:Q_{in} was fixed at 4.9, as this value maximizes denitrification under the reference conditions by balancing the nitrate flow rate to the anoxic tanks with the denitrification capacity (calculation according to the method by Henze et al. (2008) in Appendix A.7).

3.1.5 Oxygen control

An oxygen controller was added to automatically adapt the aeration to different simulated influent flow rates. For this, a PI (proportional-integral) controller with a set-point of 2 g $O_2.m^{-3}$ was used to manipulate the oxygen transfer coefficient in reactor 6, KLa6 [d^{-1}] (Figure 3.2), as described by Gernaey *et al.* (2014) (Table 3.3). The manipulated variable KLa6 [d^{-1}] was bounded between 0 and 360 d^{-1} (Gernaey *et al.*, 2014). The oxygen transfer coefficient in reactor 5, KLa5 [d^{-1}] was set equal to KLa6 and reactor 7 was operated with a KLa7 [d^{-1}] half as high, to avoid too much oxygen recycle to the anoxic tanks (Nopens *et al.*, 2010).

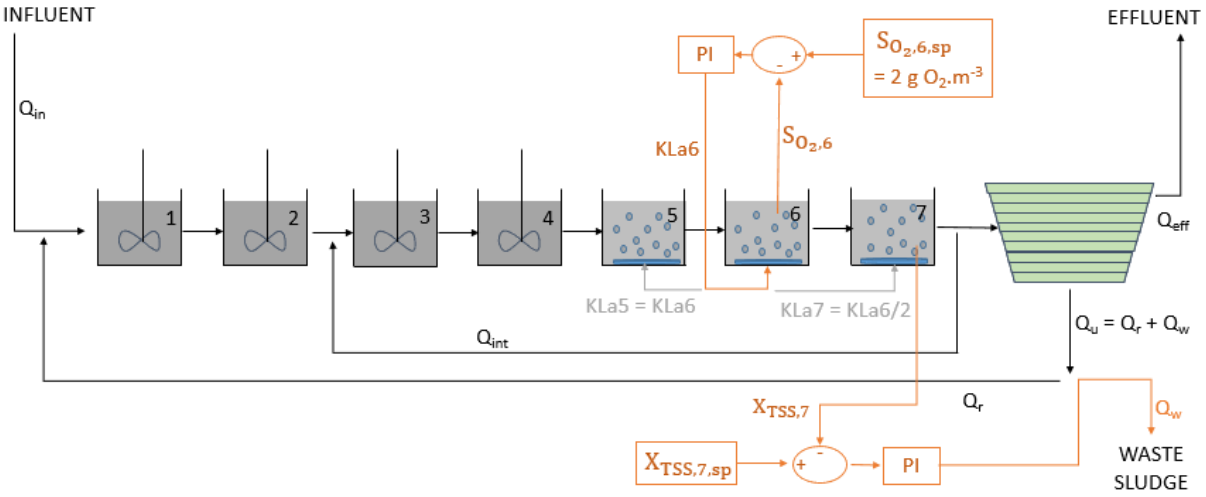

Figure 3.2: Schematic representation of the implemented control mechanisms in the continuous system. Q_{in}: influent flow rate [$m^3.d^{-1}$], Q_{eff}: effluent flow rate [$m^3.d^{-1}$], Q_u: underflow rate [$m^3.d^{-1}$], Q_r: recycle sludge flow rate [$m^3.d^{-1}$], Q_w: waste sludge flow rate [$m^3.d^{-1}$], Q_{int}: internal recycle flow rate [$m^3.d^{-1}$], KLa*i*: oxygen transfer coefficient of bioreactor *i* [d^{-1}], $S_{O2,6}$: oxygen concentration in bioreactor 6 [g $O_2.m^{-3}$], $X_{TSS,7}$: TSS concentration in bioreactor 7 [g TSS.m^{-3}], $S_{O2,6,sp}$: oxygen concentration set-point in bioreactor 6 [g $O_2.m^{-3}$], $X_{TSS,7,sp}$: TSS concentration set-point in bioreactor 7 [g TSS.m^{-3}].

Table 3.3: Parameter values of implemented PI controllers. The oxygen concentration S_{O_2} [g $O_2.m^{-3}$] in bioreactor 6 was controlled with manipulated variable KLa6 [d^{-1}] (Gernaey *et al.*, 2014). TSS control regulated the TSS concentration in bioreactor 7 with manipulated variable Q_w [$m^3.d^{-1}$] (Solon *et al.*, 2017).

Oxygen controller			TSS controller		
Parameter	**Value**	**Unit**	**Parameter**	**Value**	**Unit**
K_p	25	$m^3.(g\ O_2)^{-1}.d^{-1}$	K_p	-0.5	$m^6.(g\ TSS)^{-1}.d^{-1}$
T_i	0.002	d	T_i	7	d
$S_{O_2,6}$	2	g $O_2.m^{-3}$	$X_{TSS,7,sp}$	2-8	kg TSS.m^{-3}
$KLa6_{min}$	0	d^{-1}	$Q_{w,min}$	0	$m^3.d^{-1}$
$KLa6_{max}$	360	d^{-1}	$Q_{w,max}$	8584.1	$m^3.d^{-1}$

The model as described in this section 3.1 (Figure 3.1, operating conditions Table 3.1), adapted with fixed recycle ratios and oxygen controller will be referred to as the reference model in the continuation of this thesis.

3.2 Activated sludge model

The reference model (section 3.1) was optimized with a TSS controller to investigate the maximal treatment capacity of the continuous activated sludge system. TSS or SRT control is present in almost all full-scale applications because it ensures that the sludge is not washed out and the biological reactions can take place (Henze *et al.*, 2008). This optimized model will be further referred to as the activated sludge model.

The TSS controller was implemented into the continuous system as a PI controller mechanism that regulated the measured TSS concentration in bioreactor 7, $X_{TSS,7}$ [g TSS.m^{-3}], to the installed set-point $X_{TSS,7,sp}$ [g TSS.m^{-3}] (Figure 3.2, Table 3.3) (Solon *et al.*, 2017). The manipulated variable is the waste flow rate Q_w [m³.d^{-1}]. The values for this Q_w were bounded by the pump capacity between 0 and 8584.1 m³.d^{-1}. The latter value is equal to 0.1*$Q_{in,max}$ (as stated in BSM reports (Alex *et al.*, 2008b)) with $Q_{in,max}$ [m³.d^{-1}] the maximal flow rate of the dynamic BSM2 influent data (85 841 m³.d^{-1}) (Solon *et al.*, 2017).

3.3 Aerobic granular sludge model

The activated sludge model (section 3.2) was adapted to an aerobic granular sludge model by simulating both the effect of better settleability (section 3.3.1) and diffusion limitation (section 3.3.2).

3.3.1 Better settling sludge

The settling parameters v_0 [m.d^{-1}] and v_0' [m.d^{-1}] were increased by a factor 5 in Eq. 3.1 to represent the better settling of aerobic granular sludge (Table 3.4). Since v_0 and v_0' increase linearly with v_s [m.d^{-1}] (Eq. 3.1), the factor 5 resulted from the choice to increase the settling velocity v_s [m.d^{-1}] with a factor 5. This factor is an average value derived from literature based on two findings. On the one hand, based on formulas describing the relation between the SVI of sludge and the settling parameters v_0 and r_h [m³.(g TSS)$^{-1}$], an average factor 2 to 3 was found (Bye & Dold, 1999; Zheng *et al.*, 2006; Henze *et al.*, 2008). On the other hand, when comparing the (very divergent) reported settling velocities of aerobic granular sludge to those of activated sludge, an average factor 6 was found (Morgenroth *et al.*, 1997; Etterer & Wilderer, 2001; Wang *et al.*, 2004; Hu *et al.*, 2005; Liu *et al.*, 2005b; Anuar *et al.*, 2007; Adav *et al.*, 2008; Ni *et al.*, 2009; Thanh *et al.*, 2009; Winkler *et al.*, 2011, 2012, 2013; Kent *et al.*, 2018; Rollemberg *et al.*, 2018). Since settling velocities are widely reported and sometimes even much higher factors were found, it was tended to choose a relatively high factor 5.

Table 3.4: Adapted settling parameters (Eq. 3.1) to represent the effect of better settling in the aerobic granular sludge model.

Symbol	Settling parameter	Value	Unit
v_0'	Maximum settling velocity	1250	m.d^{-1}
v_0	Maximum Vesilind settling velocity	2370	m.d^{-1}

3.3.2 Diffusion limitation

The second aspect of aerobic granular sludge, diffusion limitation, was modelled using so-called apparent kinetics (Baeten *et al.*, 2018). Due to the compact granular structure, oxygen and other nutrients can only limited diffuse to the core of the granule, resulting in limiting biological degradation reactions. The process rates of the ASM2d model (Table A.4) are composed of typical Monod kinetics, based on half saturation coefficients K_s [$g.m^{-3}$] (Eq. 3.2). This K_s is the substrate concentration at which the process rate μ [d^{-1}] is half of the maximal value μ_{max} [d^{-1}]. Instead of describing the different process rates that occur along the radius of the granule (1D modelling), the total process rates are decreased (0D modelling) by increasing the half saturation coefficient K_s (Eq. 3.2). Since the grade of diffusion limitation in granules in continuous systems is hard to predict because it is dependent of the substrate concentration and density of the granules, two scenarios were elaborated. As a strong diffusion limitation scenario, it was chosen to increase the K_s parameters with a factor 5 (Baeten *et al.*, 2018). This was done for the K_s parameters regarding reactions where NH_4^+ or COD are the final electron donor, NO_3^- or O_2 the final electron acceptor and where PO_4^{3-} is stored as PP (Appendix A.8). Secondly, as a more moderate diffusion limitation scenario, the exact values as given by Baeten *et al.* (2018) were used (Appendix A.8). This moderate diffusion limitation scenario did not take into account the effect of competition between microbial groups on diffusion limitation. It was also considered as a second scenario because of the uncertainty on the effect of granule radius or influent composition on the grade of diffusion limitation. It is important to notice that these values by Baeten *et al.* (2018) were obtained based on a batch model and thus might not be representative for a continuous system.

$$\mu = \mu_{max} \frac{S}{K_S + S} \qquad [d^{-1}] \qquad \textbf{Eq. 3.2}$$

with μ = specific process rate [d^{-1}]

μ_{max} = maximal specific process rate [d^{-1}]

S = substrate concentration [$g.m^{-3}$]

K_S = half-saturation coefficient [$g.m^{-3}$]

3.4 Simulation procedure

3.4.1 Reference model validation

The mass balance of COD, N and P was made based on a steady state simulation to validate the reference model. Steady state of the model is obtained when biomass concentrations in the reactor and effluent concentration do not change anymore over time using a constant influent composition and flow rate (Table A.1). The elaboration of this equation in terms of COD, N and P, together with some extra explanation is given in Appendix A.9.

3.4.2 Effect of different influent flow rates on system performance

The simulation procedure as summarized in Figure 3.3 was carried out several times, completely based on steady state simulations. Firstly the procedure was used for the reference model (section 3.1) to get a first impression of the general trends and shortcomings of the model. The BSM2 constant influent data (Table A.1) was used, only with different influent flow rates Q_{in} [$m^3.d^{-1}$] for each steady state simulation according to Table 3.5. Six values for Q_{in} were chosen between the minimal (5146 $m^3.d^{-1}$) and the maximal (85 841 $m^3.d^{-1}$) flow rate found in the dynamic influent data set of BSM2 (Solon *et al.*, 2017). Later on, the same procedure was followed for the activated sludge model (section 3.2), for the activated sludge model with separately better settling sludge (section 3.3.1) and diffusion limitation (section 3.3.2) and for the aerobic granular sludge model (section 3.3.1 + 3.3.2). The separate effects of better settling sludge and diffusion limitation were simulated to investigate whether both effects are equally as important or that one effect is more important than the other. In these cases, the values for Q_{in} were step-by-step increased in order to find the exact point of failure of the system.

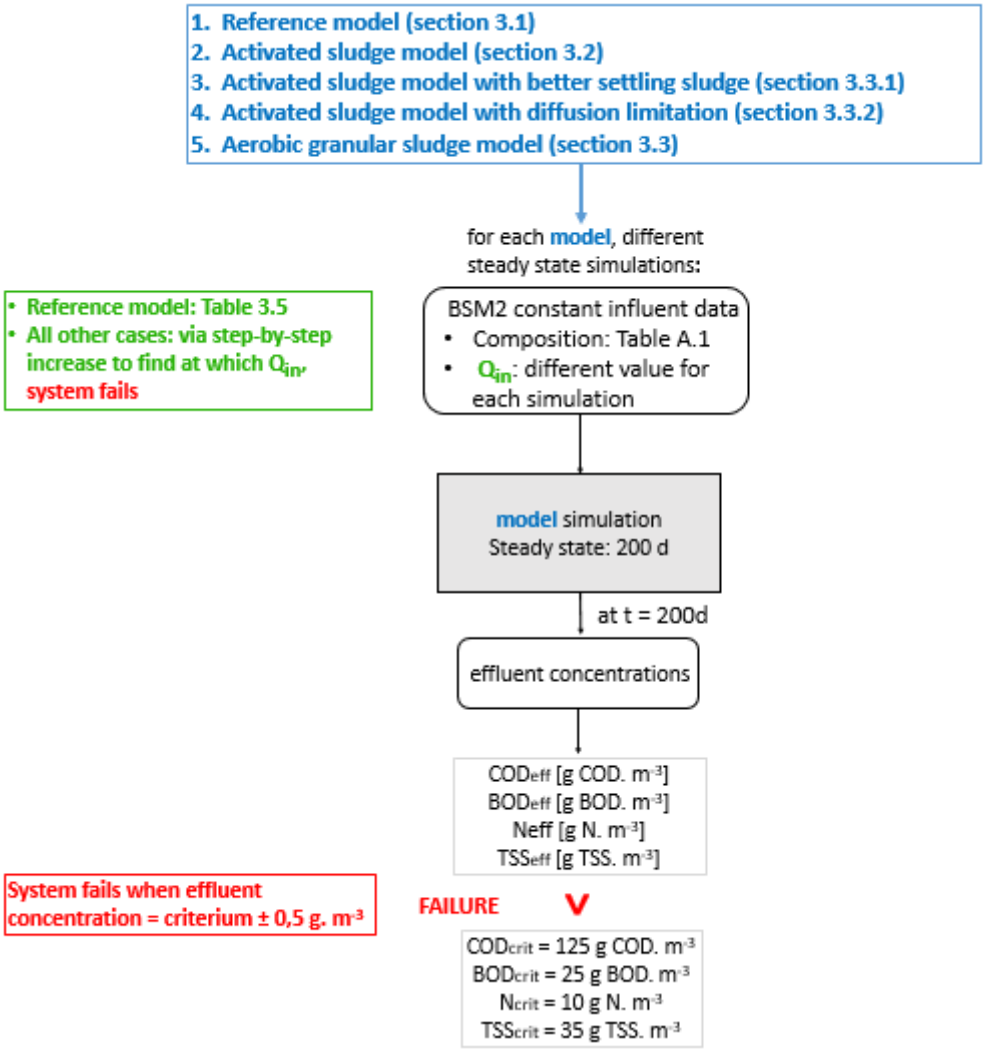

Figure 3.3: Flowchart of the steady state simulation procedure carried out on the models of the different continuous systems. Effluent criteria were based on Council of European Communities (1991).

Table 3.5: Steady state simulations of the reference model. BSM2 influent data of Table A.1 is used with varying Q_{in} [$m^3.d^{-1}$] according to this table. Associated COD and N load [$g.d^{-1}.m^{-3}$] are also given. Point 4 (20 648 $m^3.d^{-1}$) is the original value of the BSM2 data (Table A.1).

Simulation	Q_{in} [$m^3.d^{-1}$]	COD load [$g\ COD.d^{-1}.m^{-3}$]	N load [$g\ N.d^{-1}.m^{-3}$]
1	5146	225.87	18.60
2	11 796	517.74	42.62
3	18 446	809.61	66.65
4	20 648	906.28	74.61
5	34 106	1496.95	123.24
6	85 841	3767.65	310.19

Some assumptions were made in order to define the failure of the system. First of all, the primary focus of this thesis was determined to be COD, TSS and N removal. The behavior of PAO is not easy to predict and actions taken to optimize biological P removal like aeration strategy may influence other performance parameters like N effluent quality (Gernaey *et al*., 2002). Above all, excess phosphorus can still be removed using chemical precipitation (Gernaey *et al*., 2004). Secondly, in all simulations of this thesis, Q_{int}:Q_{in} was fixed at 4.9, independent of a possibly changing SRT due to the imposed TSS concentration, which would mean that the optimal value for Q_{int}:Q_{in} would change.

Based on the steady state outcomes after 200 days of simulation, the effluent quality was obtained using the simulated effluent TSS concentration TSS_{eff} [g TSS.m^{-3}] and calculated based on BSM2 effluent quality formulas for COD_{eff} [g COD.m^{-3}], BOD_{eff} [g BOD.m^{-3}] and N_{eff} [g N.m^{-3}] (Gernaey *et al.*, 2014) (Figure 3.3). These values were evaluated using the effluent criteria COD_{crit} (125 g COD.m^{-3}), BOD_{crit} (25 g BOD.m^{-3}), N_{crit} (10 g N.m^{-3}) and TSS_{crit} (35 g TSS.m^{-3}) (Council of European Communities, 1991). The standards for total TSS and N are valid for plants treating water for respectively more than 10 000 and 100 000 P.E. It was defined that the system fails when one of the effluent criteria is exceeded (Figure 3.3).

3.4.3 Maximal treatment capacity

Based on the evaluation of failure of the system, the maximal treatment capacity of the different systems was found by searching the exact value for Q_{in} at which the system failed (i.e. one effluent criterion is exceeded). It was defined that the exact value for Q_{in} was found when one of the effluent concentrations (TSS_{eff}, COD_{eff}, BOD_{eff} or N_{eff}) was in the range of its respective criterion ± 0.5 g.m^{-3}.

3.4.4 Energy consumption

To compare the energy consumption of different simulations, the pumping energy [kWh.d^{-1}], aeration energy [kWh.d^{-1}] and the mixing energy [kWh.d^{-1}] were calculated using typical BSM1 formulas (Alex *et al.*, 2008a) (Appendix A.10). To make a fair comparison between different simulations (with different influent flow rates Q_{in} [$m^3.d^{-1}$]), the outcomes [kWh.d^{-1}] were divided by Q_{in} [$m^3.d^{-1}$] to express the energy consumption per volume treated water in kWh.m^{-3}.

4. Results and discussion

This chapter compares the treatment capacity and energy consumption between the activated sludge and aerobic granular sludge model. Firstly, the reference model was validated and general trends and shortcomings were identified in section 4.1. Secondly, in section 4.2, the activated sludge model was used to determine the maximal treatment capacity of this system. Subsequently, the same was done for the aerobic granular sludge model in section 4.3. The effects of better settling sludge and diffusion limitation were both separately and simultaneously taken into account.

4.1 Reference model

The reference model was studied in this section. Firstly, the model was validated in section 4.1.1. Furthermore, the effect of varying influent flow rates on the system performance was carried out in section 4.1.2.

4.1.1 Reference model validation

To validate the model, steady state conditions need to be ensured. The reference model (section 3.1) was simulated under constant influent conditions (Table A.1). The fluctuations of effluent concentrations (Figure 4.1), as well as the biomass concentrations (Figure 4.2) stagnated already after about 100 days of simulation. To ensure steady state under different influent conditions, all further simulations were carried out with 200 days of operation.

The system failed, since the TSS concentration X_{TSS} [g TSS.m^{-3}] in the effluent exceeded TSS_{crit} (35 g TSS.m^{-3}). Hence, it seems that the influent load (0.91 kg COD.d^{-1}.m^{-3}, Table A.1) is already too high and the settler cannot sufficiently separate the sludge from the clean effluent.

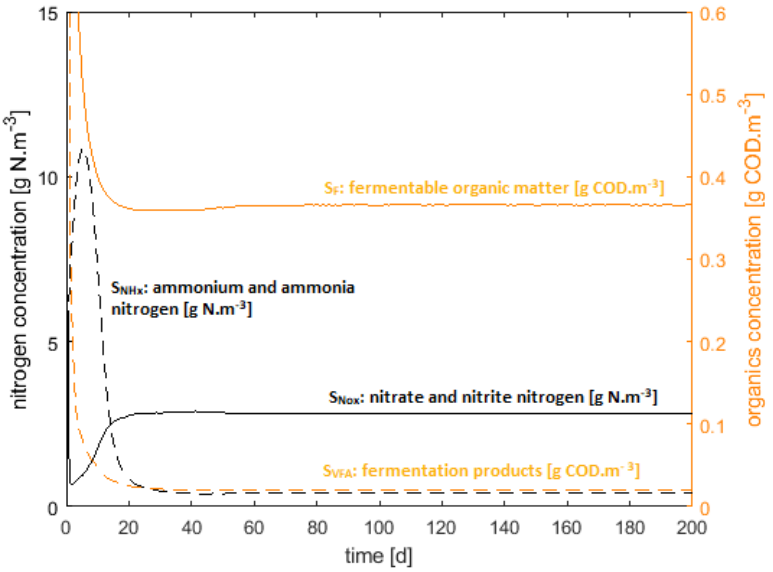

Figure 4.1: Simulated effluent concentrations as a function of time for the reference model (section 3.1) with a constant influent (Table A.1). After about 200 days there is a steady state operation.

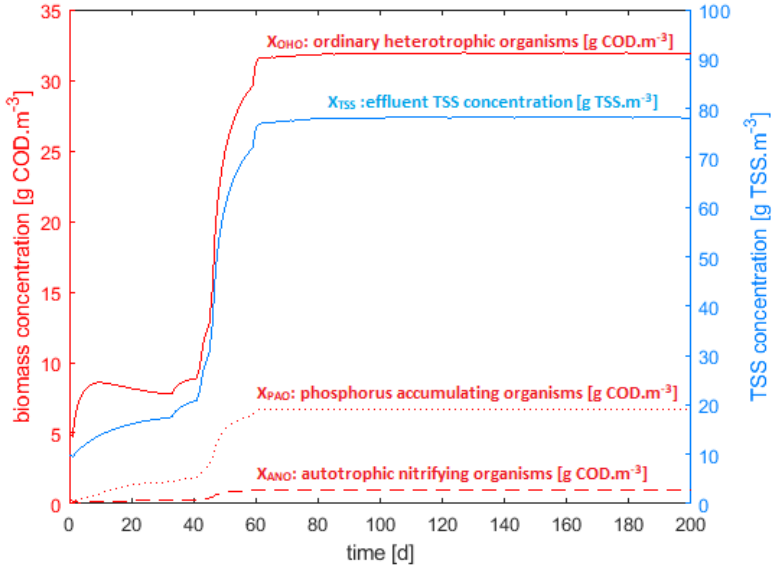

Figure 4.2: Simulated biomass concentrations as a function of time for the reference model with a constant influent (Table A.1). After about 200 days there is a steady state operation.

The oxygen control mechanism was validated by running the reference model with the constant influent data (Table A.1). In Figure 4.3, the oxygen concentrations S_{O_2} [g O_2.m^{-3}] in the aeration tanks are shown. It can be seen that the controlled variable (oxygen concentration in tank 6) reached the set-point of 2 g O_2.m^{-3}. KLa6 [d^{-1}] was the manipulated variable and based on this control strategy, KLa5 and KLa7 [d^{-1}] were set to respectively KLa6 and KLa6/2.

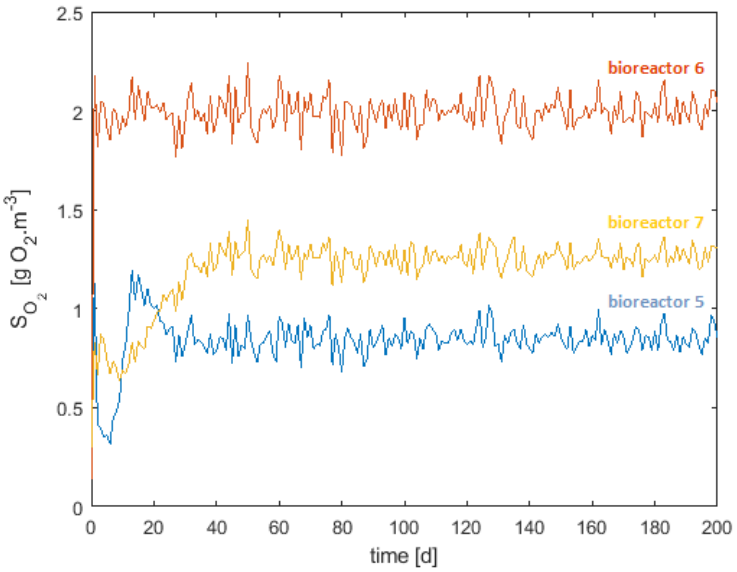

Figure 4.3: Simulated oxygen concentration S_{O_2} [g O_2.m^{-3}] as a function of time in the aeration reactors for the reference model with constant influent (Table A.1). S_{O_2} [g O_2.m^{-3}] in reactor 6 is controlled at a set-point of 2 g O_2.m^{-3}. Based on the manipulated variable KLa6 [d^{-1}], KLa5 and KLa7 were respectively set at KLa6 and KLa6/2, resulting in the visualized oxygen concentrations S_{O_2} [g O_2.m^{-3}] in bioreactor 5 and 7.

The mass balances of nitrogen (N), phosphorus (P) and organic matter (COD) over the reference model result in the in- and outgoing load of N, P and COD visualized in Figure 4.4 (Appendix A.11). The difference between the ingoing and outgoing load compared to the ingoing load of N and P were smaller than 0.01%, and of COD 0.7%. The latter deviation might be due to not fully attained steady state (although that does not seem the case based on Figures 4.1 and 4.2) or faults in the numerical algorithm. Based on this negligible deviations, it can be concluded that mass balances are closed and the model is validated.

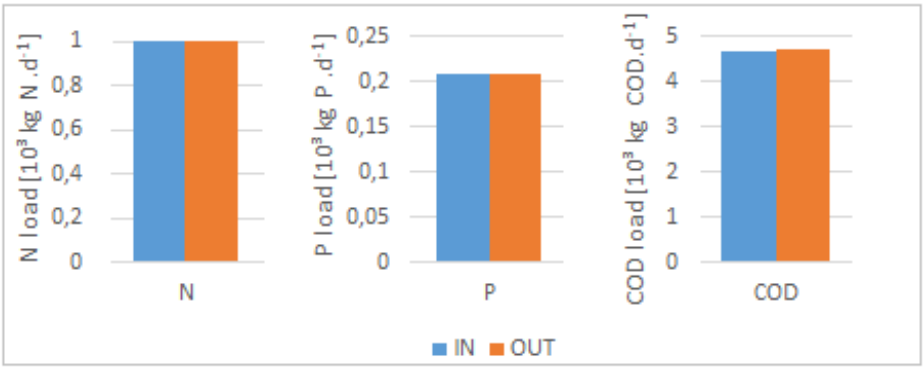

Figure 4.4: Bar plot of the ingoing and outgoing load of N, P and COD at steady state conditions (day 200 of operation). The simulation was done on the reference model using the constant BSM2 influent data (Table A.1) and based on Appendix A.11.

4.1.2 Effect of different influent flow rates on system performance

In order to investigate the effect of different influent flow rates on the performance of the reference model, the simulation procedure with the influent conditions of Table 3.5 was carried out (Figure 4.5). Important to notice is that the only fixed flow rate was the waste flow rate Q_w = 300 $m^3.d^{-1}$.

In general, the system started to fail from Q_{in} = 18 446 $m^3.d^{-1}$ on, where the TSS concentration exceeded the effluent criterion (TSS_{eff} > TSS_{crit}) (Figure 4.5(b)). The total nitrogen concentration N_{eff} exceeded the limit starting from Q_{in} = 20 648 $m^3.d^{-1}$ (the BSM2 influent data Q_{in}, Table A.1). The COD and BOD effluent criteria were exceeded from Q_{in} = 34 106 $m^3.d^{-1}$ (Figure 4.5(a)).

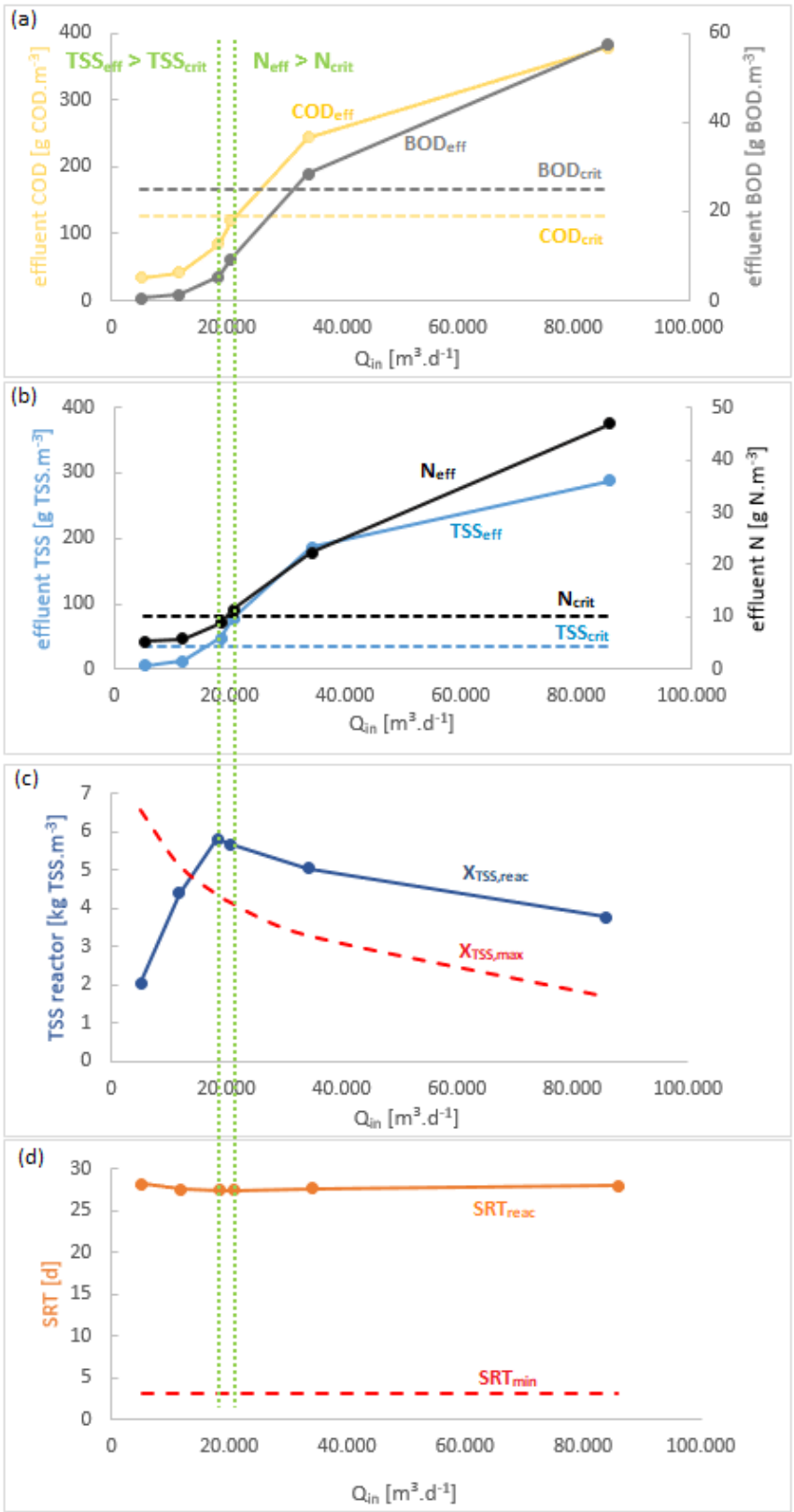

Figure 4.5: Steady state simulations of the reference model for different influent flow rates Q_{in}. (a): Effluent COD concentration COD_{eff} and effluent BOD concentration BOD_{eff}, together with respective effluent criteria COD_{crit} and BOD_{crit}. (b): Effluent TSS concentration TSS_{eff} and effluent N concentration N_{eff}, together with respective effluent criteria TSS_{crit} and N_{crit}. (c): Average TSS concentration in the biological reactor $X_{TSS,reac}$ (Eq. 4.1) compared to the theoretical maximal allowable TSS concentration in the reactor $X_{TSS,max}$ (Eq.4.2). (d): SRT_{reac} (sludge retention time) of the reactor compared to the minimal SRT for nitrification SRT_{min}.

In order to better interpret the results regarding the effluent TSS concentration (Figure 4.5 (b)), the average TSS concentration in the reactor $X_{TSS,reac}$ [kg TSS.m^{-3}] (Eq. 4.1) was compared with the theoretical maximal allowable TSS concentration in the reactor before failure of the settler $X_{TSS,max}$ [kg TSS.m^{-3}] in Figure 4.5(c) (Eq. 4.2) (Henze *et al.*, 2008). $X_{TSS,max}$ depends on the design of the settler (A_{set} [m²]) and the settleability of the sludge (r_h [m³.(g TSS)$^{-1}$], v_0 [m.h^{-1}]; Table 3.1). With this simplistic analytical formula, the observed effects were checked. Theoretically, if the TSS concentration in the reactor $X_{TSS,reac}$ becomes higher than this $X_{TSS,max}$, the settler should start failing ($TSS_{eff} > TSS_{crit}$).

$$X_{TSS,reac} = \frac{\sum_{i=1}^{7} V_i X_{TSS,i}}{V_p} \quad [g\ TSS.\ m^{-3}] \quad \textbf{Eq. 4.1}$$

with $X_{TSS,reac}$ = average TSS concentration in biological reactor [g TSS.m^{-3}]

V_i = volume of each bioreactor *i* (see Table 3.1) [m³]

$X_{TSS,i}$ = TSS concentration in bioreactor *i* [g TSS.m^{-3}]

V_p = total volume of biological reactors (13 500 m³) [m³]

$$A_{set} = \frac{Q_{set}/24}{0.8 v_0 \exp(-r_h * X_{TSS,max})} \quad [m^2] \quad \textbf{Eq. 4.2}$$

$$\Leftrightarrow X_{TSS,max} = -{r_h}^{-1} * \ln\left[\frac{Q_{set}/24}{A_{set} 0.8 v_0}\right] \quad [kg\ TSS.\ m^{-3}]$$

with Q_{set} = flow rate into settler [m³.d^{-1}]

= $Q_{in} + Q_r$ = 2.5Q_{in} (since Q_r:Q_{in} = 1.5)

v_0 = maximum Vesilind settling velocity [m.h^{-1}]

r_h = hindered zone settling parameter [m³.g^{-1}]

A_{set} = surface area of secondary settler (1500 m²) [m²]

It can be concluded that the settler started failing from an influent flow rate of 18 446 m³.d^{-1} ($TSS_{eff} > TSS_{crit}$, point 3) (Figure 4.5(b)). At this influent flow rate, the TSS concentration in the reactor peaked at 5.83 kg TSS.m^{-3} (Figure 4.5(c), point 3). Somewhere in between points 2 and 3, $X_{TSS,reac}$ exceeded $X_{TSS,max}$, which indeed corresponds with the situation where $TSS_{eff} > TSS_{crit}$. The higher Q_{in}, the higher the TSS concentration in the reactor $X_{TSS,reac}$ because more TSS is entering the reactor. However, it seems that because the influent flow rate got too high (18 446 m³.d^{-1} in point 3), $X_{TSS,reac}$ got too high and wash-out occurred significantly. Hence, the TSS concentration in the effluent increased significantly too and $TSS_{eff} > TSS_{crit}$. The settler got saturated and the maximal capacity of TSS in the settler was reached because Q_{in} got too high (18 446 m³.d^{-1}).

In order to check the N effluent quality in Figure 4.5(b), the sludge retention time (SRT_{reac} [d]) (Eq. 4.3) for the different simulations and the theoretical minimal SRT for nitrification SRT_{min} [d] were calculated (Eq. 4.4) (Figure 4.5(d)). The sludge age SRT_{reac} is calculated by dividing the mass of sludge in the reactor by the mass of sludge wasted per day (Henze *et al.*, 2008). This theory assumes that both the loss of solids with the effluent and the mass of sludge in the secondary settling tank compared to the mass in the reactor are negligible. This is reasonable when high recycle ratios (Q_r:Q_{in} > 1:1) are applied and the SRT is higher than 3 days (Henze *et al.*, 2008). SRT_{min} corresponds with the minimal sludge age to ensure

that nitrification still occurs (Eq. 4.4) (Henze *et al.*, 2008). Since it was assumed that the sludge is perfectly mixed and equally dispersed over all bioreactors, the unaerated sludge mass fraction f_{xt} was calculated based on the unaerated volumes. When SRT_{reac} becomes lower than SRT_{min}, the nitrifying biomass is theoretically washed out and nitrification starts failing, which should be comparable to $N_{eff} > N_{crit}$.

$$SRT_{reac} = \frac{\sum_{i:1}^{7} V_i X_{TSS,i}}{X_{TSS,w} Q_w} \quad [d] \qquad \textbf{Eq. 4. 3}$$

with V_i = volume of each bioreactor *i* (see Table 3.1) [m³]

$X_{TSS,i}$ = TSS concentration in bioreactor *i* [g TSS.m^{-3}]

$X_{TSS,w}$ = TSS concentration in waste stream Q_w [g TSS.m^{-3}]

Q_w = waste flow rate (300 m³.d^{-1}) [m³.d^{-1}]

$$SRT_{min} = \frac{1}{\mu_{ANO,Max}(1 - f_{xt}) - b_{ANO}} = 3.16 \quad [d] \qquad \textbf{Eq. 4. 4}$$

with $\mu_{ANO,Max}$ = maximum growth rate of X_{ANO} (0.61 d^{-1}) [d^{-1}]

f_{xt} = unaerated sludge mass fraction [-]

$= \frac{V_1 + V_2 + V_3 + V_4}{V_p} = 0.33$ [−]

b_{ANO} = decay rate of X_{ANO} (0.09 d^{-1}) [d^{-1}]

SRT_{reac} stayed practically constant for the different inflow rates at a value of 27 days (Figure 4.5(d)). This value was obtained during the model validation, which corresponds with simulation point 4 in Figure 4.5 (Q_{in} = 20 648 m³.d^{-1}) and was also used in the calculation procedure for the optimal nitrate recycle ratio, which led to Q_{int}:Q_{in} = 4.9. Hence, the system was operating under the optimal internal nitrate recycle conditions in all of the simulations, which would mean that denitrification did not fail in these simulations. SRT_{min} on the other hand, resulted in a value of 3.16 d, which corresponds with values found in literature (Henze *et al.*, 2008). SRT_{min} was far smaller than SRT_{reac} in all simulations. Theoretically, nitrification also never failed and wash-out of autotrophic biomass did not occur.

The approximately constant SRT_{reac} [d] for different Q_{in} can be explained both mathematically and physically. Mathematically, SRT_{reac} is expressed as the TSS mass in the reactor ($\sum_{i:1}^{7} V_i X_{TSS,i}$) [kg TSS] (Figure 4.5(c)) divided by the mass of sludge wasted per day (Eq. 4.3). It seems that numerator and denominator have the same profile, since the resulting SRT_{reac} stayed constant. More TSS mass was wasted when more TSS mass was present in the reactor. Physically, it can be understood that due to the fixed recycle ratio Q_r:Q_{in}, the amount of TSS recycled was adapted to the amount of TSS entering, which resulted in a more or less constant SRT_{reac}.

The formula for SRT_{reac} is not representative anymore from Q_{in} = 18 446 m³.d^{-1} (point 3) on and the outcomes cannot be interpreted. Since the settler started failing from point 3 on, a lot of TSS was leaving with the effluent, which means that SRT_{reac} should be decreasing since wash-out occurs. However, in the formula for SRT_{reac}, it is assumed that the TSS leaving with the effluent is negligible compared to the mass in the settler (or in other words: that the settling is not failing) (Eq. 4.3) (Henze *et al.*, 2008). It can be concluded that in the case that the settler is working well (points 1-2),

SRT_{reac} was indeed a reliable value since the sludge recycle ratio Q_r:Q_{in} was higher than 1 (in these simulations 1.5) and SRT > 3 days. The non-interpretable results from SRT_{reac} from point 3 on might the reason that it never came close to SRT_{min}. If TSS control would be present and the settler is working well because the TSS concentration is regulated at a constant value, the values for SRT_{reac} obtained would be more accurate and could be compared to SRT_{min}.

When having a closer look at the different contributions to N_{eff} , it was noticed that the primary reason for failure of N_{eff} from Q_{in} = 20 648 m³.d^{-1} on was high particulate concentrations (> 70% of N_{eff}) and thus the assimilation of nitrogen in biomass, X_U and XC_B [g COD.m^{-3}], due to the failure of the settler. It was only in point 6 (85 841 m³.d^{-1}) that the ammonium concentration in the effluent S_{NH_x} [g N.m^{-3}] became large (19.12 g N.m^{-3}) and thus nitrification started failing. This reasoning was also proven by plotting the biomass concentrations in bioreactor 7 for the different inflow rates Q_{in} (Figure 4.6). The autotrophic biomass X_{ANO} [g COD.m^{-3}] was still present in point 4 (N_{eff} > N_{crit}) and was only selectively washed out of the reactor in the last simulation point when nitrification started failing.

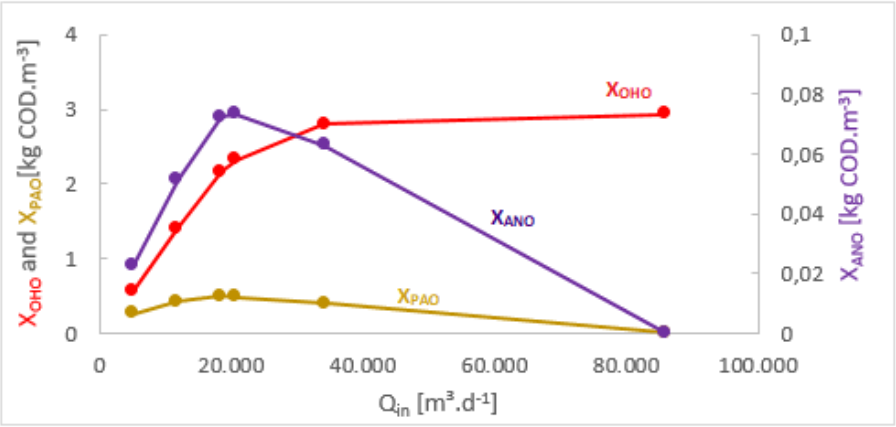

Figure 4.6: Steady state simulations of the biomass concentrations in bioreactor 7 of the reference model for different influent flow rates Q_{in}. X_{OHO}: ordinary heterotrophic organisms, X_{PAO}: phosphorus accumulating organisms and X_{ANO} :autotrophic nitrifying organism.

In conclusion, the primary inducer of failure in this reference continuous activated sludge system without TSS control is the saturation of the settler with TSS. The TSS concentration in the reactor $X_{TSS,reac}$ got too high (5.83 kg TSS.m^{-3}) in the third simulation point (18 446 m³.d^{-1}) and the activated sludge flocs could not be settled out anymore. Hence, the TSS concentration in the effluent exceeded the TSS effluent standard. Nevertheless, not so long after the settler started to fail, also N_{eff} exceeded the standard, primary because of assimilation of N in particulates. Important to realize is that no form of sludge mass control was present in these simulations. The following step is to introduce TSS control into the system. In that case, the amount of sludge wasted per day will be controlled in contrast to the fixed Q_w [m³.d^{-1}] in the previous simulations.

4.2 Activated sludge model

The TSS controller as described in section 3.2 was implemented into the system, resulting in the activated sludge model. This control mechanism was first validated (section 4.2.1), followed by a simulation procedure to investigate the effect of different influent flow rates on the system performance in section 4.2.2. Lastly, the maximal treatment capacity of the continuous activated sludge system before failure was simulated in section 4.2.3.

4.2.1 TSS control validation

To validate the TSS control mechanism described in the section 3.2, the BSM2 constant influent dataset was used (Table A.1). The TSS concentration X_{TSS} in bioreactor 7 was controlled at 4 kg TSS.m^{-3} by the manipulated variable Q_w and shown in Figure 4.7. The set-point was reached well within 200 days of steady state simulation. All further simulations in this thesis include the TSS control mechanism.

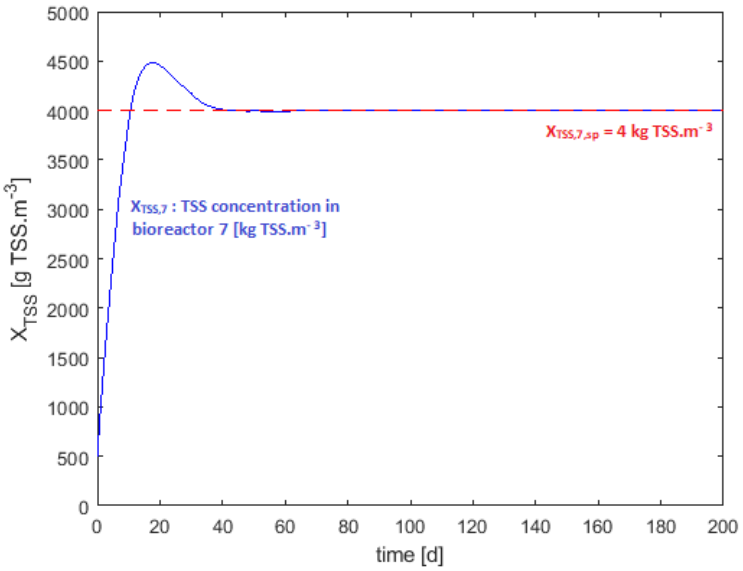

Figure 4.7: TSS concentration in bioreactor 7 $X_{TSS,7}$ [g TSS.m^{-3}] as a function of time [d] for the activated sludge model with constant BSM2 influent data (Table A.1). $X_{TSS,7}$ [g TSS.m^{-3}] was regulated at a set-point $X_{TSS,7,sp}$ of 4 kg TSS.m^{-3} using a PI controller.

4.2.2 Effect of different influent flow rates on system performance

The system was first regulated at 4 kg TSS.m^{-3} to search the maximal treatment capacity [kg COD.d^{-1}.m^{-3}] of the continuous activated sludge system with TSS control (section 3.4.2 + 3.4.3). The influent flow rate Q_{in} was changed in order to find both the loading rates at which $TSS_{eff} > TSS_{crit}$ and at which $N_{eff} > N_{crit}$. The needed values for Q_{in}, obtained via step-by-step increase, to find out where the system failed are given in Appendix A.11.

The effluent TSS concentration exceeded the legal limit when the influent flow rate Q_{in} was higher than 57 000 m³.d^{-1} (Figure 4.8(b)). Yet, the effluent nitrogen criterion was already exceeded at 31 000 m³.d^{-1}. Therefore, this lower influent flow rate corresponds to the maximal treatment capacity of 1.36 kg COD.d^{-1}.m^{-3} when the TSS concentration is controlled at 4 kg TSS.m^{-3}. COD_{eff} and BOD_{eff} were increasing for increasing Q_{in}, but remained under their effluent criterion for all simulations (Figure 4.9(a)).

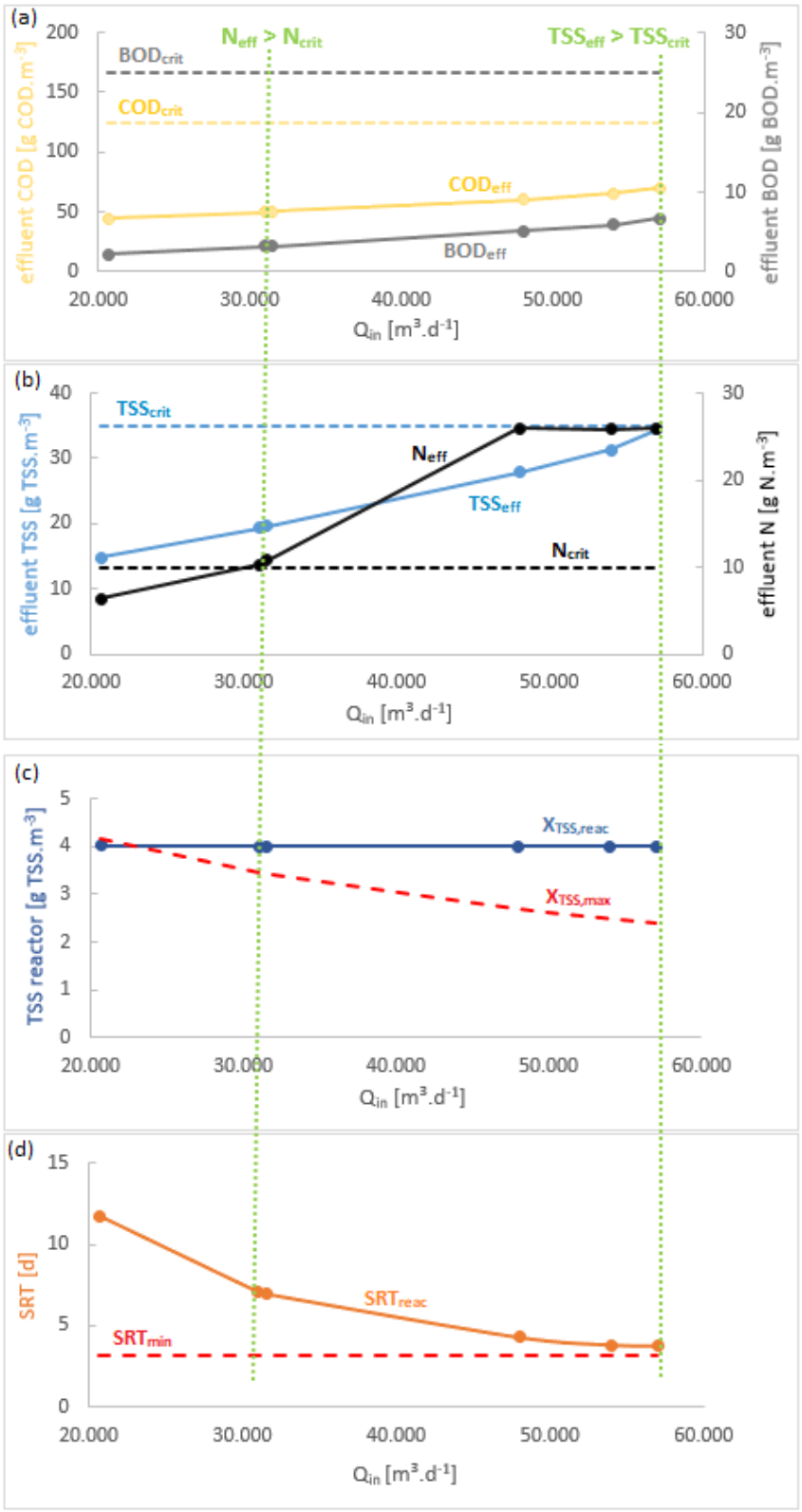

Figure 4.8: Steady state simulations of the activated sludge model regulated at X_{TSS} = 4 kg TSS.m^{-3} for different influent flow rates. (a): Effluent COD concentration COD_{eff} and effluent BOD concentration BOD_{eff}, together with respective effluent criteria COD_{crit} and BOD_{crit}. (b): Effluent TSS concentration TSS_{eff} and effluent N concentration N_{eff}, together with respective effluent criteria TSS_{crit} and N_{crit}. (c): Average TSS concentration in the biological reactor $X_{TSS,reac}$ (Eq. 4.1) compared to the theoretical maximal allowable TSS concentration in the reactor $X_{TSS,max}$ (Eq.4.2). (d): SRT_{reac} (sludge retention time) of the reactor compared to the minimal SRT for nitrification SRT_{min}.

The failure of the settler at Q_{in} = 57 000 m³.d^{-1} cannot be matched with the theoretical maximal allowable TSS concentration $X_{TSS,max}$ (Figure 4.8(c)). This deviation might be explained by the assumptions of the formula of $X_{TSS,max}$ (Eq. 4.2). In this design formula, a simplified expression for the settling velocity and a reduction factor of 0.8 were assumed. The reduction factor of 0.8 represents a 25% safety factor (1/0.8) to take into account the significant deviation of the hydrodynamics in real secondary settlers compared with the assumed 1D idealized flux theory (Ekama & Marais, 2004; Henze *et al.*, 2008; Sikic *et al.*, 2017). This safety factor was not conform with the used model and should be lower to obtain higher values for $X_{TSS,max}$.

SRT_{reac} (Eq. 4.3) decreased for the increasing inflow rates Q_{in} but did not become smaller than SRT_{min}, which theoretically would mean that autotrophic biomass was not washed out and nitrification did not fail (Figure 4.8(d)). In the calculation for SRT_{reac} (Eq. 4.3), the mass in the reactor is divided by the sludge wasted per day. Since Q_{in} kept increasing, also more TSS had to be wasted (via manipulation of Q_w) in order to keep the TSS concentration in the biological reactor constant, leading to the decreasing trend of SRT_{reac}.

The decreasing value for SRT_{reac} means that non-optimal denitrification conditions were imposed because the nitrate recycle ratio Q_{int}:Q_{in} was fixed. The optimal value for Q_{int}:Q_{in} for the first simulation point (Q_{in} = 31 000 m³.d^{-1}, SRT_{reac} = 7.08 d) would have been 3.06 (Appendix A.7). Since the installed Q_{int}:Q_{in} was 4.9, too much nitrate was recycled to the anoxic tank. Too high Q_{int}:Q_{in} is not efficient, since also a lot of O_2 is entrapped in Q_{int}, which will be used up in the anoxic tank before NO_3^-. Moreover, extra pumping energy is needed. Further research might consider to control the internal recycle ratio in order to always operate under optimal nitrate recycle conditions. However, since the COD:N ratio in the influent was not varying (Table A.1), it was assumed that the system was always operating relatively close to the optimal value and denitrification was not limited. This reasoning was proven by the composition of N_{eff} at Q_{in} = 31 000 m³.d^{-1}, which contained 51% ammonium S_{NH_x} and only 17% nitrate S_{No_x}. Hence, it seems clearly that nitrification was limited at Q_{in} = 31 000 m³.d^{-1} ($N_{eff} > N_{crit}$).

Although the legal effluent requirement for nitrogen was already not met at Q_{in} = 31 000 m³.d^{-1}, it was only from Q_{in} = 48 000 m³.d^{-1} on that the autotrophic biomass X_{ANO} was selectively washed out (Figure 4.9). When taking the ratio between the amount of ammonium leaving the system with the effluent and the amount of ammonium entering the system [kg N.d^{-1}], this resulted in 21% at Q_{in} = 31 000 m³.d^{-1} and 88% at Q_{in} = 48 000 m³.d^{-1}. Hence, nitrification was still occurring at Q_{in} = 31 000 m³.d^{-1} (however not sufficient) and only really started to fail at Q_{in} = 48 000 m³.d^{-1}, corresponding with the wash-out of autotrophic biomass.

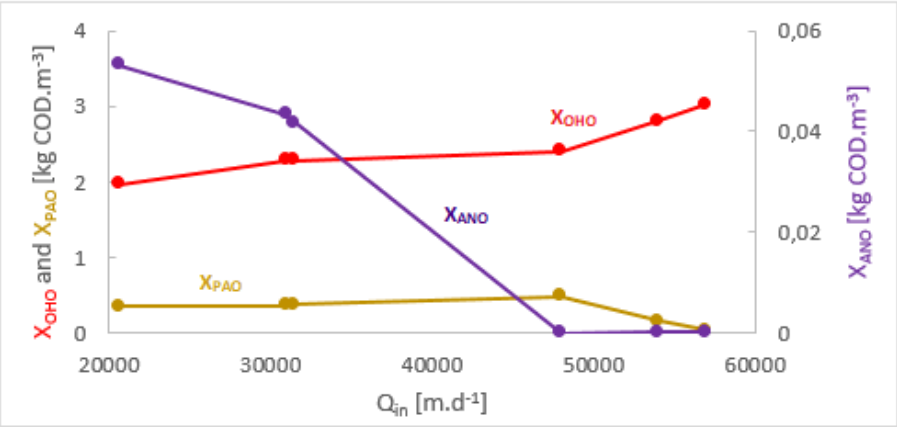

Figure 4.9: Steady state simulations of the biomass concentrations in bioreactor 7 of the activated sludge model for different influent flow rates Q_{in}. X_{OHO}: ordinary heterotrophic organisms, X_{PAO}: phosphorus accumulating organisms and X_{ANO} :autotrophic nitrifying organism.

SRT_{min} cannot be combined with these findings since SRT_{reac} at Q_{in} = 48 000 m³.d^{-1} was equal to 4.28 d, which was higher than SRT_{min} (3.16 d) (Figure 4.8(d)). The deviation between SRT_{min} and SRT_{reac} might be due to oxygen limitation in bioreactor 5 and 7 (oxygen concentration in bioreactor 6 was regulated at 2 g O_2.m^{-3}). The oxygen concentration in bioreactors 5 and 7 at Q_{in} = 48 000 m³.d^{-1} was equal to respectively 0.89 and 0.77 g O_2.m^{-3}, which is already quite small compared to a general range of 1 - 3 g O_2.m^{-3} (Nopens *et al.*, 2010). Due to this shortage of oxygen, the autotrophic bacteria might have been extra limited, resulting in a faster wash-out than theoretically expected.

In conclusion, due to the addition of TSS control, the primary inducer of failure of the system is now failure of nitrification. Due to the constant TSS concentration, the SRT of the system decreased for increasing load. At Q_{in} = 31 000 m³.d^{-1}, the SRT was already too low and nitrification was sufficiently limited, leading to $N_{eff} > N_{crit}$. From this simulation procedure at X_{TSS} = 4 kg TSS.m^{-3}, it was obtained that the maximal treatment capacity before $N_{eff} > N_{crit}$ was equal to 1.36 kg COD.d^{-1}.m^{-3} (Q_{in} = 31 000 m³.d^{-1}) and the maximal treatment capacity before $TSS_{eff} > TSS_{crit}$ was equal to 2.50 kg COD.d^{-1}.m^{-3} (Q_{in} = 57 000 m³.d^{-1}).

4.2.3 Maximal treatment capacity for different TSS concentrations

The system was subsequently regulated at respectively 2-3-5-6 kg TSS.m^{-3} and a similar simulation procedure as in section 4.2.2 was followed to find the exact loading rates where $TSS_{eff} > TSS_{crit}$ and $N_{eff} > N_{crit}$ (Figure 4.10). COD_{eff} and BOD_{eff} never failed before N_{eff} or TSS_{eff} did. The maximal treatment capacity before failure of the settler described a decreasing trend for increasing controlled TSS concentration, while the maximal treatment capacity before failure of N removal achieved a peak at a biomass concentration of 5 kg TSS.m^{-3}. At X_{TSS} = 2-3-4 kg TSS.m^{-3}, the system started failing for N removal before the settler started failing. At X_{TSS} = 5-6 kg TSS.m^{-3}, the settler failed just before N removal started failing. Lastly, it was noticed that the reference case - the reference model with BSM2 constant influent data - was located around the border between a good working system and failure.

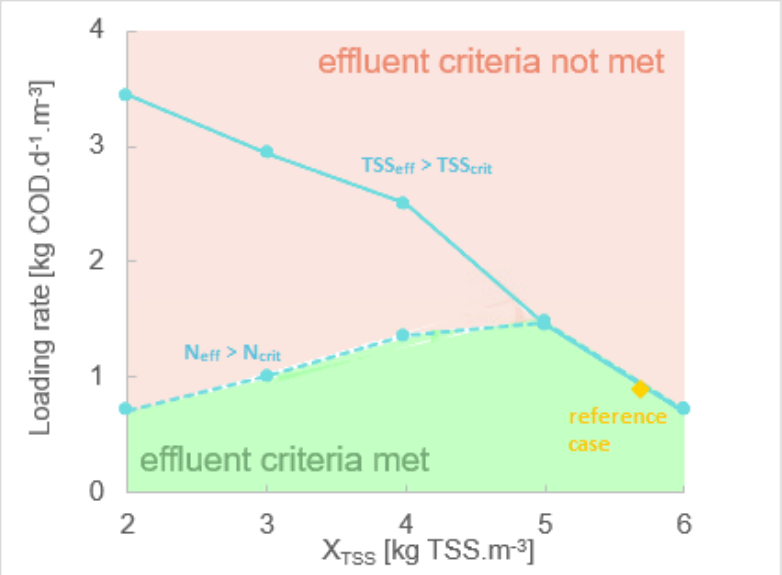

Figure 4.10: Maximal treatment capacity of the activated sludge model before failure of N removal ($N_{eff} > N_{crit}$) and before failure of the settler ($TSS_{eff} > TSS_{crit}$) as a function of the controlled TSS concentration in the biological reactor X_{TSS}. Green area: operating points where no effluent criteria is exceeded. Red area: one or more effluent criteria exceeded. Reference case according to section 3.1 and Table A.1 (influent COD load 0.9 kg COD.d^{-1}.m^{-3}).

The higher the TSS concentration in the biological reactor X_{TSS} [kg TSS.m^{-3}], the higher the TSS concentration in the water entering the settler. Due to this higher concentration, the maximal load that can be treated before the settler starts failing becomes smaller, which explains the decreasing trend of the maximal treatment capacity before failure of the settler ($TSS_{eff} > TSS_{crit}$) (Figure 4.10).

The initial increase of the maximal treatment capacity before $N_{eff} > N_{crit}$ is due to the higher controlled TSS concentration - and thus also biomass concentration - in the biological reactor. The more biomass available to treat the water (and perform COD and N removal), the higher the removal rates since these are directly proportional to the biomass concentrations (Appendix A.4). Hence, a higher treatment capacity before failure of N removal can be obtained ($N_{eff} > N_{crit}$). However, when the TSS concentration gets too high (i.e. 5 kg TSS.m^{-3}), the settler starts failing before N removal does and wash-out occurs. Due to this extensive wash-out, also N_{eff} exceeds its standard, because of assimilation of nitrogen in biomass, X_U and XC_B. Hence, although the nitrifying (X_{ANO}) and denitrifying biomass (X_{PAO} and X_{OHO}) and thus the nitrogen removal capacity kept increasing, the effluent nitrogen limit is more easily exceeded at higher TSS concentration because high concentrations of particulate-bound nitrogen leave via the effluent when the settler is overloaded.

As was already concluded in the reference model validation (section 4.1.1), the reference case was failing for TSS (Figure 4.2), which would mean that this point should fall in the red area. Due to the absence of TSS control, the TSS concentration in the reactor became too high (5.68 kg TSS.m^{-3} in point 4 in Figure 4.5(c)), leading to failure of the settler. Controlling this system with accompanied influent data at a TSS concentration around 4-5 kg TSS.m^{-3} would bring the system into the good working green area and would make sure that no wash-out occurs.

In conclusion, the maximal treatment capacity before the activated sludge system starts failing peaked at 5 kg TSS.m^{-3} and was equal to 1.46 kg COD.d^{-1}.m^{-3}. It should now be researched whether this treatment capacity could be increased by introducing aerobic granular sludge into the system.

4.3 Aerobic granular sludge model

To investigate the effect of aerobic granular sludge in a continuous system, two important effects were researched. Firstly, the effect of the better settleability of the granules (section 4.3.1 and 4.3.2). Secondly, the diffusion limitation - and together with that the possible simultaneous nitrification and denitrification in granules - was taken into account (section 4.3.3).

4.3.1 Effect of different influent flow rates on system performance: better settling sludge

The effect of better settling granules was simulated by increasing the settling velocity of the sludge with a factor 5 (section 3.3.1, Table 3.4). In a similar simulation procedure as in section 4.2.2, the system was first controlled at X_{TSS} = 4 kg TSS.m^{-3} and maximal loads before failure of N removal and the settler were searched via a step-by-step increase of Q_{in} (data in Appendix A.12). Similar trends and conclusions as in section 4.2.2 apply to this simulation. TSS_{eff} exceeded the legal requirement from Q_{in} = 207 763 m³.d^{-1} on, which means that wash-out started from this point on (Figure 4.11). N_{eff} on the other hand, exceeded its criterion starting from Q_{in} = 31 500 m³.d^{-1}, corresponding with a maximal capacity of 1.38 kg COD.d^{-1}.m^{-3}. The reason for this was again the failure of nitrification.

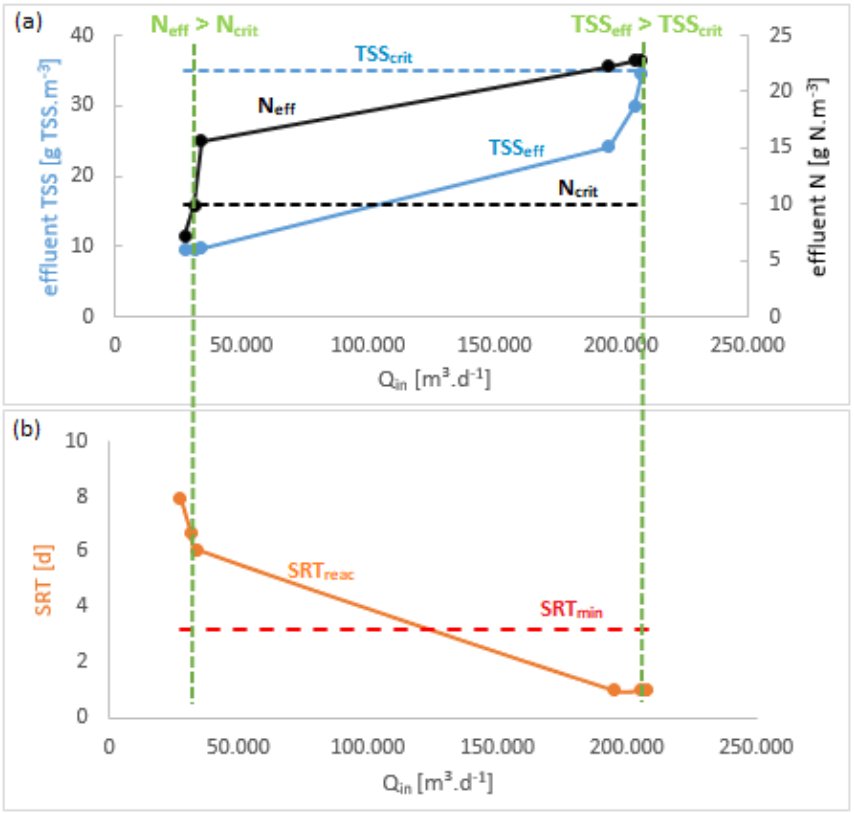

Figure 4.11: Steady state simulations of the activated sludge model with better settling sludge (increased with factor 5) controlled at 4 kg TSS.m^{-3} for different influent flow rates Q_{in}. (a): Effluent TSS concentration TSS_{eff} and effluent N concentration N_{eff}, together with their respective effluent criteria TSS_{crit} and N_{crit}. (b): The sludge retention time of the reactor SRT_{reac} (Eq. 4.3) and minimal SRT_{min} [d] (Eq. 4.4).

The system with better settling sludge now failed for N removal at Q_{in} = 31 500 m³.d^{-1}, while the activated sludge system failed at 31 000 m³.d^{-1} (Figure 4.8(b)). Although the TSS concentration was in both cases controlled at the same concentration (and thus the biomass concentration in both cases is equal), a slightly better result is obtained with better settling sludge. The only difference between both cases seems that the organic fraction of N_{eff} is slightly higher for activated sludge (32% with activated sludge vs. 25% for better settling sludge). Hence, in case of activated sludge the settler was already quite heavy loaded at a TSS concentration of 4 kg TSS.m^{-3}, leading to slightly higher particulate fractions at these influent flow rates.

Failure of the settler was significantly improved by introducing better settling sludge into the continuous system. The TSS concentration now exceeded its criterion from Q_{in} = 207 763 m³.d^{-1} on, while in case of activated sludge this was at 57 000 m³.d^{-1}. Hence, the maximal treatment capacity was increased with a factor of 3.6. Due to the better settleability of the sludge, the settler can now much more efficiently separate the sludge from the clean effluent, leading to significantly higher loads possible.

Failure of N removal was also compared with the theoretical equivalent SRT_{min}, whose value seems valid for both activated sludge and aerobic granular sludge (3.16 d). SRT_{reac} only crossed SRT_{min} between simulation points 3 and 4, while it was already at Q_{in} = 31 500 m³.d^{-1} that $N_{eff} > N_{crit}$ (Figure 4.11(b)). Although autotrophic biomass was still present in the first three points, they could not perform sufficient nitrification to keep N_{eff} low enough (similarly as in section 4.2.2). Only at higher influent loads the real wash-out occurred and nitrification failed somewhere between Q_{in} = 34 106 m³.d^{-1} and Q_{in} = 195 000 m³.d^{-1} (and $SRT_{reac} < SRT_{min}$).

4.3.2 Maximal treatment capacity for different TSS concentrations: better settling sludge

Since it could be expected that due the better settling sludge, the system can now handle higher TSS concentrations, the system was subsequently regulated at respectively 5-6-7-8 kg TSS.m^{-3}. At each TSS concentration, a similar simulation procedure resulted in values for the maximal treatment capacity [kg COD.d^{-1}.m^{-3}] before failure of N removal ($N_{eff} > N_{crit}$) and failure of the settler ($TSS_{eff} > TSS_{crit}$). These results are summarized in Figure 4.12. COD or BOD again never failed before TSS or N did. As can be noticed, the general trends in Figure 4.12 are the same as in case of activated sludge (Figure 4.10). The maximal treatment capacity before failure of the settler decreased for increasing X_{TSS} and the maximal treatment capacity before failure of N removal achieved a peak value at X_{TSS} = 6 kg TSS.m^{-3}. At X_{TSS} = 4 - 5 - 6 kg TSS.m^{-3}, the system failed because $N_{eff} > N_{crit}$, while at X_{TSS} = 7 - 8 kg TSS.m^{-3}, the system failed because $TSS_{eff} > TSS_{crit}$.

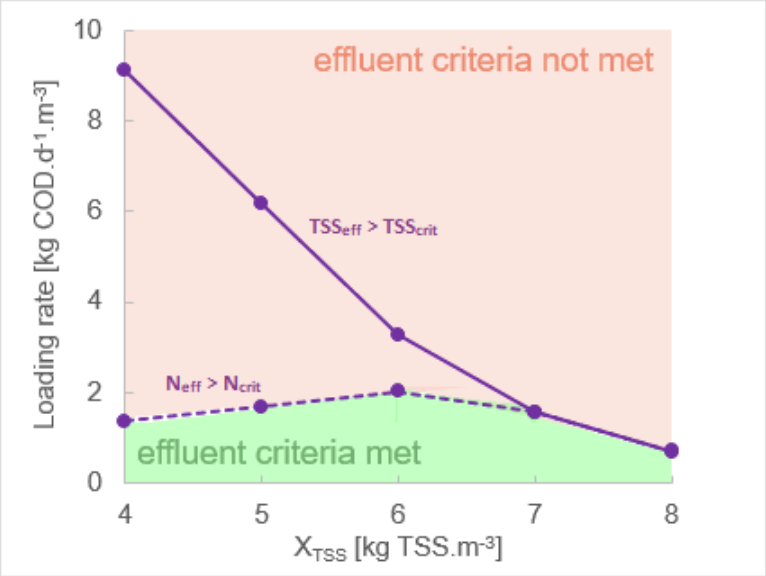

Figure 4.12: Maximal treatment capacity of the activated sludge model before failure of N removal ($N_{eff} > N_{crit}$) and before failure of the settler ($TSS_{eff} > TSS_{crit}$) as a function of the controlled TSS concentration in the biological reactor X_{TSS}. Green area: operating points where no effluent criteria is exceeded. Red area: one or more effluent criteria exceeded.

The maximal treatment capacity before failure of the settler was situated significantly higher in case of better settling sludge compared to activated sludge (at X_{TSS} = 4 - 5 - 6 kg TSS.m^{-3} an increase with respectively factor 3.6 - 4.2 - 4.7). Since the sludge has a better settleability, the downward solid fluxes in the settler are increased, leading to more efficient separation of sludge from the clean effluent. Hence, much higher loads are possible for the same X_{TSS} (i.e. the TSS concentration in the incoming water of the settler).

The maximal treatment capacity before failure of N removal described a similar pattern as in case of activated sludge, but now peaked at a higher TSS concentration of 6 kg TSS.m^{-3}. The reason for this peak is identical as in case of activated sludge. At low TSS concentrations (4 - 5 - 6 kg TSS.m^{-3}), the system failed because of failure of nitrification. The loads obtained at 4 and 5 kg TSS.m^{-3} are slightly higher compared to the activated sludge case. The reason for this is the better settling sludge and thus less organic N in the effluent. At higher TSS concentrations (7 - 8 kg TSS.m^{-3}) the settler started to fail before nitrification, resulting in assimilation of N in particulates, which caused N_{eff} to exceed N_{crit}. Hence, the difference is that the maximal treatment capacity before failure of N removal could increase until a higher TSS concentration before it was stopped by failure of the settler, due to the better settleability of the sludge. The maximal treatment capacity for the continuous system with better settling sludge was now 2.03 kg COD.d^{-1}.m^{-3}, achieved at a TSS concentration of 6 kg TSS.m^{-3}. Coming from 1.46 kg COD.d^{-1}.m^{-3} at X_{TSS} = 5 kg TSS.m^{-3} for activated sludge, an increase in maximal treatment capacity of the system of 39% was obtained.

As a critical note, the used increase factor 5 for the settling velocity was an average value based on literature findings. However, reported settling velocities in literature are very diverse, with peak values at 70 - 90 m.h^{-1}, which results in a factor higher than 10 compared to the factor 5 used in these simulations (Thanh *et al.*, 2009; Winkler *et al.*, 2012). When these values would be obtained in a continuous system, the improved effect in treatment capacity could be even higher.

4.3.3 Maximal treatment capacity: diffusion limitation

4.3.3.1 Diffusion limitation scenarios

Due to the dense and compact structure of granules, diffusion of substrates towards the core of the granule is limited, which decreases the overall removal performance (Li & Liu, 2005). Firstly, a strong diffusion limitation scenario was analyzed where the half saturation coefficients were increased with a factor 5, followed by a more moderate diffusion limitation scenario based on Baeten *et al.* (2018) (Appendix A.8). For both of these scenarios, the simulation procedure to find the maximal treatment capacity of the system was carried out twice. Once for the optimal situation of activated sludge (peak in Figure 4.10) to investigate the effect of purely diffusion limitation and one time for the optimal situation of better settling sludge (peak in Figure 4.12). It might be possible that the optimal TSS concentration of the system changed due to diffusion limitation, but this was not taken into account. Furthermore, the oxygen set-point in all of these diffusion limitation simulations was increased from 2 to 4 g $O_2.m^{-3}$. This was done in order to have sufficient nitrification, since it was found that the severe limitation had almost completely inhibited the nitrification at 2 g $O_2.m^{-3}$. This higher set-point is disadvantageous in terms of energy consumption. It might be more interesting to change the oxygen control strategy to make it more energy efficient. However, it was chosen to keep the oxygen control strategy as described in section 3.5.1 and based on BSM2 reports.

Due to the strong diffusion limitation, the maximal treatment capacity before failure of the optimal situations was sharply decreased (Figure 4.13). When looking at the effect of diffusion limitation only, i.e. in case of activated sludge with strong diffusion limitation, the maximal treatment capacity before failure of the system was decreased with 65%. If both the effects of better settling sludge and strong diffusion limitation were taken into account, the maximal treatment capacity before failure of the system decreased with 54% compared to activated sludge. The negative effect of purely diffusion limitation (-65%) clearly outweighed the positive effect of better settling sludge (+39%) since the ultimate result (-54%) is not the cumulative sum of both separate effects.

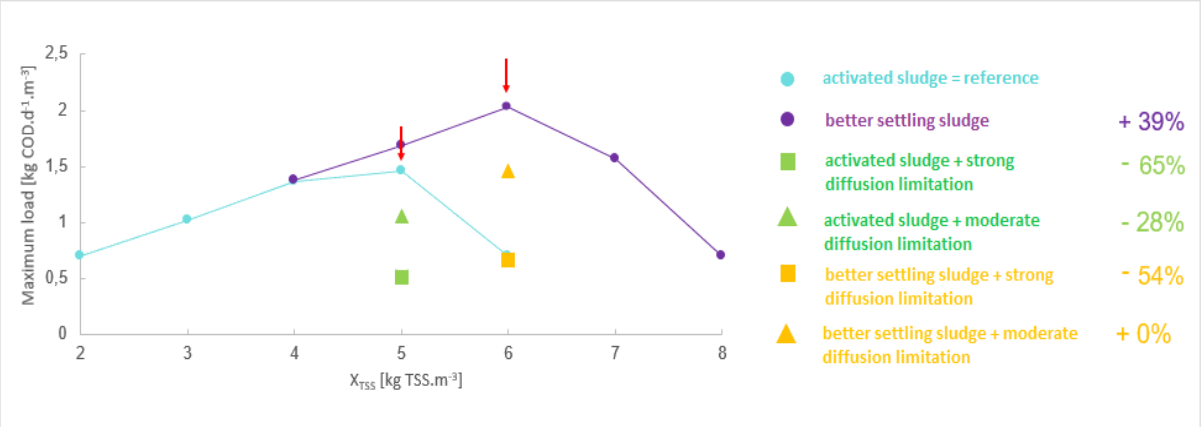

Figure 4.13 Treatment capacity [kg COD.d^{-1}.m^{-3}] of a continuous system with activated sludge (blue), better settling sludge (purple), diffusion limited sludge (green), better settling and diffusion limited sludge (yellow) in function of the imposed TSS concentration X_{TSS} [kg TSS.m^{-3}]. Squares represent the strong diffusion limitation (half saturation coefficients increase with factor 5) and triangles the moderate diffusion limitation according to Baeten *et al.* (2018). Only for the peak values in case of activated sludge and better settling sludge, the new peaks in case of the diffusion limitation are depicted. Percentage increase/decrease are expressed compared to the activated sludge system capacity, which was aimed to increase.

Under the moderate diffusion limitation, the maximal treatment capacity before failure was still extensively decreased (Figure 4.15). Based on purely diffusion limitation, the maximal load of the activated sludge system was decreased with 28%. If both the effects of better settling sludge and moderate diffusion limitation were taken into account, the maximal possible load of the system was practically equal to the original maximal treatment capacity of the continuous activated sludge system, which means that diffusion limitation (-28%) also here outweighed the effect of better settling sludge (+39%).

When comparing the optimal situation for better settling sludge with the new optima in case of moderate and strong diffusion limitation, the sludge age of these steady state simulations were respectively 7, 13 and 32 days. It seems that even though the SRT_{reac} was higher in the diffusion limitation cases and thus the biomass had more time to perform the biological removal reactions, the rates of these reactions were so severely limited that the system however already failed.

Primarily the biological conversion of the system, and more in particular N removal, was disturbed due to diffusion limitation, while the performance of the settler was not affected. Per example, 56% of N_{eff} was present in the form of S_{NH_x}[g N.m^{-3}] in case of better settling sludge with moderate diffusion limitation. Furthermore, the ammonium concentration in bioreactors 5, 6 and 7 for the same case were respectively 7.24, 6.12 and 5.31 g N.m^{-3}. Comparing this to the nitrate concentrations in bioreactors 5, 6 and 7 of 0.43, 0.99 and 1.31 g N.m^{-3} shows that it was primary nitrification that failed. Shortage of oxygen did also not seem to be the problem, since the oxygen concentration in bioreactor 6 was controlled at 4 g O_2.m^{-3} and the concentration in bioreactors 5 and 7 was around 2.8 g O_2.m^{-3} (sufficiently high compared to the half saturation coefficient $K_{O_2,ANO}$= 1 g O_2.m^{-3}). The maximal treatment capacity before failure of the settler on the other hand, stayed practically the same with diffusion limitation compared to the original situations (peak activated sludge + better settling sludge). The TSS control mechanism was regulating at the same TSS concentration as in the original situations and thus imposed the same load to the settler. However, even when comparing Q_w [m³.d^{-1}] values between the new simulations with diffusion limitation and their original simulations, no significant differences were noticed when simulating at the same Q_{in}. Hence, the biomass production was not significantly changed due to diffusion limitation. The main reason for this was probably because COD removal was still occurring properly (failure of the system was due to N removal failure), resulting in optimal growth rates for X_{OHO} and X_{PAO}, who have a higher impact on the total mass in the system than X_{ANO}.

4.3.3.2 Simultaneous nitrification and denitrification

To further investigate which reactions were limited the most, nitrification by X_{ANO} and denitrification on S_F by X_{OHO} reaction rates for respectively better settling sludge and better settling sludge with strong and moderate diffusion limitation in bioreactor 6 were plotted in Figure 4.14 (Appendix A.4). Although also PAO perform denitrification, it was chosen to only plot one denitrification reaction based on OHO to investigate the general trend, since OHO were sufficiently more present in the system (as can be seen in Figure 4.9). Even with the oxygen set-point increase, the reaction rate of nitrification in the aerobic reactor was decreased in case of moderate diffusion limitation, and even more in case of strong diffusion limitation. The denitrification rate on the other hand, was increased extensively for moderate diffusion limitation, while it was decreased for strong diffusion limitation. Important to mention is that these reaction rates are directly proportional to the biomass concentrations X_{OHO} and

X_{ANO}. Although these reactions occur in the aerobic tank, since X_{OHO} are much more abundant compared to $X_{ANO,}$ the denitrification reactions have much higher rates [g COD.d^{-1}.m^{-3}] than the nitrification ones.

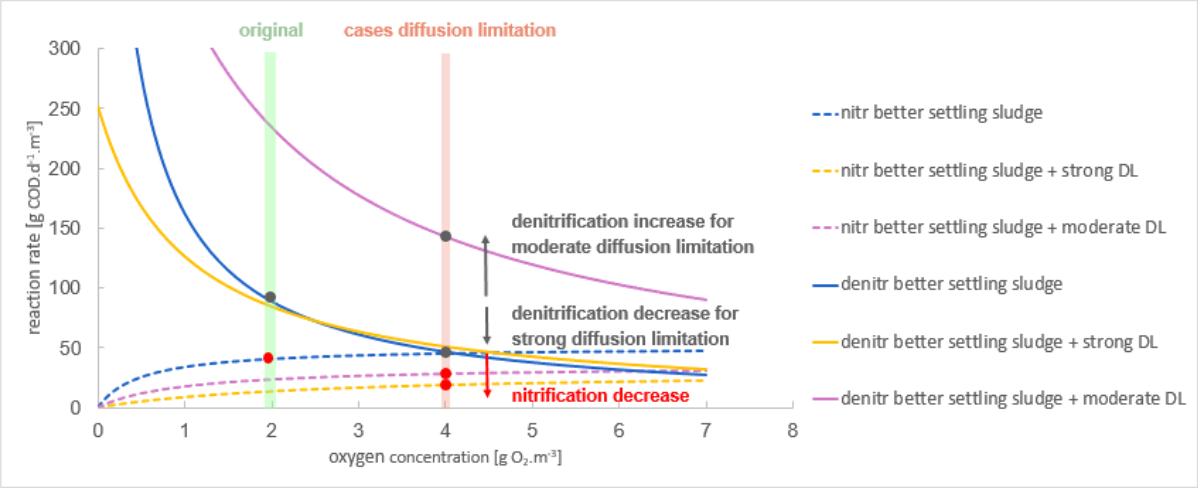

Figure 4.14: Reaction rates [g COD.d^{-1}.m^{-3}] for nitrification by X_{ANO} and denitrification on S_F by X_{OHO} as a function of the oxygen concentration in aerobic bioreactor 6, in case of absence and presence of both strong and moderate diffusion limitation (DL) (Appendix A.4, reactions 6 and 18). Absence of diffusion limitation is simulated by the optimal situation of better settling sludge, and the diffusion limitation cases represent the respective new optima. The substrate steady state concentrations of these simulations were used to calculate the reactions rates. In case of better settling sludge, the oxygen concentration was regulated at 2 g O_2.m^{-3}, while due to the diffusion limitation of aerobic granular sludge, the oxygen concentration had to be increased to 4 g O_2.m^{-3}.

The decrease in nitrification rates show that N removal, and more in particular nitrification, was the cause of failure of the system, which was more extensively for the strong than for the moderate diffusion limitation. Simultaneous nitrification and denitrification on the other hand, was clearly enhanced in case of moderate diffusion limitation compared to strong diffusion limitation. This was also confirmed by calculating the percentage simultaneous nitrification and denitrification in bioreactor 6, resulting in 30% for the strong diffusion limitation and 50% for the moderate diffusion limitation (Eq. 4.5). As a comparison, the percentage simultaneous nitrification and denitrification was already 34% in the optimal better settling sludge situation, meaning that no improvement for the strong diffusion limitation was achieved. In literature, values up till 90% are reported for batch systems (Layer *et al.*, 2020).

$$\%\text{sim nitr.}-\text{denitr.} = \frac{NO_3^- \text{ denitrified}}{NH_4^+ \text{ removed}} = \frac{\left(S_{NH_x,in} - S_{NH_x,out}\right) + S_{No_x,in} - S_{No_x,out}}{S_{NH_x,in} - S_{NH_x,out}} \quad [-] \qquad \textbf{Eq. 4. 5}$$

with S_{NH_x} = ammonium concentration [g N.m^{-3}]

S_{NO_x} = nitrate concentration [g N.m^{-3}]

To better understand the increase in denitrification rate due to diffusion limitation, the Monod terms for oxygen and nitrate in the reaction rates equations are given for the nitrification reaction by autotrophic biomass (Eq. 4.6) and the denitrification by ordinary heterotrophic organisms (Eq. 4.7) (full equation in Appendix A.4). Based on these equations, it can be seen that simultaneous nitrification

and denitrification was taken into account. The half-saturation coefficients also act as inhibition coefficients in the kinetic expressions of the reaction rates in the ASM2d model. $K_{O_2,OHO}$ [g $O_2.m^{-3}$] acts as a inhibition coefficient in the denitrification reaction, since it is placed in the nominator (Eq. 4.7). An increased inhibition coefficient decreases the inhibition of oxygen on the denitrification reaction in the aerobic tank, allowing it to occur there at a higher reaction rate than original. This is the reason that the denitrification curves for diffusion limitation are located above the one without diffusion limitation (for strong diffusion limitation only from 3 g $O_2.m^{-3}$ on). However, since $K_{O_2,OHO}$ did not change much between strong and moderate diffusion limitation, this cannot be the reason for the deviation between the denitrification rates in both cases. $K_{NO_x,OHO}$ [g $N.m^{-3}$] on the other hand, was significantly lower in case of moderate compared to strong diffusion limitation (0.58 vs. 2.50 g $N.m^{-3}$). The lower half saturation coefficient in case of moderate diffusion limitation allowed the denitrification reaction to occur more extensively, while in case of strong diffusion limitation the reaction was strongly limited, definitely with the higher oxygen concentration (Eq. 4.7).

$$\rho_{N,ANO} \sim \frac{S_{O_2}}{K_{O_2,ANO} + S_{O_2}} \qquad [\mathrm{g\ COD.\ m^{-3}.\ d^{-1}}]\ \mathbf{Eq.\ 4.6}$$

with $\rho_{N,ANO}$ = specific process rate of nitrification by ANO [g $COD.m^{-3}.d^{-1}$]

S_{O_2} = oxygen concentration [g $O_2.m^{-3}$]

$K_{O_2,ANO}$ = half saturation parameter of ANO for S_{O_2} [g $O_2.m^{-3}$]

$$\rho_{DN,OHO} \sim \frac{K_{O_2,OHO}}{K_{O_2,OHO} + S_{O_2}} * \frac{S_{No_x}}{K_{NO_x,OHO}+S_{No_x}} \qquad [\mathrm{g\ COD.\ m^{-3}.\ d^{-1}}]\ \mathbf{Eq.\ 4.7}$$

with $\rho_{DN,OHO}$ = specific process rate of denitrification by OHO [g $COD.m^{-3}.d^{-1}$]

S_{O_2} = oxygen concentration [g $O_2.m^{-3}$]

S_{No_x} = nitrate/nitrite concentration [g $N.m^{-3}$]

$K_{O_2,OHO}$ = half saturation/inhibition parameter of OHO for S_{O_2} [g $O_2.m^{-3}$]

$K_{NO_x,OHO}$ = Half saturation parameter of OHO for S_{NO_x} [g $O_2.m^{-3}$]

It seems that increasing the half saturation coefficients, and thus also increasing inhibition coefficients, affected both reactions differently due to the complex interaction between the different Monod terms. This shows that different values for half saturation coefficients strongly affect the reaction rates and thus the final maximal treatment capacity of the system. Particularly the improvement of nitrification performance should be the first concern, i.e. the optimal design and control strategies needed to optimize the nitrification rate. Only when nitrification is performing well, also the performance and optimization of simultaneous nitrification and denitrification should be revised.

4.3.3.3 Perspectives for diffusion limitation in continuous systems

The actual degree of diffusion limitation in continuous systems is hard to predict and will depend on the granule density, size, microbial population distribution and competition for substrates.
On the one hand, granules in continuous systems most likely will be smaller than in batch systems, which could result in less diffusion limitation (Jahn *et al.*, 2019). Hence, substrates do not have to diffuse that deep into the granules due to their smaller radius, which would result in less diffusion limitation. Based on this reasoning, the used values for the half saturation coefficients, which were based on batch models, might have been an overestimation. Lower values for the half saturation coefficients would also result in significantly different conclusions. The half saturation coefficient of ANO for O_2 per example, $K_{O_2,ANO}$, can vary between 0.4 and 3 g O_2.m^{-3} dependent of the type of granule (Baeten *et al.*, 2018). As a side note, less diffusion limitation would also imply that less simultaneous nitrification and denitrification can occur.
On the other hand, based on these outcomes, diffusion limitation seems to be a more important aspect in continuous systems than in batch systems due to the difference in substrate concentration. In batch systems, a gradual decrease in substrate concentrations over time occurs in the reactor. On the contrary, in continuous systems, completely mixed conditions result in low substrate concentrations. These lower substrate concentrations in continuous systems could cause even more limitation. This effect may also be seen in Eq. 3.2: the lower the substrate concentration, the lower the degradation reaction rates will be. It has to be noticed though that in the used model a sequence of seven completely mixed bioreactors is used, which already partly simulated this gradual decrease in substrate concentrations (plugflow-like). However, the diffusion limitation was still severe.
Hence, in order to counteract this more severe diffusion limitation in continuous systems, it might be interesting to keep the granules as small as possible, provided that the settling velocity is still sufficiently high to improve the biomass concentration in the system.

Since it was mostly nitrification that failed due to diffusion limitation and there did not seem to be oxygen shortage, it might be interesting to further investigate what the reason for this failure was. This could possibly be explained by the unchanged composition of microbial groups in the aerobic granular sludge system compared to the activated sludge case. OHO dominated in the system, which is representative for activated sludge, but should actually be revised for aerobic granular sludge, since these are supposed to select for slow growing organisms, i.e. PAO/GAO (de Kreuk & van Loosdrecht, 2004). This microbial composition could be the reason why nitrification failed first, since fast growing OHO strongly compete with ANO for oxygen, which would be less the case for slow growing PAO.

Hence, although these diffusion limitation scenarios did not result in a higher maximal treatment capacity than possible with the conventional activated sludge system, this does not mean that it is proven that granules in continuous systems are disadvantageous. However, also the opposite is not demonstrated. It was shown that diffusion limitation can possibly counteract the positive effect of better settling sludge of aerobic granules in continuous systems. The severity of this diffusion limitation in continuous systems is non-negligible, although it is not mentioned in literature (Kent *et al.*, 2018).

4.3.4 Energy consumption

In general, the most important contribution to the energy consumption was the aeration energy, which was significantly higher in case of aerobic granular sludge (Table 4.1). The reason for this is the higher imposed oxygen set-point, which was 4 g $O_2.m^{-3}$ for aerobic granular sludge compared to 2 g $O_2.m^{-3}$ for activated sludge. This higher set-point was imposed to counteract the severe nitrification reduction because of diffusion limitation. On top of that, the optimal situation for aerobic granular sludge is at a higher biomass concentration (6 versus 5 kg $TSS.m^{-3}$), which consumed more oxygen. As previously mentioned, the SRT values for aerobic granular sludge were higher, resulting in more endogenous respiration. Simultaneous nitrification and denitrification induces more denitrification in the aerobic tank, resulting in less nitrate that needs to be internally recycled and thus lower optimal Q_{int}, which might result in a lower oxygen set-point. This would lead to lower aeration energy needs but was not taken into account in this research since Q_{int}:Q_{in} was fixed. As for the difference between the strong and moderate diffusion limitation scenario, less limitation allows higher loads to be treated, resulting in lower energy needed per m^3 treated water.

Table 4.1: Energy contributions for the optimal activated sludge and aerobic granular sludge systems with strong and moderate diffusion limitation (DL) (Appendix A.10). Activated sludge: X_{TSS} = 5 kg $TSS.m^{-3}$ and treatment capacity 1.46 kg $COD.d^{-1}.m^{-3}$. Aerobic granular sludge: strong diffusion limitation: X_{TSS} = 6 kg $TSS.m^{-3}$ and treatment capacity 0.67 kg $COD.d^{-1}.m^{-3}$, moderate diffusion limitation: X_{TSS} = 6 kg $TSS.m^{-3}$ and treatment capacity 1.47 kg $COD.d^{-1}.m^{-3}$.

Energy contribution	Activated sludge	Aerobic granular sludge: strong DL	Aerobic granular sludge: moderate DL
Pumping energy [$Wh.m^{-3}$]	33	32	33
Aeration energy [$Wh.m^{-3}$]	215	377	308
Mixing energy [$Wh.m^{-3}$]	16	35	16
TOTAL [$Wh.m^{-3}$]	263	444	356

The pumping energy did not change much between the different simulations because of the fixed recycle ratios (Table 4.1). Since the recycle flow rates (Q_r, Q_{int}) were adapted to the influent flow rate (Q_{in}) and the energy consumption is expressed per volume of water treated (Q_{in}), the resulting value is quite constant. As a side note, it should be mentioned that some presumably beneficial aspects of aerobic granular sludge were not taken into account in this simplified simulation. First of all, due to the better settleability of the sludge, better thickening could occur, leading to higher biomass concentration in the recycle sludge Q_r and thus more energy efficient transport. This would result in lower Q_r needed to transport the same mass of sludge. However, increasing the settling velocity did not increase the TSS concentration in Q_r in the simplified model. Secondly, simultaneous nitrification and denitrification can result in a lower optimal value for the internal recycle flow rate Q_{int}. Since fixed recycle ratios Q_r:Q_{in} and Q_{int}:Q_{in} were used for simplicity, these advantage were not simulated in this thesis. These effects could have led to lower pumping energy in case of aerobic granular sludge. However, important to mention is that it was not the pumping energy that was the most important contributor to the total energy consumption, but the aeration energy.

Lastly, the mixing energy is much higher in the strong diffusion limitation scenario of aerobic granular sludge. This is because of the lower load that the system can treat. This lower maximal treatment capacity (and thus Q_{in}) was treated in the same design for all cases, leading to a higher mixing energy per m^3 of treated water.

5. General conclusions

Introducing aerobic granules in continuous systems is a new endeavor in the wastewater treatment research area , leading to a lot of research on granulation and stabilization of granules in continuous systems. However, this thesis took a step back to first of all investigate whether the operating conditions of a continuous activated sludge system are sufficiently fit in the first place to optimally benefit from the advantages of aerobic granular sludge. Assuming that it would be possible to cultivate stable granules in continuous systems and that long-term stability of the granules is achieved, the following research question was answered:

"Would continuous aerobic granular sludge plants have a higher treatment capacity and/or lower energy consumption compared to the conventional activated sludge plants with the same design and effluent criteria?".

Based on a model simulation study in Matlab, the following results were obtained:

- The treatment capacity of the modelled continuous activated sludge plant with a fixed, low TSS concentration (2-4 kg TSS.m^{-3}) was determined by failure of nitrification. The settler capacity was not limiting in this case.
- When controlling the TSS concentration in the reactor at higher set-points (5-6 kg TSS.m^{-3}), the treatment capacity was determined by settler failure, as observed by TSS concentrations exceeding the effluent standard. However, settler failure was quickly followed by an exceedance of the effluent total nitrogen limits because of the organically bound nitrogen in TSS leaving with the effluent.
- An increased settling velocity, up to a high value typical for aerobic granular sludge, led to an increased maximal treatment capacity (by 39%) which was obtained at a higher TSS set-point (6 vs 5 kg TSS.m^{-3}). Failure of nitrification was again the limiting factor at lower TSS concentrations (4 - 6 kg TSS.m^{-3}), while failure of the settler determined the treatment capacity at higher TSS concentrations (7 - 8 kg TSS.m^{-3}).
- When diffusion limitation was simulated for aerobic granular sludge, the maximal treatment capacity of the activated sludge system was decreased depending on the extent of diffusion limitation (65% in case of strong diffusion limitation and 28% for moderate diffusion limitation).
- Simulating both the higher settling velocity and diffusion limitation resulted in a decrease of the maximal treatment capacity of the system with 54% for a strong diffusion limitation scenario, compared to a practically unchanged treatment capacity in case of moderate diffusion limitation.
- The individual effects of diffusion limitation and better settling were not simply additive. The negative effect of diffusion limitation clearly outweighed the positive effect of better settling sludge in both diffusion limitation scenarios. Hence, it seems that diffusion limitation has a more severe impact in continuous systems than in batch systems, probably because of the lower substrate concentrations in continuous systems.
- Granules in continuous systems are generally smaller than in batch systems, which would lead to less diffusion limitation (Jahn *et al.*, 2019). Since the diffusion limitation parameters were based on batch models, it may be that the severity of diffusion limitation was overestimated in this thesis. It seems recommended to keep granules as small as possible while maintaining good settling properties in continuous systems.

- The energy consumption in case of aerobic granular sludge was higher than in case of activated sludge, primary because of higher aeration energy. Higher oxygen set-points were needed in case of aerobic granular sludge to counteract the severe diffusion limitation.

Overall, the results obtained in this thesis indicated that due to low substrate concentrations, diffusion limitation might be the bottleneck of aerobic granular sludge in continuous systems, possibly completely counteracting the positive effect of better settling sludge. However, based on this research, no clear statements regarding the beneficial effect of replacing activated sludge with aerobic granular sludge in continuous systems can be made. More care has to be taken in the process configuration and the optimal operating conditions of the continuous system in order to benefit from the advantages of aerobic granular sludge in existing continuous flow reactors.

6. Recommendations for further research

Overall, while the advantages of aerobic granular sludge are proven, further research is required to substantiate its added value in our existing continuous systems. This further research is situated on three domains. These domains are firstly the settling ability and diffusion limitation of aerobic granules in continuous systems, secondly the optimization of the design and operating conditions of the continuous wastewater treatment plant with aerobic granular sludge, and thirdly the differences between aerobic granules in batch and continuous systems.

The variability in settling ability and diffusion limitation of aerobic granules in continuous systems should be further investigated to quantify the associated potential of increasing the treatment capacity of the conventional activated sludge systems.

- A first important parameter is the maximal settling velocity attainable with granules in a continuous system. Based on lab-scale continuous aerobic granular sludge systems, a wide range of settling velocities is reported, with peak values around 70 - 90 $m.h^{-1}$ (Thanh *et al.*, 2009; Winkler *et al.*, 2012). This would mean that the settling velocity of granules would be around 10 times higher than that of activated sludge, compared to the average factor 5 used in this thesis. Further simulations of the aerobic granular sludge model over a range of settling velocities could quantify their effect on the optimal biomass concentration in the system and the associated maximal treatment capacity. An improvement of the maximal treatment capacity of the system due to higher settling velocities would better withstand against the negative effect of diffusion limitation.
- Furthermore, also more insight in the severity of diffusion limitation in continuous systems due to the low substrate concentrations is needed. If reliable ranges for the half saturation coefficients could be obtained based on a lab-scale continuous aerobic granular sludge system instead of the values based on batch models used in this thesis, more correct outcomes regarding the maximal treatment capacity could be obtained. Hence, it would become clear whether diffusion limitation would really be as severe as it was based on the simulations in this thesis.
- The optimal TSS concentration of the continuous aerobic granular sludge system should also be further investigated. In this research, it was assumed that the optimal TSS concentration of the system with better settling sludge would also be the optimal concentration if diffusion limitation was added, which may not be the case. To this end, the maximal treatment capacity of the aerobic granular sludge system also needs to be determined at other TSS concentrations to see where it peaked in a similar way as was done for activated sludge and better settling sludge in this thesis. Even though quite straightforward, this was not yet accomplished because of time constraints.

Optimization of the design and operating conditions of the continuous wastewater treatment plant in order to fully benefit from the advantages of aerobic granular sludge, is a second important topic for further research. In this thesis, the effect of introducing aerobic granules into the existing continuous installations was investigated, without changing anything in terms of reactor configuration and control strategies. Hence, nitrification was the primary inducer of failure of the system. This nitrification performance should be first optimized before looking at the performance of denitrification and the accompanied simultaneous nitrification and denitrification. The following steps are proposed to improve the nitrogen removal performance:

- The composition of microbial groups in the aerobic granular sludge system was the same as in case of activated sludge in this thesis. OHO dominated in the system, which is representative for activated sludge, but should actually be revised for aerobic granular sludge, since these are supposed to select for slow growing organisms, i.e. PAO/GAO (de Kreuk & van Loosdrecht, 2004). PAO are selected by applying feast-famine conditions to the system, which did not seem to be imposed enough by the seven bioreactors in series in the model. This microbial composition could be the reason why nitrification failed first, since fast growing OHO strongly compete with ANO for oxygen, which would be less the case for slow growing PAO. Optimization of the oxygen control strategy or maybe even of the process configuration (two anoxic tanks followed by three aerobic ones) may help imposing these feast-famine conditions with alternating anaerobic and aerobic phases to select for PAO (Van Loosdrecht *et al.*, 2005).
- Once full nitrification is obtained in the system, the optimal internal (nitrate) recycle flow rate should be determined and controlled to achieve maximum denitrification and thus overall nitrogen removal performance of the system. This could be done by controlling the nitrate concentration in the anoxic tank to a set-point of per example 1 g $N.m^{-3}$.
- The oxygen set-point also plays a role in the optimization of denitrification. Firstly, more anoxic reactions by DPAO could reduce the oxygen set-point needed. Secondly, the optimal oxygen set-point for simultaneous nitrification and denitrification should be imposed to optimally benefit from the aerobic granular sludge.

Lastly, more intensively investigating the differences between aerobic granules in batch and continuous systems could help to better understand the severe diffusion limitation effect in continuous systems. A greenfield operation could be considered. If a new design with aerobic granular sludge should be chosen, should a batch or continuous system be recommended? An aerobic granular sludge batch model with the same anaerobic, anoxic and aerobic HRT as in the model for the continuous system in this thesis could be used to answer this question. Based on a fixed treatment capacity, the comparison in terms of energy consumption, surface area and cost (investment + operational) of both systems could be elaborated on. Furthermore, does the optimal biomass concentration differ between a batch and continuous system? Does diffusion limitation have a more severe effect in continuous systems than batch systems, as indicated by the results obtained in this thesis? The latter question could be answered by simulating better settling sludge and diffusion limitation separately to investigate their individual contribution to the maximal treatment capacity, as was done in this thesis, but for batch systems.

7. References

Adav, S. S., Lee, D. J., Show, K. Y., & Tay, J. H. (2008). Aerobic granular sludge: Recent advances. *Biotechnology Advances*, 26(5), 411-423. doi:10.1016/j.biotechadv.2008.05.002

Alex, J., Benedetti, L., Copp, J., Gernaey, K., Jeppsson, U., Nopens, I., Pons, M., Steyer, J. & Vanrolleghem, P. (2008a). Benchmark simulation model No. 1 (BSM1). *IWA Taskgroup on Benchmarking of Control Strategies for WWTPs*, 19-20.

Alex, J., Benedetti, L., Copp, J., Gernaey, K., Jeppsson, U., Nopens, I., Pons, M., Steyer, J. & Vanrolleghem, P. (2008b). Benchmark Simulation Model No. 2 (BSM2), Tech. rep., *IWA Taskgroup on Benchmarking of Control Systems for WWTPs*.

Anuar, A. N., Ujang, Z., van Loosdrecht, M. C. M., & de Kreuk, M. (2007). Settling behaviour of aerobic granular sludge. *Water Science and Technology*, 56(7), 55-63.

Baeten, J. E., van Loosdrecht, M. C. M., & Volcke, E. I. P. (2018). Modelling aerobic granular sludge reactors through apparent half-saturation coefficients. *Water Research*, 146, 134-145. doi:10.1016/j.watres.2018.09.025

Bathe, S., de Kreuk, M. K., McSwain, B. S., & Schwarzenbeck, N. (Eds.). (2005). *Aerobic granular sludge*. London: IWA Publishing.

Bengtsson, S., de Blois, M., Wilen, B. M., & Gustavsson, D. (2018). Treatment of municipal wastewater with aerobic granular sludge. *Critical Reviews in Environmental Science and Technology*, 48(2), 119-166. doi:10.1080/10643389.2018.1439653

Beun, J. J., Hendriks, A., Van Loosdrecht, M. C. M., Morgenroth, E., Wilderer, P. A., & Heijnen, J. J. (1999). Aerobic granulation in a sequencing batch reactor. *Water Research*, 33(10), 2283-2290. doi:10.1016/s0043-1354(98)00463-1

Bye, C. M., & Dold, P. L. (1999). Evaluation of correlations for zone settling velocity parameters based on sludge volume index-type measures and consequences in settling tank design. *Water Environment Research*, 71(7), 1333-1344. doi:10.2175/106143096x122348

Caluwé, M. (November 5, 2018). *Feest bij bacteriën zorgt voor proper water*. Retrieved October 18 from https://www.phdcup.be/nieuws/feest-bij-bacterien-zorgt-voor-proper-water

Caluwe, M., Dobbeleers, T., Daens, D., Geuens, L., Blust, R., & Dries, J. (2018). SBR treatment of tank truck cleaning wastewater: sludge characteristics, chemical and ecotoxicological effluent quality. *Environmental Technology*, 39(19), 2524-2533. doi:10.1080/09593330.2017.1359342

Carrera, P., Campo, R., Mendez, R., Di Bella, G., Campos, J. L., Mosquera-Corral, A., & Val del Rio, A. (2019). Does the feeding strategy enhance the aerobic granular sludge stability treating saline effluents? *Chemosphere*, 226, 865-873. doi:10.1016/j.chemosphere.2019.03.127

Chen, Y. Y., Ju, S. P., & Lee, D. J. (2016). Aerobic granulation of protein-rich granules from nitrogen-lean wastewaters. *Bioresource Technology*, 218, 469-475.doi:10.1016/j.biortech.2016.06.120

Clayton, J. A., Ekama, G. A., Wentzel, M. C., & Marais, G. V. R. (1991). Denitrification kinetics in biological nitrogen and phosphorus removal activated sludge systems treating mmunicipal wastewaters. *Water Science and Technology*, 23(4-6), 1025-1035.

Cobelpa. (n.d.). *Waterzuiveringstation bij SAPPI Lanaken*. Retrieved November 16 from http://www.cobelpa.be/nl/ss14bis.html

Comeau, Y., Hall, K. J., Hancock, R. E. W., & Oldham, W. K. (1986). Biochemical model for Enhanced biological phosphorus removal. *Water Research*, 20(12), 1511-1521. doi:10.1016/0043-1354(86)90115-6

Corominas, L., Rieger, L., Takacs, I., Ekama, G., Hauduc, H., Vanrolleghem, P. A., Oehmen,A., Gernaey, K.V., van Loosdrecht, M.C.M., Comeau, Y. (2010). New framework for standardized notation in wastewater treatment modelling. *Water Science and Technology*, 61(4), 841-857. doi:10.2166/wst.2010.912

Corsino, S. F., Campo, R., Di Bella, G., Torregrossa, M., & Viviani, G. (2016). Study of aerobic granular sludge stability in a continuous-flow membrane bioreactor. *Bioresource Technology*, 200, 1055-1059. doi:10.1016/j.biortech.2015.10.065

Council of European Communities. (1991). *Council directive of 21 May 1991 concerning urban waste water treatment.* Retrieved March 10 from https://eur-lex.europa.eu/LexUriServ/LexUriServ.do?uri=OJ:L:1991:135:0040:0052:EN:PDF%20

de Bruin, L. M. M., de Kreuk, M. K., van der Roest, H. F. R., Uijterlinde, C., & van Loosdrecht, M. C. M. (2004). Aerobic granular sludge technology: an alternative to activated sludge? *Water Science and Technology*, 49(11-12), 1-7.

de Kreuk, M., Heijnen, J. J., & van Loosdrecht, M. C. M. (2005a). Simultaneous COD, nitrogen, and phosphate removal by aerobic granular sludge. *Biotechnology and Bioengineer*ing, 90(6), 761-769. doi:10.1002/bit.20470

de Kreuk, M. K., De Bruin, L. M. M., & Van Loosdrecht, M. C. M. (2005b). Aerobic granular sludge: From idea to pilot plant. *Aerobic granular sludge. IWA Publishing, London*, *UK*, 111-124.

de Kreuk, M. K., Kishida, N., & van Loosdrecht, M. C. M. (2007). Aerobic granular sludge - state of the art. *Water Science and Technology*, 55(8-9), 75-81. doi:10.2166/wst.2007.244

de Kreuk, M. K., & van Loosdrecht, M. C. M. (2004). Selection of slow growing organisms as a means for improving aerobic granular sludge stability. *Water Science and Technology*, 49(11-12), 9-17.

Devlin, T. R., & Oleszkiewicz, J. A. (2018). Cultivation of aerobic granular sludge in continuous flow under various selective pressure. *Bioresource Technology*, 253, 281-287. doi:10.1016/j.biortech.2018.01.056

Ekama, G. A., & Marais, P. (2004). Assessing the applicability of the ID flux theory to full-scale secondary settling tank design with a 2D hydrodynamic model. *Water Research*, 38(3), 495-506. doi:10.1016/j.watres.2003.10.026

Emis. (2015). *Actief slib systemen*. Retrieved October 8 from https://emis.vito.be/nl/techniekfiche/actief-slib-systemen

EPA, U. (1999). Wastewater technology fact sheet—sequencing batch reactors. *US Environmental Protection Agency,* Office of Water, EPA, Washington DC.

Espinosa-Ortiz, E. J., Rene, E. R., Pakshirajan, K., van Hullebusch, E. D., & Lens, P. N. L. (2016). Fungal pelleted reactors in wastewater treatment: Applications and perspectives. *Chemical Engineering Journal*, 283, 553-571. doi:10.1016/j.cej.2015.07.068

EssDe. (n.d. a). S::Select® solves the problem of bulking sludge and multiplies the capacity of the Biological Reactor. Retrieved November 26 from https://www.essde.com/s-select-fights-bulking-sludge

EssDe. (n.d. b). S::Select ® - the ideal biological activated sludge system. Retrieved November 26 from https://www.essde.com/s-select-the-ideal-biological-system

Etterer, T., & Wilderer, P. A. (2001). Generation and properties of aerobic granular sludge. Water Science and Technology, 43(3), 19-26.

European Commission. (2016, May 30). Decisions commission implementing decision (EU)

2016/902 of 30 May 2016 establishing best available techniques (BAT) conclusions, under Directive 2010/75/EU of the European Parliament and of the Council, for common waste water and waste gas treatment/ management systems in the chemical sector. *Official Journal of the European Union.* Retrieved August 26 from https://eippcb.jrc.ec.europa.eu/reference/BREF/BATC_CWW.pdf

European Commission. (2019, July 8). *Introduction to the EU Water Framework Directive*. Retrieved August 26 from https://ec.europa.eu/environment/water/water-framework/info/intro_en.htm

Flores-Alsina, X., Mbamba, C. K., Solon, K., Vrecko, D., Tait, S., Batstone, D. J., .Jeppsson, U., Gernaey, K. V. (2015). A plant-wide aqueous phase chemistry module describing pH variations and ion speciation/pairing in wastewater treatment process models. *Water Research*, 85, 255-265. doi:10.1016/j.watres.2015.07.014

Focht, D. D., & Chang, A. C. (1975). Nitrification and denitrification processes related to waste water treatment. *Advances in applied microbiology*, 19, 153-186

Ford, A., Rutherford, B., Wett, B., & Bott, C. (2016). Implementing hydrocyclones in mainstream process for enhancing biological phosphorus removal and increasing settleability through aerobic granulation. *Proceedings of WEFTEC 2016*, 2809-2822.

Franca, R. D. G., Pinheiro, H. M., van Loosdrecht, M. C. M., & Lourenco, N. D. (2018). Stability of aerobic granules during long-term bioreactor operation. *Biotechnology Advances*, 36(1), 228-246. doi:10.1016/j.biotechadv.2017.11.005

Gao, D. W., Liu, L., Liang, H., & Wu, W. M. (2011). Aerobic granular sludge: characterization, mechanism of granulation and application to wastewater treatment. *Critical Reviews in Biotechnology*, 31(2), 137-152. doi:10.3109/07388551.2010.497961

Genesis water tech. (2019, June 14). *7 Disadvantages of Using an Activated Sludge Process For Your Municipality or Company.* Retrieved October 1 from https://genesiswatertech.com/blog-post/7-disadvantages-of-using-an-activated-sludge-process-for-your-municipality-or-company/

Gernaey, K. V., Jeppsson, U., Vanrolleghem, P. A., & Copp, J. B. (Eds.). (2014). *Benchmarking of control strategies for wastewater treatment plants*. IWA Publishing.

Gernaey, K., Mussati, M., Yuan, Z., Nielsen, M. K., & Jørgensen, S. B. (2002). Control strategy evaluation for combined N and P removal using a benchmark wastewater treatment plant. *IFAC Proceedings Volumes*, 35(1), 381-386.

Gernaey, K. V., van Loosdrecht, M. C. M., Henze, M., Lind, M., & Jorgensen, S. B. (2004). Activated sludge wastewater treatment plant modelling and simulation: state of the art. *Environmental Modelling & Software*, 19(9), 763-783. doi:10.1016/j.envsoft.2003.03.005

Hauduc, H., Rieger, L., Takacs, I., Heduit, A., Vanrolleghem, P. A., & Gillot, S. (2010). A systematic approach for model verification: application on seven published activated sludge models. *Water Science and Technology*, 61(4), 825-839. doi:10.2166/wst.2010.898

He, Q. L., Zhang, S. L., Zou, Z. C., Zheng, L. A., & Wang, H. Y. (2016). Unraveling characteristics of simultaneous nitrification, denitrification and phosphorus removal (SNDPR) in an aerobic granular sequencing batch reactor. *Bioresource Technology*, 220, 651-655. doi:10.1016/j.biortech.2016.08.105

Henze, M., Gujer, W., Mino, T., & van Loosdrecht, M. C. (2000). *Activated sludge models ASM1, ASM2, ASM2d and ASM3*. IWA publishing

Henze, M., van Loosdrecht, M. C., Ekama, G. A., & Brdjanovic, D. (Eds.). (2008). *Biological wastewater treatment*. IWA publishing.

Hu, L. L., Wang, J. L., Wen, X. H., & Qian, Y. (2005). The formation and characteristics of aerobic granules in sequencing batch reactor (SBR) by seeding anaerobic granules. *Process Biochemistry*, 40(1), 5-11. doi:10.1016/j.procbio.2003.11.033

Irvine, R. L., Ketchum Jr, L. H., & Asano, T. (1989). Sequencing batch reactors for biological wastewater treatment. *Critical Reviews in Environmental Science and Technology*, *18*(4), 255-294.

Isaacs, S. H., & Henze, M. (1995). Controlled carbon source addition to an alternating nitrification denitrification wastewater treatment process including biological P-removal. *Water Research*, 29(1), 77-89. doi:10.1016/0043-1354(94)e0119-q

Ivanov, V., Tay, J. H., Liu, Q. S., Wang, X. H., Wang, Z. W., Maszenan, B. A. M., ... & Tay, S. T. L. (2005). Microstructural optimization of wastewater treatment by aerobic granular sludge. *Aerobic granular sludge. IWA Publishing, London*, *UK*, 43-52.

Jahn, L., Svardal, K., & Krampe, J. (2019). Comparison of aerobic granulation in SBR and continuous-flow plants. *Journal of Environmental Management*, 231, 953-961. doi:10.1016/j.jenvman.2018.10.101

Jeppsson, U., Alex, J., Pons, M. N., Spanjers, H., & Vanrolleghem, P. A. (2002). Status and future trends of ICA in wastewater treatment - a European perspective. *Water Science and Technology*, 45(4-5), 485-494.

Juang, Y. C., Adav, S. S., Lee, D. J., & Tay, J. H. (2010). Stable aerobic granules for continuous-flow reactors: Precipitating calcium and iron salts in granular interiors. *Bioresource Technology*, 101(21), 8051-8057. doi:10.1016/j.biortech.2010.05.078

Kawase, Y., & Moo-Young, M. (1990). Mathematical models for design of bioreactors: Applications of: Kolmogoroff's theory of isotropic turbulence. *The Chemical Engineering Journal*, *43*(1), B19-B41.

Kent, T. R., Bott, C. B., & Wang, Z. W. (2018). State of the art of aerobic granulation in continuous flow bioreactors. *Biotechnology Advances*, 36(4), 1139-1166. doi:10.1016/j.biotechadv.2018.03.015

Layer, M., Villodres, M. G., Hernandez, A., Reynaert, E., Morgenroth, E., & Derlon, N. (2020). Limited simultaneous nitrification-denitrification (SND) in aerobic granular sludge systems treating municipal wastewater: Mechanisms and practical implications. *Water research X*, 100048.

Li, D., Lv, Y. F., Zeng, H. P., & Zhang, J. (2016). Startup and long term operation of enhanced biological phosphorus removal in continuous-flow reactor with granules. *Bioresource Technology*, 212, 92-99. doi:10.1016/j.biortech.2016.04.008

Li, J., Cai, A., Ding, L. B., Sellamuthu, B., & Perreault, J. (2015). Aerobic sludge granulation in a Reverse Flow Baffled Reactor (RFBR) operated in continuous-flow mode for wastewater treatment. *Separation and Purification Technology*, 149, 437-444. doi:10.1016/j.seppur.2015.04.045

Li, J., Garny, K., Neu, T., He, M., Lindenblatt, C., & Horn, H. (2007). Comparison of some characteristics of aerobic granules and sludge flocs from sequencing batch reactors. *Water Science and Technology*, 55(8-9), 403-411. doi:10.2166/wst.2007.284

Li, Y., & Liu, Y. (2005). Diffusion of substrate and oxygen in aerobic granule. *Biochemical Engineering Journal*, 27(1), 45-52. doi:10.1016/j.bej.2005.06.012

Li, X. M., Yang, G. J., Yang, Q., Zeng, G. M., Liao, D. X., Hu, M. F., & Wu, Y. M. (2005). Simultaneous phosphorus and nitrogen removal by aerobic granular sludge in single SBR system. *Aerobic granular sludge. IWA Publishing, London*, *UK*, 71-78.

Liu, H. B., Li, Y. J., Yang, C. Z., Pu, W. H., He, L., & Bo, F. (2012). Stable aerobic granules in continuous-flow bioreactor with self-forming dynamic membrane. *Bioresource Technology*, 121, 111-118. doi:10.1016/j.biortech.2012.07.016

Liu, H. B., Xiao, H., Huang, S., Ma, H. J., & Liu, H. (2014). Aerobic granules cultivated and operated in continuous-flow bioreactor under particle-size selective pressure. *Journal of Environmental Sciences*, 26(11), 2215-2221. doi:10.1016/j.jes.2014.09.004

Liu, J., Li, J., Tao, Y. Q., Sellamuthu, B., & Walsh, R. (2017). Analysis of bacterial, fungal and archaeal populations from a municipal wastewater treatment plant developing an innovative aerobic granular sludge process. *World Journal of Microbiology & Biotechnology*, 33(1). doi:10.1007/s11274-016-2179-0

Liu, Y., & Tay, J. H. (2004). State of the art of biogranulation technology for wastewater treatment. *Biotechnology Advances*, 22(7), 533-563. doi:10.1016/j.biotechadv.2004.05.001

Liu, Y., Wang, Z. W., Qin, L., Liu, Y. Q., & Tay, J. H. (2005a). Selection pressure-driven aerobic granulation in a sequencing batch reactor. *Applied Microbiology and Biotechnology*, 67(1), 26-32. doi:10.1007/s00253-004-1820-2

Liu, Y., Wang, Z. W., & Tay, J. H. (2005b). A unified theory for upscaling aerobic granular sludge sequencing batch reactors. *Biotechnology Advances*, 23(5), 335-344. doi:10.1016/j.biotechadv.2005.04.001

Liu, Y. Q., Lan, G. H., & Zeng, P. (2015). Excessive precipitation of CaCO3 as aragonite in a continuous aerobic granular sludge reactor. *Applied Microbiology and Biotechnology*, 99(19), 8225-8234. doi:10.1007/s00253-015-6727-6

Lu, Y. Z., Wang, H. F., Kotsopoulos, T. A., & Zeng, R. J. (2016). Advanced phosphorus recovery using a novel SBR system with granular sludge in simultaneous nitrification, denitrification and phosphorus removal process. *Applied Microbiology and Biotechnology*, 100(10), 4367-4374. doi:10.1007/s00253-015-7249-y

Lübken, M., Schwarzenbeck, N., Wichern, M., & Wilderer, P. A. (2005). Modelling nutrient removal of an aerobic granular sludge lab-scale SBR using ASM3. *Aerobic granular sludge. IWA Publishing, London*, *UK*, 103-110.

Mahvi, A. H. (2008). Sequencing batch reactor: a promising technology in wastewater treatment. *Journal of Environmental Health Science & Engineering*, *5*(2), 79-90.

Manea, E. E., & Bumbac, C. (2019). Performance Evaluation of Continuous Flow Aerobic Granular Sludge Configurations. *Revista De Chimie*, 70(1), 283-285.

McSwain, B. S., Irvine, R. L., & Wilderer, P. A. (2005). Population dynamics during aerobic granule formation: lessons from denaturing gradient gel electrophoresis. *Aerobic granular sludge. IWA Publishing, London*, *UK*, 53-61.

Metcalf & Eddy. (2004). *Wastewater Engineering. Treatment and Reuse, fourth ed.* New York: McGraw Hill. Cited by Rabaey & Vlaeminck (2017).

Morales, N., Figueroa, M., Mosquera-Corral, A., Campos, J. L., & Mendez, R. (2012). Aerobic granular-type biomass development in a continuous stirred tank reactor. *Separation and Purification Technology*, 89, 199-205. doi:10.1016/j.seppur.2012.01.024

Morgenroth, E., Sherden, T., van Loosdrecht, M. C. M., Heijnen, J. J., & Wilderer, P. A. (1997). Aerobic granular sludge in a sequencing batch reactor. *Water Research*, 31(12), 3191-3194. doi:10.1016/s0043-1354(97)00216-9

Mosquera-Corral, A., Vázquez-Padín, J. R., Arrojo, B., & Campos, J. L. (2005). Nitrifying granular sludge in a Sequencing Batch. *Aerobic granular sludge. IWA Publishing, London*, *UK*, 63.

Ni, B. J., Xie, W. M., Liu, S. G., Yu, H. Q., Wang, Y. Z., Wang, G., & Dai, X. L. (2009). Granulation of activated sludge in a pilot-scale sequencing batch reactor for the treatment of low-strength municipal wastewater. *Water Research*, 43(3), 751-761. doi:10.1016/j.watres.2008.11.009

Nopens, I., Benedetti, L., Jeppsson, U., Pons, M. N., Alex, J., Copp, J. B., Gernaey, K.V., Rosen, C., Steyer, J.-P., Vanrolleghem, P. A. (2010). Benchmark Simulation Model No 2: finalisation of plant layout and default control strategy. *Water Science and Technology*, 62(9), 1967-1974. doi:10.2166/wst.2010.044

Oehmen, A., Lemos, P. C., Carvalho, G., Yuan, Z. G., Keller, J., Blackall, L. L., & Reis, M. A. M. (2007). Advances in enhanced biological phosphorus removal: From micro to macro scale. *Water Research*, 41(11), 2271-2300. doi:10.1016/j.watres.2007.02.030

Onken, U., & Weiland, P. (1983). Airlift fermenters: Construction, behavior, and uses. *Adv. biotechnol. Process.*, *1*, 67-95.

Pitman, A. R. (1991). Design considerations for nutrient removal activated sludge plants. *Water Science and Technology*, 23(4-6), 781-790.

Pronk, M., de Kreuk, M. K., de Bruin, B., Kamminga, P., Kleerebezem, R., & van Loosdrecht, M. C. M. (2015). Full scale performance of the aerobic granular sludge process for sewage treatment. *Water Research*, 84, 207-217. doi:10.1016/j.watres.2015.07.011

Pronk, M., Giesen, A., Thompson, A., Robertson, S., & van Loosdrecht, M. (2017). Aerobic granular biomass technology: advancements in design, applications and further developments. *Water Practice and Technology,* 12(4), 987-996. doi:10.2166/wpt.2017.101

Qian, F. Y., Wang, J. F., Shen, Y. L., Wang, Y., Wang, S. Y., & Chen, X. (2017). Achieving high performance completely autotrophic nitrogen removal in a continuous granular sludge reactor. *Biochemical Engineering Journal*, 118, 97-104. doi:10.1016/j.bej.2016.11.017

Rabaey, K., Vlaeminck, S. (2017). *Biotechnological processes in environmental sanitation.* Ghent University.

Ramos, C., Suarez-Ojeda, M. E., & Carrera, J. (2016). Biodegradation of a high-strength wastewater containing a mixture of ammonium, aromatic compounds and salts with simultaneous nitritation in an aerobic granular reactor. *Process Biochemistry*, 51(3), 399-407. doi:10.1016/j.procbio.2015.12.020

Rocktaschel, T., Klarmann, C., Helmreich, B., Ochoa, J., Boisson, P., Sorensen, K. H., & Horn, H. (2013). Comparison of two different anaerobic feeding strategies to establish a stable aerobic granulated sludge bed. *Water Research*, 47(17), 6423-6431.doi:10.1016/j.watres.2013.08.014

Rollemberg, S. L. D., Barros, A. R. M., Firmino, P. I. M., & dos Santos, A. B. (2018). Aerobic granular sludge: Cultivation parameters and removal mechanisms. *Bioresource Technology*, 270, 678-688. doi:10.1016/j.biortech.2018.08.130

Royal HaskoningDHV. (2020a). *Nereda® Plants.* Retrieved May 25 2020 from https://www.royalhaskoningdhv.com/en-gb/nereda/nereda-plants

Royal HaskoningDHV. (2020b). *Nereda Utrecht plant.* Retrieved May 25 2020 from https://www.royalhaskoningdhv.com/en-gb/nereda

Royal HaskoningDHV. (2020c). *The Netherlands – Epe.* Retrieved May 25 2020 from https://www.royalhaskoningdhv.com/en-gb/nereda/nereda-plants/the-netherlands-epe/474

Schwarzenbeck, N., & Wilderer, P. A. (2005). Treatment of food industry effluents in a granular sludge SBR. *Aerobic granular sludge. IWA Publishing, London*, *UK*, 95-102.

Shannon, K. E., Lee, D. Y., Trevors, J. T., & Beaudette, L. A. (2007). Application of real-time quantitative PCR for the detection of selected bacterial pathogens during municipal wastewater treatment. *Science of the Total Environment*, 382(1), 121-129. doi:10.1016/j.scitotenv.2007.02.039

Shaw, A., Watts, J., Fairey, A. W., & Iler, M. (2009). Intelligent sequencing batch reactor control from theory, through modelling, to full-scale application. *Water Science and Technology, 59*(1), 167-173. doi:10.2166/wst.2009.861

Sikic, T., Meijer, S. C. F., Sirac, S., Matosic, M., & Brdjanovic, D. (2017). Five methods for secondary settler design. Filtration & Separation, 54(4), 28-31.

Simon, J., Wiese, J., & Steinmetz, H. (2006). A comparison of continuous flow and sequencing batch reactor plants concerning integrated operation of sewer systems and wastewater treatment plants. *Water Science and Technology, 54*(11-12), 241-248. doi:10.2166/wst.2006.814

Solon, K., Flores-Alsina, X., Mbamba, C. K., Ikumi, D., Volcke, E. I. P., Vaneeckhaute, C., Ekama, G., Vanrolleghem, P.A., Batstone, D.J., Gernaey, K.V., Jeppsson,U. (2017). Plant-wide modelling of phosphorus transformations in wastewater treatment systems: Impacts of control and operational strategies. *Water Research*, 113, 97-110. doi:10.1016/j.watres.2017.02.007

Takacs, I., Patry, G. G., & Nolasco, D. (1991). A dynamic model of the clarification thickening process. *Water Research*, 25(10), 1263-1271. doi:10.1016/0043-1354(91)90066-y

Tarpagkou, R., & Pantokratoras, A. (2014). The influence of lamellar settler in sedimentation tanks for potable water treatment - A computational fluid dynamic study. *Powder Technology*, 268, 139-149. doi:10.1016/j.powtec.2014.08.030

Tay, J. H., Liu, Q. S., Liu, Y., Show, K. Y., Ivanov, V., & Tay, S. T. L. (2005). A comparative study of aerobic granulation in pilot-and laboratory-scale SBRs. *Aerobic granular sludge. IWA Publishing, London*, *UK*, 125-133.

Thanh, B. X., Visvanathan, C., & Ben Aim, R. (2009). Characterization of aerobic granular sludge at various organic loading rates. *Process Biochemistry*, 44(2), 242-245. doi:10.1016/j.procbio.2008.10.018

Tobey, J. A., & Smets, H. (1996). The Polluter-Pays Principle in the Context of Agriculture and the Environment. *World Economy*, 19(1), 63-87.

Van der Roest, H. F., De Bruin, L. M. M., Gademan, G., & Coelho, F. (2011). Towards sustainable waste water treatment with Dutch Nereda® technology. *Water Practice and Technology*, *6*(3).

Van Haandel, A. C, & Van der Lubbe, J. (2007). *Handbook biological waste water treatment : design and optimisation of activated sludge systems.* Leidschendam: Quist Publishing.

Van Loosdrecht, M. C. M., de Kreuk, M. K., & Heijnen, J. J. (2005). The unity of biofilm structures. *Aerobic granular sludge. IWA Publishing, London*, *UK*, 1-5.

Vlaamse milieumaatschappij. (2019a, March). *Zuiveringsgraad in Vlaanderen.* Retrieved August 27 from https://www.milieurapport.be/milieuthemas/waterkwaliteit/andere/zuiveringsgraad

Vlaamse milieumaatschappij. (2019b, July). *Riolerings- en zuiveringsgraden.* Retrieved August 27 from https://www.vmm.be/data/riolerings-en-zuiveringsgraden

Vrecko, D., Gernaey, K. V., Rosen, C., & Jeppsson, U. (2006). Benchmark Simulation Model No 2 in Matlab-Simulink: Towards plant-wide WWTP control strategy evaluation. *Water Science and Technology,* 54(8), 65-72. doi:10.2166/wst.2006.773

Wagner, M., Loy, A., Nogueira, R., Purkhold, U., Lee, N., & Daims, H. (2002). Microbial community composition and function in wastewater treatment plants. *Antonie Van Leeuwenhoek International Journal of General and Molecular Microbiology*, 81(1-4), 665-680. doi:10.1023/a:1020586312170

Wang, Q., Du, G. C., & Chen, J. (2004). Aerobic granular sludge cultivated under the selective pressure as a driving force. *Process Biochemistry*, 39(5), 557-563. doi:10.1016/s0032-9592(03)00128-6

Wavin. (2017, January 17). *Pros and Cons of separating rainwater from sewers to prevent sewer*

overflow in urban areas. Retrieved September 25 from https://www.wavin.com/en-en/News-Cases/News/Pros-and-Cons-of-separating-rainwater-from-sewers-to-prevent-sewer-overflow-in-urban-areas

Wery, N., Lhoutellier, C., Ducray, F., Delgenes, J. P., & Godon, J. J. (2008). Behaviour of pathogenic and indicator bacteria during urban wastewater treatment and sludge composting, as revealed by quantitative PCR. *Water Research*, 42(1-2), 53-62. doi:10.1016/j.watres.2007.06.048

Winkler, M. K. H., Bassin, J. P., Kleerebezem, R., de Bruin, L. M. M., van den Brand, T. P. H., & van Loosdrecht, M. C. M. (2011). Selective sludge removal in a segregated aerobic granular biomass system as a strategy to control PAO-GAO competition at high temperatures. *Water Research*, 45(11), 3291-3299. doi:10.1016/j.watres.2011.03.024

Winkler, M. K. H., Bassin, J. P., Kleerebezem, R., van der Lans, R., & van Loosdrecht, M. C. M. (2012). Temperature and salt effects on settling velocity in granular sludge technology. *Water Research*, 46(12), 3897-3902. doi:10.1016/j.watres.2012.04.034

Winkler, M. K. H., Kleerebezem, R., Strous, M., Chandran, K., & van Loosdrecht, M. C. M. (2013). Factors influencing the density of aerobic granular sludge. *Applied Microbiology and Biotechnology*, 97(16), 7459-7468. doi:10.1007/s00253-012-4459-4

Xin, X., Lu, H., Yao, L., Leng, L., & Guan, L. (2017). Rapid Formation of Aerobic Granular Sludge and Its Mechanism in a Continuous-Flow Bioreactor. *Applied Biochemistry and Biotechnology*, 181(1), 424-433. doi:10.1007/s12010-016-2221-6

Yuan, Z. G., Pratt, S., & Batstone, D. J. (2012). Phosphorus recovery from wastewater through microbial processes. *Current Opinion in Biotechnology*, 23(6), 878-883. doi:10.1016/j.copbio.2012.08.001

Zeng, W., Li, L., Yang, Y. Y., Wang, S. Y., & Peng, Y. Z. (2010). Nitritation and denitritation of domestic wastewater using a continuous anaerobic-anoxic-aerobic (A(2)O) process at ambient temperatures. *Bioresource Technology*, 101(21), 8074-8082. doi:10.1016/j.biortech.2010.05.098

Zheng, Y. M., Yu, H. Q., Liu, S. H., & Liu, X. Z. (2006). Formation and instability of aerobic granules under high organic loading conditions. *Chemosphere*, 63(10), 1791-1800. doi:10.1016/j.chemosphere.2005.08.055

Zhou, D. D., Liu, M. Y., Gao, L. L., Shao, C. Y., & Yu, J. (2013a). Calcium accumulation characterization in the aerobic granules cultivated in a continuous-flow airlift bioreactor. *Biotechnology Letters*, 35(6), 871-877. doi:10.1007/s10529-013-1157-y

Zhou, D. D., Liu, M. Y., Wang, J., Dong, S. S., Cui, N., & Gao, L. L. (2013b). Granulation of activated sludge in a continuous flow airlift reactor by strong drag force. *Biotechnology and Bioprocess Engineering*, 18(2), 289-299. doi:10.1007/s12257-012-0513-4

Zou, J. T., Tao, Y. Q., Li, J., Wu, S. Y., & Ni, Y. J. (2018). Cultivating aerobic granular sludge in a developed continuous-flow reactor with two-zone sedimentation tank treating real and low-strength wastewater. *Bioresource Technology*, 247, 776-783. doi:10.1016/j.biortech.2017.09.088

Appendix

Appendix A.1: BSM2 constant influent data

Table A.1: BSM2 constant influent data. The 20 variables presented here form the variables set simulated in the model. They consist of the 19 state variables as given in Table 3.2, supplemented with the flow rate Q.

Symbol	Value	Unit	Reference
$\mathbf{S_{O_2}}$	0	g O_2.m^{-3}	Alex *et al.* (2008b)
$\mathbf{S_F}$	34.91	g COD.m^{-3}	Alex *et al.* (2008b)
$\mathbf{S_{VFA}}$	23.27	g COD.m^{-3}	Alex *et al.* (2008b)
$\mathbf{S_U}$	27.23	g COD.m^{-3}	Alex *et al.* (2008b)
$\mathbf{S_{NH_x}}$	23.86	g N.m^{-3}	Alex *et al.* (2008b)
$\mathbf{S_{N_2}}$	0	g N.m^{-3}	Solon *et al.* (2017)
$\mathbf{S_{No_x}}$	0	g N.m^{-3}	Alex *et al.* (2008b)
$\mathbf{S_{PO_4}}$	5.96	g P.m^{-3}	Solon *et al.* (2017)
$\mathbf{S_{Alk}}$	7	mole HCO_3^-.m^{-3}	Alex *et al.* (2008b)
$\mathbf{X_U}$	92.50	g COD.m^{-3}	Alex *et al.* (2008b)
$\mathbf{XC_B}$	363.94	g COD.m^{-3}	Alex *et al.* (2008b)
$\mathbf{X_{OHO}}$	50.68	g COD.m^{-3}	Alex *et al.* (2008b)
$\mathbf{X_{PAO}}$	0	g COD.m^{-3}	Alex *et al.* (2008b)
$\mathbf{X_{PAO,PP}}$	0	g P.m^{-3}	Solon *et al.* (2017)
$\mathbf{X_{PAO,Stor}}$	0	g COD.m^{-3}	Solon *et al.* (2017)
$\mathbf{X_{ANO}}$	0	g COD.m^{-3}	Alex *et al.* (2008b)
$\mathbf{X_{TSS}}$	380.34	g TSS.m^{-3}	Alex *et al.* (2008b)
$\mathbf{X_{MeOH}}$	0	g $Fe(OH)_3$.m^{-3}	Solon *et al.* (2017)
$\mathbf{X_{MeP}}$	0	g $FePO_4$.m^{-3}	Solon *et al.* (2017)
Q_{in}	20 648.36	m^3.d	Alex *et al.* (2008b)

Appendix A.2: Stoichiometric parameters of ASM2d

Table A.2: Stoichiometric parameters of ASM2d and their respective value at 14.86°C, unit and reference. The notation is based on Corominas *et al.* (2010).

Symbol	Definition	Value	Unit	Reference
$f_{S_U\_XC_B,hyd}$	Fraction of inert COD generated in hydrolysis	0.00	g COD.(g COD)$^{-1}$	Henze *et al.* (2000)
Y_{OHO}	Yield for X_{OHO} growth	0.625	g COD.(g COD)$^{-1}$	Henze *et al.* (2000)
Y_{PAO}	Yield for X_{PAO} growth per $X_{PAO,PHA}$	0.625	g COD.(g COD)$^{-1}$	Henze *et al.* (2000)
$Y_{PP\_Stor,PAO}$	Yield for $X_{PAO,PP}$ requirement (PO_4 release) per $X_{PAO,Stor}$ stored	0.40	g P.(g COD)$^{-1}$	Henze *et al.* (2000)
$Y_{Stor\_PP,PAO}$	Yield for $X_{PAO,PP}$ storage per $X_{PAO,Stor}$ utilized	0.20	g COD.(g P)$^{-1}$	Henze *et al.* (2000)
Y_{ANO}	yield of autotrophic biomass per NO_3^- -N	0.24	g COD.(g N)$^{-1}$	Henze *et al.* (2000)
$f_{X_U\_Bio,lys}$	Fraction of X_U generated in biomass decay	0.10	g COD.(g COD)$^{-1}$	Henze *et al.* (2000)
$i_{N\_S_U}$	N content of S_U	0.06003	g N.(g COD)$^{-1}$	Solon *et al.* (2017)
$i_{N\_S_F}$	N content of S_F	0.03352	g N.(g COD)$^{-1}$	Solon *et al.* (2017)
$i_{N\_X_U}$	N content of X_U	0.06003	g N.(g COD)$^{-1}$	Solon *et al.* (2017)
$i_{N\_XC_B}$	N content of XC_B	0.03352	g N.(g COD)$^{-1}$	Solon *et al.* (2017)
$i_{N\_X_{Bio}}$	N content of biomass (X_{OHO}, X_{PAO}, X_{ANO})	0.08615	g N.(g COD)$^{-1}$	Solon *et al.* (2017)
$i_{P\_S_U}$	P content of S_U	0.00649	g P.(g COD)$^{-1}$	Solon *et al.* (2017)
$i_{P\_S_F}$	P content of S_F	0.00559	g P.(g COD)$^{-1}$	Solon *et al.* (2017)
$i_{P\_X_U}$	P content of X_U	0.00649	g P.(g COD)$^{-1}$	Solon *et al.* (2017)
$i_{P\_XC_B}$	P content of XC_B	0.00559	g P.(g COD)$^{-1}$	Solon *et al.* (2017)
$i_{P\_X_{Bio}}$	P content of biomass (X_{OHO}, X_{PAO}, X_{ANO})	0.02154	g P.(g COD)$^{-1}$	Solon *et al.* (2017)
$i_{TSS\_X_U}$	TSS to COD ratio for X_U	0.75	g TSS.(g COD)$^{-1}$	Henze *et al.* (2000)
$i_{TSS\_XC_B}$	TSS to COD ratio for XC_B	0.75	g TSS.(g COD)$^{-1}$	Henze *et al.* (2000)
$i_{TSS\_X_{Bio}}$	TSS to COD ratio for biomass (X_{OHO}, X_{PAO}, X_{ANO})	0.90	g TSS.(g COD)$^{-1}$	Henze *et al.* (2000)

Appendix A.3: Kinetic parameters of ASM2d

Table A.3: Kinetic parameters of ASM2d and their respective value and unit at 14.86°C based on Henze *et al.* (2000), with corrections of Hauduc *et al.* (2010). The notation is based on Corominas *et al.* (2010).

Symbol	Definition	Value	Unit
Hydrolysis of particulate substrate XC_B			
$q_{XC_B\_SB,hyd}$	Maximum specific hydrolysis rate	2.46	d^{-1}
$\eta_{qhyd,Ax}$	Correction factor for anoxic hydrolysis	0.60	-
$\eta_{qhyd,An}$	Correction factor for anaerobic hydrolysis	0.40	-
$K_{O_2,hyd}$	Half saturation/inhibition parameter for S_{O_2}	0.20	g $O_2.m^{-3}$
$K_{NO_x,hyd}$	Half saturation/inhibition parameter for S_{NO_x}	0.50	g $N.m^{-3}$
$K_{XC_B,hyd}$	Half saturation parameter for XC_B/X_{OHO}	0.10	g COD.(g COD)$^{-1}$
Heterotrophic organisms X_{OHO}			
$\mu_{OHO,Max}$	Maximum growth rate of X_{OHO}	4.23	d^{-1}
$q_{S_F\_VFA,Max}$	Rate constant for fermentation	2.11	g COD.(g COD)$^{-1}.d^{-1}$
$\eta_{\mu OHO,Ax}$	Reduction factor for anoxic growth of X_{OHO}	0.80	-
b_{OHO}	Decay rate for X_{OHO}	0.28	d^{-1}
$K_{O_2,OHO}$	Half saturation/inhibition parameter for S_{O_2}	0.20	g $O_2.m^{-3}$
$K_{S_F,OHO}$	Half saturation parameter for S_F	4.00	g $COD.m^{-3}$
$K_{S_F,fe}$	Half saturation parameter for fermentation of S_F	4.00	g $COD.m^{-3}$
$K_{S_{VFA},OHO}$	Half saturation parameter for S_{VFA}	4.00	g $COD.m^{-3}$
$K_{NO_x,OHO}$	Half saturation/inhibition parameter for S_{NO_x}	0.50	g $N.m^{-3}$
$K_{NH_x,OHO}$	Half saturation parameter for S_{NH_x}	0.05	g $N.m^{-3}$
$K_{PO_4,OHO}$	Half saturation parameter for S_{PO_4}	0.01	g $P.m^{-3}$
$K_{Alk,OHO}$	Half saturation parameter for S_{Alk}	0.10	(mole HCO_3^-).m^{-3}
Phosphorus accumulating organisms X_{PAO}			
q_{PAO,VFA_Stor}	Rate constant for S_{VFA} uptake rate ($X_{PAO,Stor}$ storage)	2.46	g COD.(g COD)$^{-1}.d^{-1}$
q_{PAO,PO_4_PP}	Rate constant for storage of $X_{PAO,PP}$	1.23	g P.(g COD)$^{-1}.d^{-1}$
$\mu_{PAO,Max}$	Maximum growth rate of X_{PAO}	0.82	d^{-1}
$\eta_{\mu\ PAO}$	Reduction factor for anoxic growth of X_{PAO}	0.60	-
b_{PAO}	Decay rate of X_{PAO}	0.14	d^{-1}
$b_{PP\_PO_4}$	Rate constant for lysis of $X_{PAO,PP}$	0.14	d^{-1}
b_{Stor_VFA}	Rate constant for respiration of $X_{PAO,Stor}$	0.14	d^{-1}
$K_{O_2,PAO}$	Half saturation/inhibition parameter for S_{O_2}	0.20	g $O_2.m^{-3}$
$K_{NO_x,PAO}$	Half saturation parameter for S_{NO_x}	0.50	g $N.m^{-3}$
$K_{S_{VFA},PAO}$	Half saturation parameter for S_{VFA}	4.00	g $COD.m^{-3}$
$K_{NH_x,PAO}$	Half saturation parameter for S_{NH_x}	0.05	g $N.m^{-3}$
$K_{PO_4,PAO,upt}$	Half saturation parameter for S_{PO_4} uptake ($X_{PAO,PP}$ storage)	0.20	g $P.m^{-3}$
$K_{PO_4,PAO,nut}$	Half saturation parameter for S_{PO_4} as nutrient (X_{PAO} growth)	0.01	g $P.m^{-3}$
$K_{Alk,PAO}$	Half saturation parameter for S_{Alk}	0.10	(mole HCO_3^-).m^{-3}
K_{S,fPP_PAO}	Half saturation parameter for $X_{PAO,PP}/X_{PAO}$	0.01	g P.(g COD)$^{-1}$

$f_{PP\_PAO,Max}$	Maximum ratio of $X_{PAO,PP}/X_{PAO}$	0.34	g P.(g COD)$^{-1}$
K_{I,fPP_PAO}	Half inhibition parameter for $X_{PAO,PP}/X_{PAO}$	0.02	g P.(g COD)$^{-1}$
K_{fStor_PAO}	Saturation constant for $X_{PAO,Stor}/X_{PAO}$	0.01	g COD.(g COD)$^{-1}$
Autotrophic nitrifying organisms X_{ANO}			
$\mu_{ANO,Max}$	Maximum growth rate of X_{ANO}	0.61	d^{-1}
b_{ANO}	Decay rate of X_{ANO}	0.09	d^{-1}
$K_{O_2,ANO}$	Half saturation parameter for S_{O_2}	0.50	g O_2.m^{-3}
$K_{NH_x,ANO}$	Half saturation parameter for S_{NH_x}	1.00	g N.m^{-3}
$K_{Alk,ANO}$	Half saturation parameter for S_{Alk}	0.50	(mole HCO_3^-).m^{-3}
$K_{PO_4,ANO}$	Half saturation parameter for S_{PO_4}	0.01	g P.m^{-3}
Precipitation			
k_{PRE}	Rate constant for P precipitation	1.00	m^3.(g $Fe(OH)_3$)$^{-1}$.d^{-1}
k_{RED}	Rate constant for redissolution	0.60	d^{-1}
$K_{Alk,PRE}$	Saturation coefficient for alkalinity	0.50	(mole HCO_3^-).m^{-3}

Appendix A.4: Process rates of ASM2d

Table A.4: Process rate equations ρ_j [g.m^{-3}.d^{-1}] for each process *j* of the ASM2d model based Henze *et al.* (2000), with corrections of Hauduc *et al.* (2010).The kinetic parameters can be found in Appendix A.3. The notation is based on Corminas *et al.* (2010). In these equations, it is assumed that lysis of biomass only occurs under aerobic conditions.

Process	Rate
1. Aerobic hydrolysis	$q_{XC_B\_SB,hyd}\frac{S_{O_2}}{K_{O_2,hyd}+S_{O_2}}\frac{(XC_B/X_{OHO})}{K_{XC_B,hyd}+(XC_B/X_{OHO})}X_{OHO}$
2. Anoxic hydrolysis	$q_{XC_B\_SB,hyd}\eta_{qhyd,Ax}\frac{K_{O_2,hyd}}{K_{O_2,hyd}+S_{O_2}}\frac{S_{No_x}}{K_{NO_x,hyd}+S_{No_x}}\frac{(XC_B/X_{OHO})}{K_{XC_B,hyd}+(XC_B/X_{OHO})}X_{OHO}$
3. Anaerobic hydrolysis	$q_{XC_B\_SB,hyd}\eta_{qhyd,An}\frac{K_{O_2,hyd}}{K_{O_2,hyd}+S_{O_2}}\frac{K_{NO_x,hyd}}{K_{NO_x,hyd}+S_{No_x}}\frac{(XC_B/X_{OHO})}{K_{XC_B,hyd}+(XC_B/X_{OHO})}X_{OHO}$
4. Aerobic growth X_{OHO} on S_F	$\mu_{OHO,Max}\frac{S_{O_2}}{K_{O_2,OHO}+S_{O_2}}\frac{S_F}{K_{S_F,OHO}+S_F}\frac{S_F}{S_F+S_{VFA}}\frac{S_{NH_x}}{K_{NH_x,OHO}+S_{NH_x}}\frac{S_{PO_4}}{K_{PO_4,OHO}+S_{PO_4}}\frac{S_{Alk}}{K_{Alk,OHO}+S_{Alk}}X_{OHO}$
5. Aerobic growth X_{OHO} on S_{VFA}	$\mu_{OHO,Max}\frac{S_{O_2}}{K_{O_2,OHO}+S_{O_2}}\frac{S_{VFA}}{K_{S_{VFA},OHO}+S_{VFA}}\frac{S_{VFA}}{S_F+S_{VFA}}\frac{S_{NH_x}}{K_{NH_x,OHO}+S_{NH_x}}\frac{S_{PO_4}}{K_{PO_4,OHO}+S_{PO_4}}\frac{S_{Alk}}{K_{Alk,OHO}+S_{Alk}}X_{OHO}$
6. Anoxic growth X_{OHO} on S_F	$\mu_{OHO,Max}\eta_{\mu OHO,Ax}\frac{K_{O_2,OHO}}{K_{O_2,OHO}+S_{O_2}}\frac{S_{No_x}}{K_{NO_x,OHO}+S_{No_x}}\frac{S_F}{K_{S_F,OHO}+S_F}\frac{S_F}{S_F+S_{VFA}}\frac{S_{NH_x}}{K_{NH_x,OHO}+S_{NH_x}}\frac{S_{PO_4}}{K_{PO_4,OHO}+S_{PO_4}}\frac{S_{Alk}}{K_{Alk,OHO}+S_{Alk}}X_{OHO}$
7. Anoxic growth X_{OHO} on S_{VFA}	$\mu_{OHO,Max}\eta_{\mu OHO,Ax}\frac{K_{O_2,OHO}}{K_{O_2,OHO}+S_{O_2}}\frac{S_{No_x}}{K_{NO_x,OHO}+S_{No_x}}\frac{S_{VFA}}{K_{S_{VFA},OHO}+S_{VFA}}\frac{S_{VFA}}{S_F+S_{VFA}}\frac{S_{NH_x}}{K_{NH_x,OHO}+S_{NH_x}}\frac{S_{PO_4}}{K_{PO_4,OHO}+S_{PO_4}}\frac{S_{Alk}}{K_{Alk,OHO}+S_{Alk}}X_{OHO}$
8. Fermen-tation	$q_{S_F\_VFA,Max}\frac{K_{O_2,OHO}}{K_{O_2,OHO}+S_{O_2}}\frac{K_{NO_x,OHO}}{K_{NO_x,OHO}+S_{No_x}}\frac{S_F}{K_{S_F,fe}+S_F}\frac{S_{Alk}}{K_{Alk,OHO}+S_{Alk}}X_{OHO}$
9. Lysis X_{OHO}	$b_{OHO}X_{OHO}$
10. Storage $X_{PAO,Stor}$	$q_{PAO,VFA\_Stor}\frac{S_{VFA}}{K_{S_{VFA},PAO}+S_{VFA}}\frac{S_{Alk}}{K_{Alk,PAO}+S_{Alk}}\frac{X_{PAO,PP}/X_{PAO}}{K_{S,fPP\_PAO}+X_{PAO,PP}/X_{PAO}}X_{PAO}$

Process	Rate
11. Aerobic storage $X_{PAO,PP}$	$q_{PAO,PO_4\_PP} \frac{S_{O_2}}{K_{O_2,PAO}+S_{O_2}} \frac{S_{PO_4}}{K_{PO_4,PAO,upt}+S_{PO_4}} \frac{S_{Alk}}{K_{Alk,PAO}+S_{Alk}} \frac{(X_{PAO,Stor}/X_{PAO})}{K_{fStor\_PAO}+(X_{PAO,Stor}/X_{PAO})} \frac{f_{PP\_PAO,Max}-X_{PAO,PP}/X_{PAO}}{K_{I,fPP\_PAO}+f_{PP\_PAO,Max}-X_{PAO,PP}/X_{PAO}} X_{PAO}$
12. Anoxic storage of $X_{PAO,PP}$	$q_{PAO,PO_{4PP}} \eta_{\mu PAO} \frac{K_{O_2,PAO}}{K_{O_2,PAO}+S_{O_2}} \frac{S_{No_x}}{K_{NO_x,PAO}+S_{No_x}} \frac{S_{PO_4}}{K_{PO_4,PAO,upt}+S_{PO_4}} \frac{S_{Alk}}{K_{Alk,PAO}+S_{Alk}} \frac{(X_{PAO,Stor}/X_{PAO})}{K_{fStor\_PAO}+(X_{PAO,Stor}/X_{PAO})} \frac{f_{PP\_PAO,Max}-X_{PAO,PP}/X_{PAO}}{K_{I,fPP\_PAO}+f_{PP\_PAO,Max}-X_{PAO,PP}/X_{PAO}} X_{PAO}$
13. Aerobic growth X_{PAO} on $X_{PAO,Stor}$	$\mu_{PAO,Max} \frac{S_{O_2}}{K_{O_2,PAO}+S_{O_2}} \frac{S_{NH_x}}{K_{NH_x,PAO}+S_{NH_x}} \frac{S_{PO_4}}{K_{PO_4,PAO,nut}+S_{PO_4}} \frac{S_{Alk}}{K_{Alk,PAO}+S_{Alk}} \frac{(X_{PAO,Stor}/X_{PAO})}{K_{fStor\_PAO}+(X_{PAO,Stor}/X_{PAO})} X_{PAO}$
14. Anoxic growth X_{PAO} on $X_{PAO,Stor}$	$\mu_{PAO,Max} \eta_{\mu,PAO} \frac{K_{O_2,PAO}}{K_{O_2,PAO}+S_{O_2}} \frac{S_{No_x}}{K_{NO_x,PAO}+S_{No_x}} \frac{S_{NH_x}}{K_{NH_x,PAO}+S_{NH_x}} \frac{S_{PO_4}}{K_{PO_4,PAO,nut}+S_{PO_4}} \frac{S_{Alk}}{K_{Alk,PAO}+S_{Alk}} \frac{(X_{PAO,Stor}/X_{PAO})}{K_{fPHA\_PAO}+(X_{PAO,Stor}/X_{PAO})} X_{PAO}$
15. Lysis X_{PAO}	$b_{PAO} X_{PAO} \frac{S_{Alk}}{K_{Alk,PAO}+S_{Alk}}$
16. Lysis $X_{PAO,PP}$	$b_{PP\_PO_4} X_{PAO,PP} \frac{S_{Alk}}{K_{Alk,PAO}+S_{Alk}}$
17. Lysis $X_{PAO,Stor}$	$b_{Stor\_VFA} X_{PAO,Stor} \frac{S_{Alk}}{K_{Alk,PAO}+S_{Alk}}$
18. Aerobic growth X_{ANO}	$\mu_{ANO,Max} \frac{S_{O_2}}{K_{O_2,ANO}+S_{O_2}} \frac{S_{NH_x}}{K_{NH_x,ANO}+S_{NH_x}} \frac{S_{PO_4}}{K_{PO_4,ANO}+S_{PO_4}} \frac{S_{Alk}}{K_{Alk,ANO}+S_{ALK}} X_{ANO}$
19. Lysis X_{ANO}	$b_{ANO} X_{ANO}$
20. precipi-tation	$k_{PRE} S_{PO_4} X_{MeOH}$
21. redisso-lution	$k_{RED} X_{MeP} \frac{S_{Alk}}{K_{Alk,PRE}+S_{Alk}}$

Appendix A.5. **Table A.5: Complete stoichiometric ASM2d matrix consisting of the stoichiometric coefficients $\nu_{j,I}$ for component *i* in process *j* (Henze *et al.*, 2000). Notation based on Corominas *et al.* (2010). The stoichiometric parameters can be found in Appendix A.2.**

Process	S_{O_2}	S_F	S_{VFA}	S_U	S_{NH_4}	S_{N_2}	S_{NO_x}	S_{PO_4}	S_{Alk}	X_U	XC_B	X_{OHO}	X_{PAO}	$X_{PAO,}$	$X_{PAO,}$	X_{ANO}	X_{TSS}	X_{MeOH}	X_{MeP}
1. Aerobic hydrolysis		$1-f_{S_{U\_XC_B,hyd}}$		$f_{S_{U\_XC_B,hyd}}$	$i_{N\_XC_B} - i_{N\_S_U} f_{S_{U\_XC_B,hyd}} - i_{N\_S_F}(1 - f_{S_{U\_XC_B,hyd}})$			$i_{P\_XC_B} - i_{P\_S_U} f_{S_{U\_XC_B,hyd}} - i_{P\_S_F}(1 - f_{S_{U\_XC_B,hyd}})$	alk_1		-1					$-i_{TSS\_XC_B}$		
2. Anoxic hydrolysis		$1-f_{S_{U\_XC_B,hyd}}$		$f_{S_{U\_XC_B,hyd}}$	$i_{N\_XC_B} - i_{N\_S_U} f_{S_{U\_XC_B,hyd}} - i_{N\_S_F}(1 - f_{S_{U\_XC_B,hyd}})$			$i_{P\_XC_B} - i_{P\_S_U} f_{S_{U\_XC_B,hyd}} - i_{P\_S_F}(1 - f_{S_{U\_XC_B,hyd}})$	alk_1		-1					$-i_{TSS\_XC_B}$		
3. Anaerobic hydrolysis		$1-f_{S_{U\_XC_B,hyd}}$		$f_{S_{U\_XC_B,hyd}}$	$i_{N\_XC_B} - i_{N\_S_U} f_{S_{U\_XC_B,hyd}} - i_{N\_S_F}(1 - f_{S_{U\_XC_B,hyd}})$			$i_{P\_XC_B} - i_{P\_S_U} f_{S_{U\_XC_B,hyd}} - i_{P\_S_F}(1 - f_{S_{U\_XC_B,hyd}})$	alk_1		-1					$-i_{TSS\_XC_B}$		
4. Aerobic growth X_{OHO} on S_F	$\frac{-(1-Y_{OHO})}{Y_{OHO}}$	$\frac{-1}{Y_{OHO}}$			$\frac{i_{N\_S_F}}{Y_{OHO}} - i_{N\_X_{Bio}}$			$\frac{i_{P\_S_F}}{Y_{OHO}} - i_{P\_X_{Bio}}$	alk_2			1				$i_{TSS\_X_{Bio}}$		
5. Aerobic growth X_{OHO} on S_F	$\frac{-(1-Y_{OHO})}{Y_{OHO}}$		$\frac{-1}{Y_{OHO}}$		$-i_{N\_X_{Bio}}$			$-i_{P\_X_{Bio}}$	alk_3			1				$i_{TSS\_X_{Bio}}$		
6. Anoxic growth X_{OHO} on S_F		$\frac{-1}{Y_{OHO}}$			$\frac{i_{N\_S_F}}{Y_{OHO}} - i_{N\_X_{Bio}}$	$\left(\frac{1-Y_{OHO}}{40/14\,Y_{OHO}}\right)$	$-\left(\frac{1-Y_{OHO}}{40/14\,Y_{OHO}}\right)$	$\frac{i_{P\_S_F}}{Y_{OHO}} - i_{P\_X_{Bio}}$	$+\frac{alk_2}{14*40/14*Y_{OHO}}\frac{1-Y_{OHO}}{}$			1				$i_{TSS\_X_{Bio}}$		
7. Anoxic growth X_{OHO} on S_{VFA}			$\frac{-1}{Y_{OHO}}$		$i_{N\_X_{Bio}}$	$\left(\frac{1-Y_{OHO}}{40/14\,Y_{OHO}}\right)$	$-\left(\frac{1-Y_{OHO}}{40/14\,Y_{OHO}}\right)$	$-i_{P\_X_{Bio}}$	$+\frac{alk_3}{14*40/14*Y_{OHO}}\frac{1-Y_{OHO}}{}$			1				$i_{TSS\_X_{Bio}}$		

$$alk_1 = \frac{i_{N\_XC_B} - i_{N\_S_U} f_{S_{U\_XC_B,hyd}} - i_{N\_S_F}(1-f_{S_{U\_XC_B,hyd}})}{14} - \frac{i_{P\_XC_B} - i_{P\_S_U} f_{S_{U\_XC_B,hyd}} - i_{P\_S_F}(1-f_{S_{U\_XC_B,hyd}})}{31/1.5},\ alk_2 = \frac{\frac{i_{N\_S_F}}{Y_{OHO}} - i_{N\_X_{Bio}}}{14} - \frac{\frac{i_{P\_S_F}}{Y_{OHO}} - i_{P\_X_{Bio}}}{31/1.5},\ alk_3 = \frac{-i_{N\_X_{Bio}}}{14} - \frac{-i_{P\_X_{Bio}}}{31/1.5} + \frac{1}{64Y_{OHO}}$$

Process	S_{O_2}	S_F	S_{VFA}	S_U	S_{NH_4}	S_{N_2}	S_{NO_x}	S_{PO_4}	S_{Alk}	X_U	XC_B	X_{OHO}	X_{PAO}	$X_{PAO,PP}$	$X_{PAO,Stor}$	X_{ANO}	X_{TSS}	X_{MeOH}	X_{MeP}
8. Fermentation		-1	1		$i_{N\_S_F}$			$i_{P\_S_F}$	$\frac{i_{N\_S_F}}{14} - \frac{i_{P\_S_F}}{31/1.5} - \frac{1}{64}$										
9. Lysis X_{OHO}					$i_{N\_X_{Bio}} - i_{N\_X_U} f_{X_{U\_Bio,lys}} - i_{N\_XC_B}(1 - f_{X_{U\_Bio,lys}})$			$i_{P\_X_{Bio}} - i_{P\_X_U} f_{X_{U\_Bio,lys}} - i_{P\_XC_B}(1 - f_{X_{U\_Bio,lys}})$	alk_4	$f_{X_{U\_Bio,lys}}$	1-$f_{X_{U\_Bio,lys}}$	-1					$i_{TSS\_X_U} f_{X_{U\_Bio,lys}} + i_{TSS\_XC_B}(1 - f_{X_{U\_Bio,lys}}) - i_{TSS\_X_{Bio}}$		
10. Storage $X_{PAO,Stor}$			-1					$Y_{PP\_Stor,PAO}$	$Y_{PP\_Stor,PAO} * (\frac{1.5-1}{31} + \frac{1}{64})$					$-Y_{PP\_Stor,PAO}$	1		$-3.23Y_{PP\_Stor,PAO} + 0.6$		
11. Aerobic storage $X_{PAO,PP}$		$-Y_{Stor\_PP,PA}$						-1	$\frac{1.5-1}{31}$					1	$-Y_{Stor\_PP,PAO}$		3.23-0.6$Y_{Stor_PP,PAO}$		
12. Anoxic storage of $X_{PAO,PP}$						$\frac{Y_{Stor\_PP,PAO}}{\frac{40}{14}}$	$-\frac{Y_{Stor\_PP,PAO}}{\frac{40}{14}}$	-1	$\frac{\frac{1.5-1}{31}}{+\frac{Y_{Stor\_PP,PAO}}{14*40/14}}$					1	$-Y_{Stor\_PP,PAO}$		3.23-0.6$Y_{Stor_PP,PAO}$		
13. Aerobic growth X_{PAO} on $X_{PAO,Stor}$		$\frac{-(1-Y_{PAO})}{Y_{PAO}}$			$-i_{N\_X_{Bio}}$			$-i_{P\_X_{Bio}}$	$\frac{i_{N\_X_{Bio}}}{14} - \frac{-i_{P\_X_{Bio}}}{31/1.5}$				1		$\frac{-1}{Y_{PAO}}$		$i_{TSS\_X_{Bio}} - \frac{0.6}{Y_{PAO}}$		
14. Anoxic growth X_{PAO} on $X_{PAO,Stor}$					$-i_{N\_X_{Bio}}$	$\frac{(1-Y_{PAO})}{\frac{40}{14}Y_{PAO}}$	$-\frac{(1-Y_{PAO})}{\frac{40}{14}Y_{PAO}}$	$-i_{P\_X_{Bio}}$	alk_5				1		$\frac{-1}{Y_{PAO}}$		$i_{TSS\_X_{Bio}} - \frac{0.6}{Y_{PAO}}$		

$alk_4 = \frac{i_{N\_X_{Bio}} - i_{N\_X_U} f_{X_{U\_Bio,lys}} - i_{N\_XC_B}(1-f_{X_{I,H}})}{14} - \frac{i_{P\_X_{Bio}} - i_{P\_X_U} f_{X_{U\_Bio,lys}} - i_{P\_XC_B}(1-f_{X_{U\_Bio,lys}})}{31/1.5}$, $alk_5 = \frac{i_{N\_X_{Bio}}}{14} - \frac{-i_{P\_X_{Bio}}}{31/1.5} + \frac{(1-Y_{PAO})}{14*40/14*Y_{PAO}}$

Process	S_{O_2}	S_F	S_{VFA}	S_U	S_{NH_4}	S_{N_2}	S_{NO_x}	S_{PO_4}	S_{Alk}	X_U	XC_B	X_{OHO}	X_{PAO}	$X_{PAO,PP}$	$X_{PAO,Stor}$	X_{ANO}	X_{TSS}	X_{MeOH}	X_{MeP}
15. Lysis X_{PAO}					$i_{N\_X_{Bio}} - i_{N\_X_U} f_{X_{U\_Bio,lys}} - i_{N\_XC_B}(1 - f_{X_{U\_Bio,lys}})$			$i_{P\_X_{Bio}} - i_{P\_X_U} f_{X_{U\_Bio,lys}} - i_{P\_XC_B}(1 - f_{X_{U\_Bio,lys}})$	alk$_6$	$f_{X_{U\_Bio,lys}}$	1-$f_{X_{U\_Bio,lys}}$		-1				$i_{TSS\_X_U} f_{X_{U\_Bio,lys}} + i_{TSS\_XC_B}(1 - f_{X_{U\_Bio,lys}}) - i_{TSS\_X_{Bio}}$		
16. Lysis $X_{PAO,PP}$								1	$\frac{1.5-1}{31}$					-1			-3.23		
17. Lysis $X_{PAO,Stor}$			1						$\frac{-1}{64}$						-1		-0.6		
18. Aerobic growth X_{ANO}	$\frac{-(\frac{64}{14} - Y_{ANO})}{Y_{ANO}}$				$-i_{N\_X_{Bio}} - \frac{1}{Y_{ANO}}$	$\frac{1}{Y_{ANO}}$		$-i_{P\_X_{Bio}}$	alk$_7$							1	$i_{TSS\_X_{Bio}}$		
19. Lysis X_{ANO}					$i_{N\_X_{Bio}} - i_{N\_X_U} f_{X_{U\_Bio,lys}} - i_{N\_XC_B}(1 - f_{X_{U\_Bio,lys}})$			$i_{P\_X_{Bio}} - i_{P\_X_U} f_{X_{U\_Bio,lys}} - i_{P\_XC_B}(1 - f_{X_{U\_Bio,lys}})$	alk$_8$	$f_{X_{U\_Bio,lys}}$	1-$f_{X_{U\_Bio,lys}}$					-1	$i_{TSS\_X_U} f_{X_{U\_Bio,lys}} + i_{TSS\_XC_B}(1 - f_{X_{U\_Bio,lys}}) - i_{TSS\_X_{Bio}}$		
20. precipitation								-1	$\frac{1.5}{31}$								1.42	-3.45	4.87
21. redissolution								1	$\frac{-1.5}{31}$	$f_{X_{U\_Bio,lys}}$	1-$f_{X_{U\_Bio,lys}}$						-1.42	3.45	-4.87

$\text{alk}_6 = \frac{i_{N\_X_{Bio}} - i_{N\_X_U} f_{X_{U\_Bio,lys}} - i_{N\_XC_B}(1-f_{X_{U\_Bio,lys}})}{14} - \frac{i_{P\_X_{Bio}} - i_{P\_X_U} f_{X_{U\_Bio,lys}} - i_{P\_XC_B}(1-f_{X_{U\_Bio,lys}})}{31/1.5}$,

$\text{alk}_7 = \frac{i_{P\_X_{Bio}} - 1/Y_{ANO}}{14} - \frac{-i_{P\_X_{Bio}}}{31/1.5} - \frac{1}{14Y_{ANO}}$, $\text{alk}_8 = \frac{i_{N\_X_{Bio}} - i_{N\_X_U} f_{X_{U\_Bio,lys}} - i_{N\_XC_B}(1-f_{X_{U\_Bio,lys}})}{14} -$

$\frac{i_{P\_X_{Bio}} - i_{P,X_I} f_{X_{U\_Bio,lys}} - i_{P,X_S}(1-f_{X_{U\_Bio,lys}})}{31/1.5}$

Appendix A.6: Simulation of state variables

The simulation of 20 variables (Table 3.2, Q [m³.d^{-1}]) in both the bioreactors and the settler was carried out by making mass balances based on the ASM2d model. In the biological tank, the balance is made over each bioreactor for each state variable. As an example, the differential equation for X_{OHO} [g COD.m^{-3}] in bioreactor *i* is given in Eq. A.6.1 (Alex *et al.*, 2008b). The reaction term $r_{X_{OHO}}$ [g COD.m^{-3}.d^{-1}] was calculated using Eq. A.6.2. For each state variable *i* concerned (in case of X_{OHO} [g COD.m^{-3}]: *i* = 12), the sum over all processes *j* of the product ($\nu_{j,i}\rho_j$) was made (see Appendix Table A.4 and A.5). The mass balances then resulted in differential equations to be solved by the model, thereby enabling a simulation of the concentration of the state variables in the each bioreactor and in each layer of the settler over time (Henze *et al.*, 2000). In the settler on the other hand, mass balances over X_{TSS} [g TSS.m^{-3}] for each layer were made. Using these simulated TSS concentrations, all other particulate concentrations were calculated assuming that the proportions between them were the same as in the influent stream. The concentration of the soluble state variables is independent of settling and just based on the fluxes in each layer (Alex *et al.*, 2008b). All the differential equations in the Simulink model were solved by the solver ode 45.

$$\frac{dX_{OHO,i}}{dt} = \frac{1}{V_i}\left(Q_{i-1}X_{OHO,i-1} + r_{X_{OHO}}V_i - Q_iX_{OHO,i}\right) \quad (i = 2,4,5,6,7) \quad [\text{g COD.m}^{-3}\text{d}^{-1}] \qquad \textbf{Eq. A. 6. 1}$$

with $X_{OHO,i}$ = X_{OHO} in bioreactor *i* [g COD.m^{-3}.d^{-1}]

Q_i = effluent flow rate of bioreactor *i* [m³.d^{-1}]

V_i = volume of bioreactor *i* (only bioreactors with 1 influent flow) [m³]

r_{XOHO} = reaction rate of X_{OHO} ($=r_{12}$) [g COD.m^{-3}.d^{-1}]

$$r_i = \sum \nu_{j,i}\rho_j \quad \text{over all processes } j \qquad \textbf{Eq. A.6.2}$$

with r_i = reaction rate of state variable *i* [g *i*.m^{-3}.d^{1}]

$\nu_{j,i}$ = stoichiometric coefficient for component *i* in process *j* [g *i*.(g *k*)$^{-1}$](A.4)

ρ_j = process rate of process *j* [g *k*.m^{-3}.d^{-1}] (A.3)

k = component upon which process *j* is based (with $\nu_{j,k}$ = +1 or -1)

Appendix A.7: Calculation optimal internal recycle ratio $(Q_{int}:Q_{in})_{opt}$

This section contains the calculation procedure as followed by Henze *et al.* (2008) to calculate the optimal internal recycle ratio $(Q_{int}:Q_{in})_{opt}$. Since simulations of the reference model (section 3.1) showed a sludge retention time (SRT) of 27 days, this value was also used in the calculation of the optimal internal recycle ratio.

- $(Q_{int}: Q_{in})_{opt} = \frac{-B+\sqrt{B^2+4AC}}{2A}$ $[-]$ **Eq. A. 7. 1**

with $A = \frac{O_s}{2.86}$

$B = N_c - D_{p1} + \frac{(s+1)O_a+sO_s}{2.86}$

$C = (s+1)\left(D_{p1} - \frac{sO_s}{2.86}\right) - sN_c$

s	=	underflow sludge recycle ratio Q_r:Q_{in} (1.5)	[-]
O_a	=	oxygen concentration in Q_{int} * (2 g $O_2.m^{-3}$)	[g $O_2.m^{-3}$]
O_s	=	oxygen concentration in Q_r * (1 g $O_2.m^{-3}$)	[g $O_2.m^{-3}$]
N_c	=	nitrification capacity (Eq. A.7.2)	[g $N.m^{-3}$]
D_{p1}	=	denitrification potential (Eq. A.7.3)	[g $N..m^{-3}$]

Table A.7.1 Calculation results of $(Q_{int}:Q_{in})_{opt}$ [-] (Eq. A.7.1).

Symbol	Value	Source	Symbol	Value
s	1.5	assumption	A	0.35
O_a	2 g $O_2.m^{-3}$	Henze *et al.* (2008)	B	3.98
O_s	1 g $O_2.m^{-3}$	Henze *et al.* (2008)	C	27.90
N_c	33.48 g $N.m^{-3}$	Eq. A.7.2	$(Q_{int}: Q_{in})_{opt}$	4.90
D_{p1}	31.77 g $N..m^{-3}$	Eq. A.7.3		

- $N_c = N_{ti} - N_s - N_{te}$ $[g\ N.\ m^{-3}]$ **Eq. A. 7. 2**

with $N_{ti} = \left[\begin{matrix} S_{NH_x} + S_{N_2} + S_{No_x} + i_{N\_S_U}S_U + i_{N\_S_F}S_F + i_{N\_X_U}X_U \\ +i_{N\_XC_B}XC_B + i_{N\_X_{Bio}}(X_{OHO} + X_{PAO} + X_{ANO}) \end{matrix}\right]_{in}$ **Eq. A.7.2.1**

with all these values obtained from BSM2 influent data (Table A.1)

N_s = concentration of influent N incorporated into the sludge mass [g $N.m^{-3}$]

$= \frac{i_{N\_X_{Bio}}}{SRT}\left[\frac{(S_{F,in}+S_{VFA,in}+XC_{B,in})Y_H SRT}{1+b_H SRT}\left(1 + f_{X_{U_{Bio}},lys}b_H SRT\right) + X_{U,in}SRT\right]$ **Eq. A.7.2.2**

with $i_{N\_X_{Bio}}$ = N content of biomass (X_{OHO}, X_{PAO}, X_{ANO}) [g $N.(g\ COD)^{-1}$]

SRT = sludge retention time [d]

$S_{F,in}$, $S_{VFA,in}$, $XC_{B,in}$: BSM2 influent data (Table A.1)

Y_H = Yield for heterotrophic growth [g $COD.(g\ COD)^{-1}$]

(=Y_{OHO} = Y_{PAO} (Table A.2))

b_H = Decay rate of heterotrophs (= average of b_{OHO} and b_{PAO} (Table A.3)) [d^{-1}]

$f_{X_{U\,Bio},lys}$ = Fraction of X_U generated in biomass decay [g COD.(g COD)$^{-1}$]

N_{te} = organic nitrogen in the effluent [g N.m^{-3}]

$$= \frac{K_{n,15}(b_{ANO}+{}^{1}/_{SRT})}{(1-f_{x1})\mu_{ANO,Max}-(b_{ANO}+{}^{1}/_{SRT})} + f_{N'ous}N_{ti} \qquad \textbf{Eq. A.7.2.3}$$

with $K_{n,15}$ = ammonium half saturation constant at 15°C [g N.m^{-3}]

b_{ANO} = Decay rate of X_{ANO} [d^{-1}]

SRT = sludge retention time [d]

f_{x1} = anoxic volume fraction of bioreactor [-]

$$= \frac{V_3+V_4}{V_p} = 0.22$$

$\mu_{ANO,Max}$ = Maximum growth rate of X_{ANO} [d^{-1}]

$f_{N'ous}$ = unbiodegradable soluble organic N fraction

- $$D_{p1} = \frac{(S_{F,in}+S_{VFA,in})(1-Y_H)}{2.86} + \frac{K_2 f_{x1}(S_{F,in}+S_{VFA,in}+XC_{B,in})f_{cv}Y_H SRT}{1+b_H SRT} \quad [g\ N.\ m^{-3}] \quad \textbf{Eq. A. 7. 3}$$

with K_2 = specific rate of denitrification in anoxic bioreactor at 15°C [g N.(g VSS)$^{-1}$.d^{-1}]

f_{cv} = COD/VSS ratio (VSS = volatile suspended solids) [g COD.(g VSS)$^{-1}$]

Table A.7.2 Calculation results of N_c [g N.m^{-3}] (Eq. A.7.2) and D_{p1} [g N.m^{-3}] (Eq. A.7.3).

Symbol	Value	Source	Symbol	Value	Source	Symbol	Value
$i_{N\_X_{Bio}}$	0.08615 g N.(g COD)$^{-1}$	Table A.2	b_{ANO}	0.09 d^{-1}	Table A.3	N_{ti}	48.78 g N.m^{-3}
SRT	27 d	ass.	f_{x1}	0.22	model design	N_{te}	1.99 g N.m^{-3}
Y_H	0.625 g COD.(g COD)$^{-1}$	Table A.2	$\mu_{ANO,Max}$	0.61 d^{-1}	Table A.3	N_s	13.31 g N.m^{-3}
b_H	0.21 d^{-1}	Table A.3	$f_{N'ous}$	0.03	Henze *et al.* (2008)	N_c	33.48 g N.m^{-3}
$f_{X_{U\,Bio},lys}$	0.10 g COD.(g COD)$^{-1}$	Table A.2	K_2	0.069 g N. (g VSS)$^{-1}$.d^{-1}	Henze *et al.* (2008)		
$K_{n,15}$	1.45 g N.m^{-3}	Henze *et al.* (2008)	f_{cv}	1.45 g COD.(g VSS)$^{-1}$	Henze *et al.* (2008)	D_{p1}	31.77 g N..m^{-3}

Appendix A.8: Modelling effect of diffusion limitation.

The half saturation coefficients in the kinetic process rates as given in Table A.4 were increased to simulate the effect of diffusion limitation. This was done for the K_s [g.m^{-3}] parameters in reactions where NH_4^+ or COD are the final electron donor, where NO_3^- of O_2 are the final electron acceptor and where PO_4^{3-} is stored as PP. In Table A.8, the changed half saturation coefficients, together with these new values for both the strong diffusion limitatio scenario (increase factor 5) and moderate diffusion limitation scenario based on Baeten *et al.* (2018) are given. When the value was not given in Baeten *et al.* (2018), the same value as in the strong scenario was taken. It can be noticed that for $K_{O_2,OHO}$ [g O_2.m^{-3}] and $K_{S_F,OHO}$ [g COD.m^{-3}] a higher value was used in the moderate case compared to the strong case. The reason for this is that for the strong diffusion limitation scenario, the average worst limitation (which is regarding $K_{O_2,OHO}$ and $K_{S_F,OHO}$ on about a factor 5 in Baeten *et al.* (2018) compared to the original situation) was taken as factor for all coefficients. However, the exact values were slightly higher and retained in the moderate case scenario.

Table A.8: Changed half saturation coefficients K_s [g.m^{-3}] to simulate the effect of diffusion limitation. These values are used to calculate the process rates (Table A.3) in the ASM2d model. All other kinetic parameters in the expressions in Table A.4 stayed the same as listed in Table A.3. Two scenarios were investigated: strong diffusion limitation (indicated as DL in table) scenario (increase parameters with factor 5) and the moderate diffusion limitation scenario with values based on Baeten *et al.* (2018).

Symbol	Definition	Original value	Strong DL	Moderate DL	Unit
$K_{O_2,OHO}$	Half saturation/inhibition parameter for S_{O_2}	0.20	1.00	1.13	g O_2.m^{-3}
$K_{S_F,OHO}$	Half saturation parameter for S_F	4.00	20.00	20.77	g COD.m^{-3}
$K_{S_F,fe}$	Half saturation parameter for ferm. of S_F	4.00	20.00	20.00	g COD.m^{-3}
$K_{S_{VFA},OHO}$	Half saturation parameter for S_{VFA}	4.00	20.00	14.43	g COD.m^{-3}
$K_{NO_x,OHO}$	Half saturation/inhibition parameter for S_{NO_x}	0.50	2.50	0.58	g N.m^{-3}
$K_{O_2,PAO}$	Half saturation/inhibition parameter for S_{O_2}	0.20	1.00	0.58	g O_2.m^{-3}
$K_{NO_x,PAO}$	Half saturation parameter for S_{NO_x}	0.50	2.50	0.63	g N.m^{-3}
$K_{S_{VFA},PAO}$	Half saturation parameter for S_{VFA}	4.00	20.00	20.00	g COD.m^{-3}
$K_{PO_4,PAO,upt}$	Half saturation parameter for S_{PO_4} uptake	0.20	1.00	1.00	g P.m^{-3}
$K_{O_2,ANO}$	Half saturation parameter for S_{O_2}	0.50	2.50	1.00	g O_2.m^{-3}
$K_{NH_x,ANO}$	Half saturation parameter for S_{NH_x}	1.00	5.00	5.00	g N.m^{-3}

Appendix A.9: Mass balances based on N, P and COD over the system.

Since concentrations in the system are not changing anymore over time in steady state, the mass balance of COD, N and P over the system could be made to check if the model was correct. This means that the change of mass over time (dm/dt) is zero (Eq. A.9.1; Henze *et al.*, 2000). The mass coming into the system [kg.d^{-1}] ('in') is equal to the mass leaving the system ('out') (Eq. A.9.1). The balance can be composed based on total N, total P and COD, leading to equations Eq. A.9.2, A.9.3 and A.9.4. Explanation of symbols: see Table 3.2 and Table A.2. Indices 'in, 'w' and 'eff' refer to respectively influent, waste and effluent stream. In the equations for N and P, conversion factors (Table A.2) are used to compose the mass balance. In case of COD, the conversion factors are immediately substituted into the equation (Eq. A.9.3). Per example, the factor -64/14 g COD.(g NO_3-N)$^{-1}$ is obtained using the stoichiometry of the nitrification reaction. Furthermore, also the oxygen added to the aeration bioreactors is taken into account in this equation using the oxygen transfer coefficients KLa [d^{-1}].

$$\frac{dm}{dt} = V_{TOT}\frac{dC}{dt} = in - out + reaction = 0 \qquad [g.d^{-1}] \qquad \textbf{Eq. A. 9. 1}$$

with m = mass in system (COD, N or P) [g]

V_{TOT} = total volume of the system (19 500 m³) [m³]

C = total concentration N, P or COD in the system [g.m^{-3}]

$$Q_{in} * \left[S_{NH_x} + S_{N_2} + S_{No_x} + i_{N\_S_U}S_U + i_{N\_S_F}S_F + i_{N\_X_U}X_U + i_{N\_XC_B}XC_B + i_{N\_X_{Bio}}(X_{OHO} + X_{PAO} + X_{ANO})\right]_{in} =$$
$$Q_w * \left[S_{NH_x} + S_{N_2} + S_{No_x} + i_{N\_S_U}S_U + i_{N\_S_F}S_F + i_{N\_X_U}X_U + i_{N\_XC_B}XC_B + i_{N\_X_{Bio}}(X_{OHO} + X_{PAO} + X_{ANO})\right]_{w} +$$
$$Q_{eff} * \left[S_{NH_x} + S_{N_2} + S_{No_x} + i_{N\_S_U}S_U + i_{N\_S_F}S_F + i_{N\_X_U}X_U + i_{N\_XC_B}XC_B + i_{N\_X_{Bio}}(X_{OHO} + X_{PAO} + X_{ANO})\right]_{eff}$$

(see Tables 3.2 and A. 2) $[g\ N.d^{-1}]$ **Eq. A. 9. 2**

$$Q_{in} * \left[S_{PO_4} + X_{PAO,PP} + i_{P\_S_U}S_U + i_{P\_S_F}S_F + i_{P\_X_U}\mathbf{X_U} + i_{P\_XC_B}\mathbf{XC_B} + i_{P\_X_{Bio}}(X_{OHO} + X_{PAO} + X_{ANO})\right]_{in} =$$
$$Q_w * \left[S_{PO_4} + X_{PAO,PP} + i_{P\_S_U}S_U + i_{P\_S_F}S_F + i_{P\_X_U}\mathbf{X_U} + i_{P\_XC_B}\mathbf{XC_B} + i_{P\_X_{Bio}}(X_{OHO} + X_{PAO} + X_{ANO})\right]_{w} +$$
$$Q_{eff} * \left[S_{PO_4} + X_{PAO,PP} + i_{P\_S_U}S_U + i_{P\_S_F}S_F + i_{P\_X_U}\mathbf{X_U} + i_{P\_XC_B}\mathbf{XC_B} + i_{P\_X_{Bio}}(X_{OHO} + X_{PAO} + X_{ANO})\right]_{eff}$$

(see Tables 3.2 and A. 2) $[g\ P.d^{-1}]$ **Eq. A. 9. 3**

$$Q_{in} * \left[S_F + S_{VFA} + S_U + X_U + XC_B + X_{PAO,Stor} + X_{OHO} + X_{PAO} + X_{ANO} + (-1) * S_{O_2} + (-\tfrac{64}{14}) * S_{No_x} + \left(-\tfrac{24}{14}\right) * S_{N_2}\right]_{in} + (-1) * \sum_{i=5}^{7} KLa_i V_i (S^*_{O_2} - S_{O_2,i}) =$$
$$Q_w * \left[S_F + S_{VFA} + S_U + \mathbf{X_U} + \mathbf{XC_B} + X_{PAO,Stor} + X_{OHO} + X_{PAO} + X_{ANO} + (-1) * S_{O_2} + (-\tfrac{64}{14}) * S_{No_x} + \left(-\mathbf{\tfrac{24}{14}}\right) * S_{N_2}\right]_{w} + Q_{eff} * \left[S_F + S_{VFA} + S_U + \mathbf{X_U} + \mathbf{XC_B} + X_{PAO,Stor} + X_{OHO} + X_{PAO} + X_{ANO} + (-1) * S_{O_2} + (-\tfrac{64}{14}) * S_{No_x} + \left(-\mathbf{\tfrac{24}{14}}\right) S_{N_2}\right]_{eff}$$

(see Tables 3.2 and A. 2) $[g\ COD.d^{-1}]$ **Eq. A. 9. 4**

with KLa_i = oxygen transfer coefficient of bioreactor *i* (average over last 100 days of steady state simulation) [d^{-1}]

V_i = volume of each bioreactor *i* (see Table 3.2) [m³]

$S^*_{O_2}$ = oxygen saturation concentration in water (8 g O_2.m^{-3}) [g O_2.d^{-1}]

$S_{O_2,i}$ = oxygen concentration in bioreactor *i* (average over last 100 days of steady state simulation) [g O_2.d^{-1}]

Appendix A.10: Formulas for pumping, aeration and mixing energy based on BSM reports

Eq. A.10.1, A.10.2, A.10.3 were used to calculate the pumping (PE), aeration (AE) and mixing (ME) energy based on formulas found in BSM reports (Alex *et al.*, 2008a).

$$PE = 0.004Q_{int} + 0.008Q_r + 0.05Q_w \quad [kWh.d^{-1}] \mathbf{Eq.A.10.1}$$

with Q_{int} = internal flow rate Q_{int} at steady state [$m^3.d^{-1}$]

Q_r = recycle flow rate Q_r at steady state [$m^3.d^{-1}$]

Q_w = waste flow rate Q_w at steady state [$m^3.d^{-1}$]

$$AE = \frac{S_{O_2}^*}{1.8 * 1000} \sum_{i=5}^{7} V_i KLa_i \quad [kWh.d^{-1}] \mathbf{Eq.A.10.2}$$

with $S_{O_2}^*$ = oxygen saturation concentration in water (8 g $O_2.m^{-3}$) [g $O_2.d^{-1}$]

V_i = volume of bioreactor *i* (see Table 3.1) [m^3]

KLa_i = oxygen transfer coefficient of bioreactor *i* [d^{-1}]

$$ME = 24 \sum_{i=1}^{4} 0.005V_i \quad [kWh.d^{-1}] \mathbf{Eq.A.10.3}$$

with V_i = volume of bioreactor *i* (see Table 3.1) [m^3]

Appendix A.11: Influent data of simulations activated sludge model at X_{TSS} = 4 kg TSS.m^{-3}

Table A.11: Steady state simulations of the continuous model with activated sludge controlled at 4 kg TSS.m^{-3}. Different influent flow rates Q_{in} [m^3.d^{-1}] and associated COD load [kg COD.d^{-1}.m^{-3}] and N load [kg N.d^{-1}.m^{-3}] used to find the maximal treatment capacity before $TSS_{eff} > TSS_{crit}$ and $N_{eff} > N_{crit}$ are given. These loads were calculated by multiplying the COD/N concentrations in the influent with Q_{in} [m^3.d^{-1}] and dividing by the volume of the biological reactor (13 500 m^3). All other influent data were according to Table A.1.

Simulation	Q_{in} [m^3.d^{-1}]	COD load [kg COD.d^{-1}.m^{-3}]	N load [kg N.d^{-1}.m^{-3}]
1	31 000	1.36	0.11
2	31 500	1.38	0.11
3	48 000	2.11	0.17
4	54 000	2.37	0.20
5	57 000	2.50	0.21

Appendix A.12: Influent data of simulations activated sludge model with better settling sludge at X_{TSS} = 4 kg TSS.m^{-3}

Table A.12: Steady state simulations of the activated sludge model with better settling sludge (increased with factor 5) controlled at 4 kg TSS.m^{-3}. Different influent flow rates Q_{in} [m³.d^{-1}] and associated COD load [kg COD.d^{-1}.m^{-3}] and N load [kg N.d^{-1}.m^{-3}] used to find the maximal treatment capacity before $TSS_{eff} > TSS_{crit}$ and $N_{eff} > N_{crit}$ are given. These loads were calculated by multiplying the COD/N concentrations in the influent with Q_{in} [m³.d^{-1}] and dividing by the volume of the biological reactor (13 500 m³). All other influent data were according to Table A.1.

Simulation	Q_{in} [m³.d^{-1}]	COD load [kg COD.d^{-1}.m^{-3}]	N load [kg N.d^{-1}.m^{-3}]
1	27 500	1.21	0.10
2	31 500	1.38	0.11
3	34 106	1.50	0.12
4	195 000	8.56	0.70
5	205 000	9.00	0.74
6	207 763	9.12	0.75